# Polarized Protein Sorting in Hippocampal Neurons

By

**Greta Glover**

A Dissertation

Presented to the Neuroscience Graduate Program
and the Oregon Health & Science University
School of Medicine
in partial fulfillment of
the requirements for the degree of
Doctor of Philosophy

December 2005

School of Medicine
Oregon Health & Science University

---

CERTIFICATE OF APPROVAL

---

This is certify that the Ph.D. dissertation of

Greta H. Glover

has been approved

Mentor/Advisor

Member

Member

Member

Member

## Table of Contents



## Chapter 1 Introduction


THANKS GARY-
THANK YOU SEMICOLON
(you are the king of punctuation marks)
THANKS Stefanie, for all your accurate answers, and for everything else!
for teaching me the basics — writing, speaking, thinking, etc...

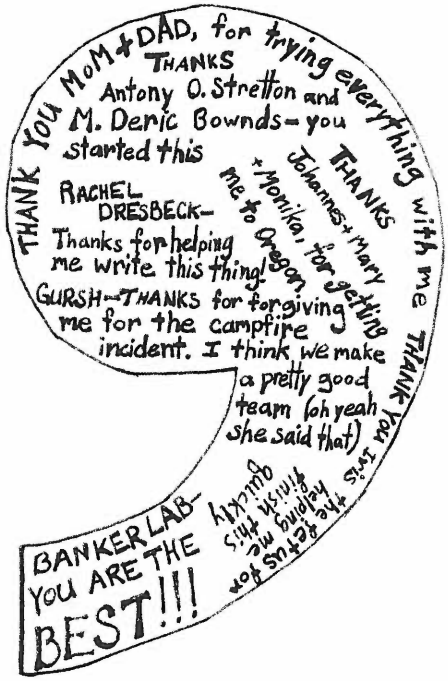
THANK YOU MOM + DAD, for trying everything with me
THANKS Antony O. Stretton and M. Deric Bownds - you started this
THANKS Johannes + Mary + Monika, for getting me to Oregon
RACHEL DRESBECK- Thanks for helping me write this thing!
GURSH - THANKS for forgiving me for the campfire incident. I think we make a pretty good team (oh yeah she said that)
THANK YOU for helping me finish this quickly
BANKER LAB- YOU ARE THE BEST!!!

## Abstract

Neurons develop from an initially spherical shape into morphologically complex, polarized cells. Neuronal function is closely tied to the establishment of two subdomains, the axon and the dendrites. Different plasma membrane proteins are localized to each of these two subdomains; this differential targeting underlies all aspects of neuronal function. The studies in this dissertation examine the mechanisms that mediate polarized protein targeting in neurons.

After plasma membrane proteins are synthesized, they are actively transported to their final destination in vesicular intermediates. A sorting signal present in the protein sequence is thought to drive interactions necessary to incorporate proteins into transport vesicles, which are then delivered to the proper destination. This general model for polarized protein sorting is not understood in any great detail. By studying the vesicles that carry axonal and dendritic proteins, and the sorting signals that are thought to drive cargo selection into these vesicles, the mechanisms involved in the establishment of axonal and dendritic protein localization can be determined.

The use of the GFP tag has revolutionized imaging of transport vesicles in live cells, and the development of GFP color variants that can be used in combination (such as CFP and YFP) makes it possible to watch two different proteins travel at the same time in the same cell (Keller et al. 2001; Kaether et al. 2000; Polischuk et al. 2004). The experiments in Chapter 2 applied dual-color, CFP/YFP imaging of transport carriers to a key issue in nerve cell biology, and an issue of importance to cell biology in general: characterizing the vesicle populations that deliver proteins to distinct domains on the plasma membrane. The findings from this study indicate that axonal and dendritic

proteins are sorted into separate transport vesicle populations soon after their synthesis, and do not intersect in a dendritic endosomal population. In addition, this separation into different vesicle populations is dependant on an intact sorting signal, since a dendritic protein containing mutations in its sorting signal was found in the same vesicle population as an axonal marker. These results can be applied to further study of additional axonal and dendritic markers to determine whether the results in Chapter 2 are representative of all polarized proteins.

This study of the vesicle populations involved in axonal and dendritic sorting (Chapter 2) was supplemented by a pair of studies that aimed to expand current knowledge of the identity of dendritic sorting signals. In Chapters 3 and 4, potential dendritic sorting signals in four different proteins were assessed by quantitative analysis of dendritic polarity. In two of these markers, EAAT3 and EGFR, novel dendritic sorting signals were identified; meanwhile, the other two markers tested, FcRγII-B2 and CD44, were not dendritic, even though they contained putative di-leucine-based sorting signals that direct these proteins to the basolateral domain in epithelial cells. These studies have added to the numbers of dendritic sorting signals identified, and have also challenged the model that proteins sorted to the basolateral domain in epithelia will be sorted to the dendrites in neurons.

# List of Figures

# List of Tables

## List of Abbreviations

| | |
|---|---|
| AEE | Apical Early Endosome |
| AMPAR | α-Amino-3-hydroxyl-5-Methyl-4-Isoxazoleropionic Acid Receptor |
| AP | Adaptor Protein |
| ARE | Apical Recycling Endosome |
| ARF1 | ADP-ribosylation Factor 1 |
| BAR | Bin, Amphiphysin, Rvs |
| BEE | Basolateral Early Endosome |
| BFA | Brefeldin A |
| CE | Common Endosome |
| CFP | Cyan Fluorescent Protein |
| CHO | Chinese Hamster Ovary |
| CK2 | Casein Kinase 2 |
| CLEM | Correlative Light-Electron Microscopy |
| COP | Coatamer Protein |
| DNER | Delta-Notch-like Epidermal Growth Factor Receptor |
| dsRed | Red Fluorescent Protein from *Discosoma* |
| EAAT | Excitatory Amino Acid Transporter |
| EEA1 | Early Endosome Antigen 1 |
| EGFR | Epidermal Growth Factor Receptor |
| EM | Electon Microscopy or Micrograph |
| ER | Endoplasmic Reticulum |
| ERES | Endoplasmic Reticulum Exit Site(s) |
| ERGIC-53 | ER-Golgi Intermediate Compartment 53 |
| FAPP2 | Phosphatidylinositol-4-phosphate Adaptor Protein 2 |
| GABA | Gamma-Amino Butyric Acid |
| GFP | Green Fluorescent Protein |
| GGA | Golgi-localized, Gamma-adaptin-containing, Arf-binding |
| GPI | Glycosylphosphatidylinositol |
| HEK | Human Embryonic Kidney |
| LDLR | Low Density Lipoprotein Receptor |
| MDCK | Madin-Darby Canine Kidney |
| NgCAM | Neuron-glia Cell Adhesion Molecule |
| NMDAR | N-methyl, D-aspartate Receptor |
| PACS-1 | Phophofurin Acidic Cluster Sorting Protein 1 |
| pIgR | Poly Immunoglobulin Receptor |
| PP2A | Protein Phosphatase 2A |
| Ptk2 | *Potorous tridactylis* Kangaroo Rat Kidney |
| PX | Phox Homology |
| RFP | Red Fluorescent Protein |
| SAC | Sub-apical Compartment |
| SH3 | Src Homology Domain |
| SNARE | Soluble NSF-attachment Protein Receptor |

| | |
|---|---|
| SNX1 | Sorting Nexin 1 |
| SPR | Surface Plasmon Resonance |
| Tf | Transferrin |
| TfR | Transferrin Receptor |
| TGN | *trans* Golgi Network |
| ts045VSV-G | Vesicular Stomatitis Virus G Protein, mutant strain ts045 |
| VHS | Vps27, Hrs, STAM domain |
| VSV | Vesicular Stomatitis Virus |
| VSV-G | Vesicular Stomatitis Virus G Protein |
| VTC | Vesiclular-Tubular Clusters |
| YFP | Yellow Fluorescent Protein |

# Chapter 1 Introduction

## 1-1 Overview

The plasma membrane is at the center of neuronal function. A single neuron has two major tasks: to sense neurotransmitter that has been deposited into the extracellular space, and to deposit neurotransmitter into that space. These tasks both occur at the plasma membrane; they also occur at separate domains of the plasma membrane, the dendrites and the axon. Neurons form an elaborate dendritic tree within which postsynaptic terminals are localized, while presynaptic terminals are localized to a single, long axon, allowing electrochemical signals to propogate over long distances. To support these and other distinct roles, different plasma membrane proteins are targeted to each of these two subdomains, ensuring proper neuronal function.

The mechanism for sorting membrane proteins to one domain or the other has been described in general terms, though the molecular details are less clear. Studies of other polarized cells, such as epithelial cells, have indicated that sorting occurs first along the biosynthetic pathway, as proteins are packaged into transport intermediates at the *trans*-Golgi network, and also in the recycling pathway, as proteins cycle between the plasma membrane and endosomes. The cellular mechanisms responsible for such polarized protein sorting in neurons are the subject of this dissertation.

Two different lines of inquiry were followed in these studies. First, dual-color live cell fluorescence microscopy techniques were developed to enable visualization of the vesicles responsible for carrying axonal and dendritic proteins to their respective surface domains. This technique allowed multiple pairs of proteins to be compared and

has led to a preliminary understanding of the organization of polarized trafficking pathways in neurons. The majority of my time and effort was devoted to this first project. Second, motifs that mediate dendritic targeting were examined and compared to motifs that mediate targeting in epithelial cells. These studies, along with others published in the last several years, resulted in the correction of a widespread theory that proposed a parallel between targeting in epithelial cells and targeting in neurons. A brief synopsis of these two projects is provided below.

### 1-1.1 Vesicle Populations Involved in Polarized Sorting in Neurons

Our knowledge of the mechanisms underlying polarized sorting in neurons is limited. What are the rules that govern the sorting of polarized proteins into post-Golgi carriers as they are synthesized and transported to their final destination? Does sorting in endosomes parallel sorting at the Golgi? To answer these questions, I made pairwise comparisons between several polarized membrane proteins to determine if they are sorted into the same or different vesicle populations. I tagged proteins with CFP or YFP (two distinguishable color variants of GFP), which enabled me to view pairs of proteins at the same time, in the same cell, and determine whether or not they are sorted into the same transport vesicles. These experiments showed that axonal and dendritic proteins are segregated into separate vesicle populations in the biosynthetic pathway. In addition, an axonal marker (Neuron-glia Cell Adhesion Molecule, NgCAM) never intersected with endosomes containing either of two dendritic markers, Low density lipoprotein receptor (LDLR) or Transferrin Receptor (TfR). When the dendritic sorting signal in LDLR was

mutated, the marker was packaged in the same vesicle with the axonal protein instead of being segregated into a separate dendritic vesicle population. These results indicate that axonal and dendritic proteins are sorted into separate vesicle populations in the biosynthetic pathway, and they remain in separate populations even as dendritic markers are endocytosed and recycled. In addition, these studies show that an intact dendritic sorting signal is necessary for sorting into the appropriate vesicle population.

### 1-1.2 Dendritic Sorting Signals: A Comparison With Epithelial Cells

The second goal of this dissertation was to further evaluate the proposed parallel between basolateral sorting in epithelial cells and dendritic sorting in neurons. Historically, investigations of polarized trafficking have been performed on polarized epithelial cells. Like neurons, epithelial cells also have two surface domains: basolateral and apical. One significant pair of studies showed that a marker known to be targeted to the basolateral domain of epithelial cells was targeted to the dendritic domain of neurons; correspondingly, an apical marker was shown to be targeted to the axon (Dotti et al., 1993; Dotti and Simons, 1990). This model was extremely appealing due to its simplicity and testability. The Banker lab and others began to evaluate the model for other basolateral and apical proteins.

Initially, further studies led to a refinement of the model. While other basolateral proteins were also found to be targeted to dendrites, apical proteins were present in approximately equal amounts on the surface of axons and dendrites—that is, they were unpolarized (Jareb and Banker, 1998; West et al., 1997). To further explore the

epithelial/neuronal parallel, I participated in two collaborative efforts to examine the localization of several other proteins in neurons (Cheng et al., 2002; Silverman et al., 2005). The principal findings of these studies were that 1) basolateral proteins expressed in neurons are sometimes dendritic, and sometimes unpolarized, and 2) there is at least one apical protein that is targeted to dendrites, using the same cytoplasmic peptide sorting signal in both cell types. As a result of these studies, as well as others published in recent years (Coco et al., 1999; Ghavami et al., 1999; Jareb and Banker, 1998; Kryl et al., 1999; Poyatos et al., 2000), the original model has been significantly modified.

In Chapter 1, an introduction to the field of protein trafficking will provide background for these studies. Current and past literature on the topics of intracellular vesicular traffic and protein sorting will be reviewed, with special attention given to discussion of studies on polarized sorting. Chapter 2 reports experiments to determine how axonal and dendritic proteins are sorted in hippocampal neurons, while Chapters 3 and 4 report experiments that compare sorting signals in epithelia and neurons. Specifically, Chapter 3 analyzes a novel sorting signal in the Excitatory Amino Acid Transporter 3 (EAAT3) that directs apical targeting in epithelia, and dendritic targeting in neurons. Chapter 4 examines a class of basolateral sorting signals, the di-leucine-based signals, in neurons. Finally, Chapter 5 discusses the results of the experiments in Chapters 2-4 and suggests follow-up studies.

## 1-2 Cell Polarity

While neurons are a very extreme case of a cell type with two distinct domains, they are certainly not the only polarized cell type. In fact, most of what we know about how a cell becomes polarized is based on experiments done in other cell types. Many cell types have surface subdomains that carry out distinct functions within a single cell. For example, the basolateral and apical domains of epithelial cells each contain their own populations of membrane proteins, which are integral to the cell's function. A monolayer of epithelial cells, joined by tight junctions, acts as a permeablity barrier which regulates the passage of ions and solute from one compartment to another (Alberts et al. 1994). Yeast also spend much of their time in a polarized state. Both budding and mating yeast preferentially deliver proteins to one part of the plasma membrane (Chant, 1999). In fact, most cells undergo some sort of assymetrical reorganization of their plasma membranes as part of their function, even if this form of polarity is not permanent. Dividing oocytes and neuroblasts, migrating fibroblasts, and T cells forming immunological synapses are all examples of cells that contain a specialized plasma membrane subdomain and can be considered polarized (Alberts et al., 1994). Some features of this transient polarity and the more permanent polarity observed in neurons and epithelia are likely similar. For example, the initial induction of polarity in dividing drosophila neuroblasts, fertilized eggs of *C. elegans*, and

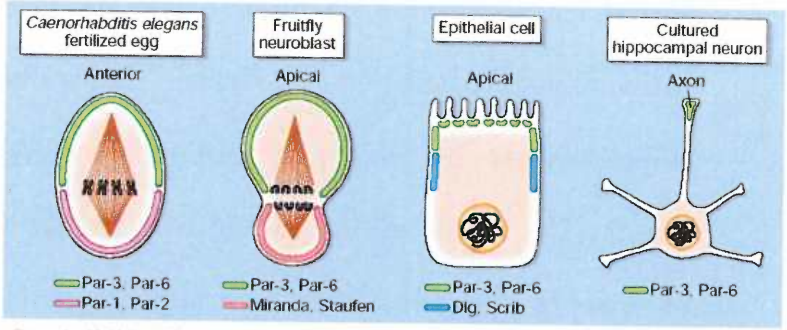


Figure 1. Multiple cell types are either transiently or permanently polarized (from Rolls and Doe, 2003)

in polarizing epithelia all involve polarized distribution of members of the Par family of proteins (Rolls and Doe, 2003). This family has recently been receiving a great deal of attention from neuroscientists, since several studies have suggested the involvement of Par proteins in the initial establishment of polarity in neurons (Nishimura et al., 2004; Nishimura et al., 2005; Rolls and Doe, 2004; Shi et al., 2003).

### 1-2.1 Study of Neuronal Polarity Using Hippocampal Cell Culture

Low-density dissociated hippocampal culture is a well-described system used commonly to study phenomena related to neuronal polarity. In culture, hippocampal neurons develop from small spherical cells into polarized neurons according to a characteristic developmental scheme (Banker and Goslin, 1998; Dotti et al., 1988). Dissociated hippocampal neurons from E18 rat embryos are plated on glass coverslips coated with polylysine. Shortly after plating, the cells extend a flat mesh of lamellipodia. By the time the cells have been in culture for half a day, these lamellipodia have coalesced at several sites to form short processes. These processes are dynamic, extending and retracting for 12-24 hours. These cells, now in culture for about 1 day, are still unpolarized. At this point, one of the minor processes enters a period of steady growth. This neurite will become the axon, and can be distinguished from the other processes by immunocytochemical markers: the cell is beginning to become polarized. After a period of axonal growth, the dendrites begin to develop by 2-4 days in culture, elongating, branching, and developing their characteristic taper. The cells continue to

develop, the dendrites branching further and developing spines, and the axons continuing to elongate and branch, forming complex synaptic networks.

Primary neuronal cell culture is not without its problems. Optimal growth conditions are not perfectly defined, and variables in culture reagents can cause cells to clump together or to develop axons and dendrites at a slower rate or to make shorter axons. These are all signs to beware, since repeat experiments may produce different outcomes in cultures in which neuronal growth does not follow the characteristic steps outlined above.

For many cell biology studies, immortalized cell lines have been developed as models for primary cells. Such cell lines allow a large population of identical cells to be experimented upon at once. In the case of neurons, there are some cell lines that extend long processes and may even develop some synaptic-like structures; however, neuronal cell lines that reproduce the structure and function of axons and dendrites observed in the brain do not exist (Craig and Banker, 1994). Therefore, it is preferable to work in primary cell culture; discoveries made in cultured neurons are almost certain to be directly applicable to neurons in the brain. Several recent studies of polarized plasma membrane proteins in neurons show that protein localization is the same in culture as *in vivo* or in acute slice preparations (Benson et al., 1998; Cheng et al., 2002; Conti et al., 1998; Mitsui et al., 2005). In addition, the changes in gene expression that occur during the development of polarity are similar *in vivo* and *in vitro*, though the rate of these changes may be slightly faster in the brain (Dabrowski et al., 2003). Even the

electrophysiological profiles of Excitatory Postsynaptic Currents and Miniature End-Plate Potentials are similar in hippocampal slices and in culture (K. Tovar pers. comm.).

However, there is a limit to the similarities between culture and the brain; influences from surrounding cells can change electrical properties (London and Segev, 2001), and since axons in culture are not myelinated, the timing and amplitude of action potentials is different. It is likely that any neuronal functions that involve cell-cell interactions will not be identical in the two systems since the density and organization of neurons in culture is completely different from that in the brain. Still, the feasibility of experimentation in culture, along with the likelihood that most processes are similar in the two systems, makes hippocampal culture the best method for studying neuronal polarity. Recent improvements in live-cell imaging of neurons in the intact brain provide hope that someday culture systems will become obsolete and the brain will be studied directly in a living animal; this approach has already been widely applied to the study of nervous systems of small animals such as fruit flies and zebrafish (Lichtman and Fraser, 2001; Niell and Smith, 2004).

## 1-3 Sorting Membrane Proteins Along the Exocytic and Recycling Pathways

Plasma membrane domains such as axons and dendrites maintain their own resident transmembrane proteins despite the fact that plasma membrane lipids and proteins are replaced many times throughout the life of a neuron. There must be some mechanism in place that allows organized turnover so that the distinct compositions of the axonal and dendritic plasma membranes are maintained over time. Because of the

geometry of the neuron, plasma membrane proteins are not likely to diffuse from the axon to the dendrite, or vice versa, during their lifetime (Khanin et al., 1998). Delivery of a particular protein to one domain in a membrane-bound vesicle is thought to be sufficient for maintaining its polarized distribution.

A crucial step in transmembrane protein targeting is thought to occur during formation of vesicles that carry proteins from one subcellular location to another. In many cases, transmembrane proteins contain peptide sequences within their cytoplasmic domains that act like "zip codes," telling the cell's sorting machinery where the protein belongs. The transmembrane protein cargo to be delivered interacts with the cell's sorting machinery, which consists of soluble proteins such as adaptor complexes. Sorting signals in transmembrane proteins are decoded by these adaptor complexes; this interaction leads to concentration of cargo proteins into budding vesicles. For these vesicles to be transported along microtubules, and for their fusion with the plasma membrane, additional factors are also recruited. Vesicles are finally cut free by a scission event, which involves the dynamin protein family in many instances (Praefcke and McMahon, 2004).

Transmembrane proteins are packaged into vesicles at several organelles within a cell. The mechanism for cargo packaging and vesicle formation is thought to be similar in principle at these different subcellular sites (Rodriguez-Boulan and Musch, 2005). In the biosynthetic pathway, newly synthesized transmembrane proteins travel from the endoplasmic reticulum (ER) to the Golgi complex in vesicles, and then again from the Golgi to the plasma membrane. After arrival at the plasma membrane, vesicles mediate

endocytosis and recycling of many transmembrane proteins. A summary of current knowledge of the various vesicle packaging steps that are taken by a typical plasma membrane protein is provided in this section, to serve as background for the experiments performed in Chapter 2.

### 1-3.1 Biosynthetic Pathway: The Endoplasmic Reticulum

#### 1-3.1a Structure and Function of the Endoplasmic Reticulum

The endoplasmic reticulum (ER) is a continuous membrane network present throughout the cytosol, and it is the entry point for the secretory pathway. The ER is capable of expanding dramatically to accommodate increased secretion or other ER functions (Chevet et al., 2001); it often makes up 50% of the total membrane in a secretory cell (Federovitch et al., 2005; Wiest et al., 1990). Although it is a single continuous membrane, the ER is compartmentalized into three major functional domains: smooth ER, rough ER and transitional elements (or ER exit sites; ERES). The smooth ER functions mainly in calcium storage, as well as in drug handling and in lipid and steroid synthesis (Levine and Rabouille, 2005). The rough ER, studded with ribosomes, is specialized for protein synthesis and folding. Transmembrane and secreted proteins are targeted to the rough ER via a signal recognition peptide present in their primary sequences (Martoglio and Dobberstein, 1998). As these proteins are folded, various ER quality control measures ensure proper folding and target improperly folded proteins for

degradation (Chevet et al., 2001). Incorrectly folded proteins are re-translocated to the cytosol, where they are degraded, while correctly folded proteins are exported from the ER at ERES (Levine and Rabouille, 2005). ERES are thought to be stable ER subdomains specialized for cargo exit (Aridor et al., 2001; Hammond and Glick, 2000).

1-3.1b Vesicle Formation at ER Exit Sites

ERES are the primary sites of vesicle formation in the ER, and the molecular mechanisms responsible for vesicle budding are relatively well characterized. Components of the Coatamer Protein II complex (COPII), along with other cofactors, concentrate transmembrane and soluble protein cargo into budding vesicles that will be delivered from ERES to the next station in the secretory pathway, the Golgi complex. The details of COPII vesicle formation will be left for discussion in Section 1-5.2 of this chapter.

From *in vitro* budding assays of yeast COPII-driven vesicle synthesis, it was shown that COPII vesicles are 60nm spherical structures (Matsuoka et al., 2001). Studies using electron microscopy showed that proteins accumulate in clusters of multiple vesicular and tubular membranes soon after exit from the ER (Farquhar and Palade, 1998). The relationship between the small vesicles seen in *in vitro* budding assays and the vesicular-tubular clusters (VTCs) seen in cells was unclear at this point. Some thought that small COPII vesicles linked to form VTCs, which were then transported along microtubules to the Golgi complex (Saraste and Kuismanen, 1984); others hypothesized that VTCs were stable ER-to-Golgi intermediate compartments, where

small COPII vesicles from the ER would fuse, then COPI vesicles would bud off and deliver cargo the rest of the way to the Golgi (Hauri and Schweizer, 1992).

By using GFP to tag cargo and study its movement from ER to Golgi in live cells, it became possible to directly visualize the transport of cargo and therefore characterize the carriers involved. Practically all of these live-cell imaging studies have relied on a single cargo marker— a temperature sensitive mutant form of VSV-G, an envelope protein from the Vesicular Stomatitis Virus. The mutant VSV-G (named tsO45VSV-G) has been popular because its exit from the ER can be easily controlled. Folding of newly synthesized tsO45VSV-G can be reversibly blocked by incubation at 39.5° C. Upon cooling cells below this restrictive temperature, a population of tsO45VSV-G is exported synchronously from the ER, allowing vesicles to form and be transported. By incubating cells expressing GFP-tagged tsO45VSV-G at 39.5° C, then cooling the cells to 32° C on the fluorescence microscope, vesicles containing tsO45VSV-G-GFP could be characterized as they moved from ER to Golgi. When these ER-derived cargo molecules were studied in living cells, it became evident that the vesicles that deliver cargo from ER to Golgi are not the 60 nm vesicles seen in the *in vitro* assays. Instead they are pleiomorphic vesicles and tubules that move on microtubules towards the Golgi complex.

This result argued that the vesicular-tubular clusters seen in electron micrographs were in fact the transport intermediates that carry cargo from ER to Golgi. But at the resolution of light microscopy, it was not possible to confirm whether these structures were single tubular carriers or multiple vesicles linked together. This question has recently been resolved through the use of correlative light-electron microscopy, in which

vesicle transport is imaged in living cells using GFP, then, after processing cells for EM, the same vesicles are visualized at the EM level. In this study, it was shown that moving transport intermediates visualized in living cells were of two types: clusters of vesicles that moved in concert and labeled for COPI, and long tubules that seemed to move faster than the clusters and were free of COPI or COPII staining (Mironov et al. 2003). The long tubules may represent a new type of carrier, while the moving clusters correspond to the VTCs observed previously. Small, 60nm vesicles containing VSV-G were not observed, even at ER exit sites. Perhaps small vesicles may be present only in yeast, or may be an artifact of the *in vitro* budding assay in which they were observed.

Another study of ER-to-Golgi carriers using live cell imaging showed that vesicles containing cargo bound for the extracellular space, in this case a secreted marker consisting of the signal sequence of prolactin coupled to dsRED, behave much differently than vesicles containing a resident ER-to-Golgi trafficking protein, GFP-ERGIC-53 (ER-to-Golgi Intermediate Compartment-53). This study used a 15° C block to arrest protein exit from previously characterized vesicular-tubular clusters that accumulate in what is known as the ERGIC (Kuismanen and Saraste, 1989). After warming cells to 32° C and making two-color movies, signal sequence-dsRED and GFP-ERGIC-53 colocalized in 30% of transport vesicles (Ben-Tekaya et al., 2005). In addition, vesicles labeled by ERGIC-53 did not move vectorially from ER to Golgi, like those labeled by VSV-G-GFP did. These data introduce the possibility that multiple vesicle populations are produced during ER-to-Golgi transport. The vesicles observed in this study were pleiomorphic, again indicating that small COPII vesicles were not transporting cargo. Further studies

using such two-color imaging techniques will help to better understand the nature of sorting between the ER and Golgi.

### 1-3.1c The ER in Hippocampal Neurons

In hippocampal neurons, the rough ER and ERES are restricted to the soma and dendrites, while smooth ER is present throughout the cytosol in both axonal and somatodendritic regions (Aridor et al., 2004; Bartlett and Banker, 1984a; Bartlett and Banker, 1984b; Horton and Ehlers, 2003a; Krijnse-Locker et al., 1995). Recent studies have confirmed that the markers that label ERES in yeast and mammalian fibroblasts also label ERES in dendrites. A particularly intriguing study was performed by Horton and Ehlers (2003) in cultured hippocampal neurons. By live cell imaging of tsO45VSV-G-GFP after accumulation in the ER, they showed that vesicles originating at ERES moved bidirectionally in dendrites. This contrasts with studies of tsO45VSV-G-GFP in fibroblasts, in which vesicles moved inwards towards a perinuclear Golgi complex (Hirschberg et al., 1998; Presley et al., 1997a). Horton and Ehlers also showed that Golgi markers were not exclusively restricted to the perinuclear region; instead, they found "Golgi outposts" (stained with two different Golgi-specific enzymes) far out into dendrites, which would provide both anterogradely- and retrogradely-moving ER-derived carriers with a Golgi-like destination. This brings up the possibility that there could be multiple destinations for proteins as they exit the ER in neurons—targeting different proteins either directly to subdomains in the dendrites (such as postsynaptic sites), or through a perinuclear Golgi, as in other mammalian cell types. I have not observed such

Golgi outposts in hippocampal cultures in the Banker lab, even using the exact same marker as Horton and Ehlers; therefore, I remain skeptical that these outposts exist. Nevertheless, a few recent studies indicate that multiple vesicle types may be produced at the ER, or at least that the vesicle formation machinery in the ER may have multiple mechanisms for interpreting peptide signals in cargo proteins (Muniz et al., 2001; Soza et al., 2004).

### 1-3.2 Biosynthetic Pathway: The Golgi Complex

From the ER, proteins move to the Golgi apparatus. Most models of protein sorting focus on the Golgi as the central "post office" where cargo is sorted and packaged into vesicles to be delivered to different cellular destinations (Gu et al., 2001; Rodriguez-Boulan and Musch, 2005). Although little is known about the sorting capabilities of the Golgi apparatus in neurons, this organelle is known to be extremely important for polarized sorting in other cell types. Since polarized sorting is the subject of this dissertation, emphasis will be given to review of the literature pertaining to the role of the Golgi in polarized protein targeting, although general exit pathways from the Golgi will also be discussed.

#### 1-3.2a Golgi Structure and Function

The Golgi is a collection of about seven stacked membranous saccules, or cisternae, located in the perinuclear region of most cells. Newly synthesized transmembrane and secreted proteins undergo a series of post-translational modifications

in the Golgi complex. For example, after initiation of glycosylation in the ER, additional steps are carried out by a series of sequentially acting glycosylation enzymes that reside in the Golgi, with earlier acting enzymes localized to the *cis* cisternae, and later acting enzymes to the medial and *trans* cisternae. Once glycosylation is complete, proteins exit the Golgi at the *trans* side and are transported in vesicles to endosomes, lysosomes, the plasma membrane, or back to the ER (Puthenveedu and Linstedt, 2005). Early structural studies of the Golgi indicated that both the *cis* and *trans* cisternae consisted of many convoluted tubules, which are thought to be involved in protein entry to and exit from the Golgi apparatus. Originally it was thought that only the last *trans* cisterna was specialized for packaging and export (Griffiths, Pfeiffer et al. 1985), but recent studies

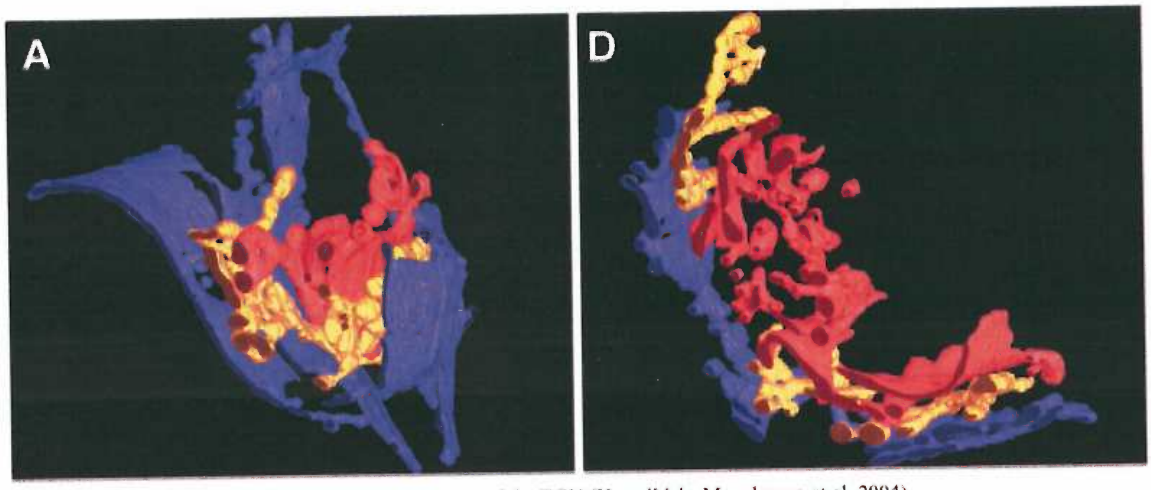


Figure 2. 3-D reconstruction of the last three cisternae of the TGN (Howell lab- Mogelsvang et al. 2004)

using cryofixation and High Voltage EM have indicated that the last three cisternae on the *trans* side are all involved in vesicle formation leading to protein export (Griffiths et al., 1985; Ladinsky et al., 1994; Ladinsky et al., 1999). In addition, it was determined that the each of last three *trans* cisternae of the Golgi give rise to different budding profiles. The most *trans* cisterna produced solely clathrin buds, the next two produced

non-clathrin buds that could not be distinguished from one another but may still represent two different coat types. This would indicate that separate cisternae could be specialized for different exit pathways that deliver cargo to different destinations such as the plasma membrane, an endosome, or back to the ER, and cargo destined for exit by one of these pathways might arrive at the *trans*-Golgi already pre-sorted.

Vesicle budding profiles at the *trans* Golgi were initially observed in electron micrographs. Coated buds about 60-130nm in diameter were observed emanating from tubular extensions of the Golgi. It was thought that these buds gave rise to round vesicles that pinched off and either diffused through the cytoplasm or were transported along cytoskeletal elements (Rothman and Wieland, 1996). As has been the case for ER-to-Golgi vesicles, the dynamics and morphology of vesicles formed at the *trans* Golgi have been best revealed by live-cell imaging of GFP chimerae. Multiple studies observing various vesicle-associated GFP chimerae at the Golgi have lead to a consensus about the general characteristics of vesicles in the constitutive and lysosomal pathways (Hirschberg et al., 1998; Polishchuk et al., 2003; Puertollano et al., 2003; Waguri et al., 2003). It has become clear that small 60-130nm buds, though they are present, do not correspond to the carriers that mediate cargo export from the Golgi. Instead, various forms and sizes of vesicles and tubules are observed. Some studies show that these vesicles can contain multiple tubular extensions and even small fenestrae characteristic of the morphology of *trans* Golgi stacks (Polishchuk et al., 2003; Polishchuk et al., 2000). In addition to observations of their pleiomorphic morphology, the formation of Golgi-derived vesicles over a period of seconds has been observed in live cells. In most studies, tubular

extensions appear to be pulled off of the Golgi by force; the final vesicle fission event seems to be caused by this pulling. Often at the moment a vesicle breaks off from the Golgi, a residual piece of membrane is seen to recoil and collapse back into the Golgi. These events occur along microtubules, and rely on a microtubule-based motor, kinesin, to generate force (Polishchuk et al., 2003).

### 1-3.2b Pathways for Exit From the *trans* Golgi

After their synthesis in the ER, several classes of proteins continue along a common route through the Golgi complex. These include lysosomal enzymes, constitutively secreted soluble molecules, resident transmembrane proteins and regulated secretory proteins (Farquhar, 1985; Griffiths and Simons, 1986; Keller and Simons, 1997). Immunocytochemistry studies have found that these proteins are all in the same Golgi stacks (Bergmann et al., 1981), and all contain carbohydrate or lipid modifications characteristic of those catalyzed by resident Golgi enzymes (Kornfeld and Kornfeld, 1985). Somewhere between the last Golgi cisterna and their final destination, these proteins must be sorted for delivery to the correct domain. Several classic studies using electron microscopy and biochemistry have provided indirect evidence to support the existence of at least four different types of vesicles emerging from the *trans*-Golgi network: vesicles targeted to lysosomes, regulated secretory vesicles, and two types of constitutive secretory vesicles, basolateral and apical. Regulated secretory proteins are concentrated up to 200x when they are packaged into secretory granules (Salpeter and Farquhar, 1981), and they fuse with the plasma membrane in response to an intracellular

$Ca^{2+}$ increase (Martin, 1997). In contrast, constitutively exocytosed proteins are not concentrated dramatically nor do they undergo signal-mediated exocytosis. These two types of proteins have been shown to use different pathways from the Golgi to the cell surface (Gumbiner and Kelly, 1982; Moore and Kelly, 1985) and are thus assumed to be sorted into different carrier vesicles at the *trans*-Golgi network. Analysis of constitutive secretory vesicles destined for different plasma membrane domains of polarized epithelial cells has revealed differential sorting of apical and basolateral membrane proteins (Simons and Fuller, 1985). Studies of immunoelectron micrographs showed that a constitutively secreted protein (Albumin or Transferrin) is packaged into the same vesicle as a resident transmembrane protein (VSV-G) (Strous et al., 1983). In 1967, Friend and Farquhar demonstrated that lysosomal hydrolases bud from the Golgi in coated vesicles (Friend and Farquar, 1967). These coats appeared to be absent from both constitutive and regulated secretory vesicles (Burgess and Kelly, 1987; Griffiths and Simons, 1986).

### 1-3.2c Polarized Protein Sorting at the *trans*-Golgi Network

In the constitutive secretory pathway, it is thought that the first step in localizing different proteins to separate plasma membrane domains is to sort them into separate vesicle populations for export from the Golgi. Several early studies (briefly referred to above) of apical and basolateral targeting in epithelia have led to this dominant paradigm. While these studies do not directly address the sorting of axonal and dendritic proteins in neurons, they do lay the foundation for the experiments in Chapter 2, and will therefore be discussed in detail here.

In epithelial cells, the basolateral and apical domains, which are separated by tight junctions, are known to contain a different constellation of membrane proteins (Simons and Fuller, 1985). This cell type, often in the form of the polarized epithelial cell line MDCK (Madin-Darby Canine Kidney), has been widely used to study the generation of membrane protein polarity. Excellent early work was performed by exploiting properties of enveloped RNA viruses. Rodriguez-Boulan and Sabatini (1978) observed that in MDCK cells, vesicular stomatitis virus (VSV) buds only from the basolateral domain, while influenza virus buds only from the apical domain (Rodriguez-Boulan and Sabatini, 1978). This provided a good model system with which to study the polarized transport of proteins. The fact that exit from the Golgi is blocked at 20° C (Matlin and Simons, 1983) was used to study the trafficking of VSV-G by synchronizing its exit from the Golgi. When the block was released, VSV-G was transported directly from the Golgi to the basolateral cell surface without stopping at endosomes (labeled with HRP uptake) or the apical cell surface (Griffiths et al., 1985). This confirmed that the *trans*-Golgi, rather than the endosome or the cell surface, was the site of polarized sorting. When MDCK cells were infected with either influenza or VSV and then subjected to vesicle immunoisolation and sucrose gradient separation, it was found that two viral proteins (VSV-G from VSV, and HA from influenza) were transported in vesicles that had slightly different densities. By 2-D gel electropheresis, the two vesicle fractions (VSV-G-containing and HA-containing) were found to contain some of the same proteins, but also some different proteins (Wandinger-Ness et al., 1990). This sorting was present even in non-polarized cells in which HA and VSV-G are not restricted to different cell

surface domains (Musch et al., 1996; Yoshimori et al., 1996). These studies use indirect evidence to show that apical and basolateral proteins are sorted into different vesicles at the Golgi.

Biochemical methods such as immunoprecipitation and gradient centrifugation have proven to be technically difficult when used to purify different transport vesicle populations from the same cell. For this reason, many biochemistry labs are turning to microscopy of GFP chimerae to visualize sorting in live cells, allowing vesicles to be observed in a relatively natural environment: a transfected cell. By visualizing exocytosis of vesicles containing GFP-tagged proteins at the plasma membrane, Kreitzer et al. (2003) showed that the apical marker p75 and the basolateral marker Low density lipoprotein receptor (LDLR) fuse at different sites on the cell surface of polarized MDCK cells, implying that they must reside in different post-Golgi vesicles (Kreitzer et al., 2003).

Coexpressing pairs of proteins tagged with different color variants of GFP, although technically more demanding than single-color imaging, offers a direct method to determine whether two proteins are present in the same vesicle population. This approach has not yet been applied to cube-shaped polarized epithelia because the vesicles move too rapidly to track them in three dimensions, but it has been used to compare the trafficking of apical and basolateral markers in flatter, unpolarized cells. A recent study used two-color live cell imaging of the GFP color variants CFP and YFP to directly examine the vesicle populations that carry polarized proteins (Keller, 2001). This study examined Ptk2 cells coexpressing an apical marker, a CFP-tagged

glycosylphosphatidylinositol motif (GPI-CFP), and a basolateral marker, VSV-G-YFP, in cells subjected to a 20° C block. Upon warming cells to 32° C, live-cell imaging of vesicle transport in two colors showed that the apical and basolateral markers labeled different populations of vesicles. This study has been contradicted by another group that used identical markers, but different cell types, to perform the same two-color CFP/YFP imaging of Golgi-derived vesicles (Polishchuk et al., 2004). Polishchuk et al. found the two markers in the same vesicle population in HEK, CHO and unpolarized MDCK cells. The authors interpreted these results (in combination with additional results from the same study) as evidence that apical and basolateral markers were first transported in the same vesicle population to the basolateral domain, then the apical protein was subsequently endocytosed from the basolateral side and redirected to the apical domain by transcytosis. It is not entirely clear why these two studies found such different results. There is good evidence that sorting of apical and basolateral proteins into separate vesicles is preserved even in unpolarized cells (Musch et al., 1996; Rustom et al., 2002; Wandinger-Ness et al., 1990; Yoshimori et al., 1996). Nevertheless, the use of different cell types by the two groups is one possible cause of the discrepancy. Because some proteins are known to be sorted differently in different cell types, or even at different developmental stages of the same cell type (Bastaki et al., 2002; Wollner et al., 1992), it is obviously important to perform such experiments in the cell type of interest.

Such two-color studies enable comparison of many different markers in a pairwise fashion, which allows the model to be tested, expanded and refined for multiple polarized proteins. So far, technical constraints have prevented the direct visualization of

Golgi-derived vesicles containing apical and basolateral proteins in polarized cells. Polarized neurons provide a distinct advantage over MDCK cells: they lie flat when cultured on glass coverslips, so following vesicles in axons and dendrites, which are no more than 2-3 um thick, is possible. In Chapter 2, such two-color experiments were performed in cultured neurons. While these experiments proved to be technically demanding, especially in the early phases of study, continuing improvements in the quality of both the detection of fluorophores and the fluorophores themselves are slowly transforming such experiments into relatively routine procedures. These experiments are just the beginning of a series of comparisons between various neuronal markers that will almost certainly lead to a dramatic increase in our understanding of polarized trafficking pathways in neurons and the genesis and maintenance of axonal and somatodendritic surface domains.

### 1-3.3 Endosomes: Endocytosis, Recycling, Protein Sorting

After membrane proteins are folded, exported from the Golgi, and delivered to their destination, it is almost certain that they are not finished being shuttled around the cell. For example, after arrival at the plasma membrane, many receptors are endocytosed and then either recycled to the surface or targeted for degradation. Likewise, membrane proteins initially targeted to the endosome/lysosome system are often subsequently retrieved to the Golgi complex. Some polarized proteins are targeted to one surface domain immediately after exit from the Golgi, only to be endocytosed and directed to a different surface domain via the endosomal system (transcytosis). The vesicle trafficking

pathways of the endosomal/recycling system are varied, and the literature can be difficult to follow, since many endosome varieties are referred to by multiple names, and since characterization of the endosomal system has uncovered different types of endosomes that are not necessarily present in all cell types.

Because the term "endosome" can include many different organelles and trafficking pathways in different cell types, I will describe the main endosomal types in polarized and unpolarized cells in general terms, as well as the main pathways that lead from place to place. After establishing this general context, I will focus on some details of endocytosis and recycling that pertain to polarized sorting in neurons.

### 1-3.3a Endosomal Compartments in Unpolarized Cells and Polarized Epithelia

In unpolarized cells such as fibroblasts, surface proteins are endocytosed into the early endosome. Many proteins are endocytosed in a clathrin-dependent fashion; the classic molecular mechanism dictates that cytoplasmic endocytosis signals in transmembrane proteins interact with the adaptor complex AP-2, which interacts with clathrin to stimulate vesicle formation (Pearse and Robinson, 1990). Although this is the textbook mechanism for endocytosis, it is becoming clear that AP-2 is not always involved, and different sub-types of clathrin-mediated endocytosis likely operate in

Figure 3. An Early Endosome; white spots are gold-labeled LDL internalised for 5 minutes (from J. Heuser, *in* Greunberg 2001)

endocytosis of different cargo proteins (Perret et al., 2005). In addition, although clathrin-mediated endocytosis appears to be the predominant mode of entry, other types of endocytosis have also been proposed, such as caveolae-mediated endocytosis, though they are not as well characterized (Hommelgaard et al., 2005; Perret et al., 2005).

It is thought that the early endosome contains proteins endocytosed by many routes (Bishop, 2003). Structurally, early endosomes contain vesicular and tubular elements that form subdomains. These domains are likely to be important for separating cargo into different vesicles for exit from the early endosome (Gruenberg, 2001). After leaving the early endosome, cargo can continue on three main routes: to the Golgi, to the late endosome and then lysosome, or to the plasma membrane via recycling. The latter recycling pathway can proceed either directly from the early endosome or after passing through a second sorting endosome located near the nucleus (Sheff et al., 2002).

In polarized epithelial cells, apical and basolateral proteins are first internalized into separate apical and basolateral early endosomes (AEE and BEE). Polarized epithelia have a common endosome (CE), also called the sub-apical compartment (SAC). They also have a second associated endosome, the apical recycling

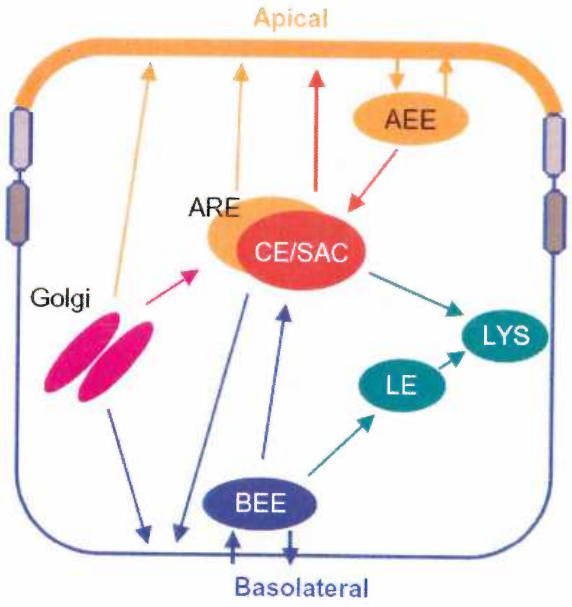


Figure 4. Endsomes and Trafficking Pathways in Epithelia (Heokstra et al. 2004)

endosome (ARE), that may be partly continuous with the CE/SAC (Hoekstra et al., 2004). The endosomal system of polarized epithelia is interconnected by multiple pathways, and different polarized proteins may not all follow the same itinerary. One excellent study follows the trafficking pathways of three different basolateral markers in order to compare the dynamics of three endocytic pathways in polarized epithelia: recycling, transcytosis, and lysosomal delivery (Brown et al., 2000). In this study, fluorescently labeled ligands for three basolateral transmembrane receptors were imaged over time, and colocalization between them was analyzed at various times after endocytosis. After two minutes, all three ligands were endocytosed into the same compartment (the early endosome). By ten minutes, Transferrin (a basolateral recycling protein) and IgA (a marker of the basolateral-to-apical transcytosis pathway) became segregated from the lysosome-bound ligand LDL, appearing to occupy separate subdomains of the same membranous structure, which is localized to the apical part of the cytoplasm. After fifteen minutes, IgA and Transferrin began to be segregated from one another. IgA moved to an even more apical, rab11-positive compartment (probably the apical recycling endosome), while Tf remained in the same recycling endosome (probably the common endosome/sub-apical compartment). Studies such as this one are valuable for comparing traffic routes taken by different endocytosed proteins.

A combination of morphology and endosome-specific protein markers has been used to classify the various endosomal subtypes. For example, just as the ER can be recognized by its reticular morphology and the Golgi by its ribbon-like structure, late endosomes can be recognized by the presence of free internal vesicles (Murk et al.,

2003). The apical recycling endosome can be distinguished from the common endosome or early endosomes by its apical localization, and also by the presence of small vesicles between 100-200 nm in diameter (Futter et al., 1998; Rahner et al., 2000). Other endosome types are more difficult to identify based on structure alone since multiple endosome types contain vesicular and tubular subdomains of similar morphology (Gruenberg, 2001). Early and recycling endosomes are both tubular, though they can be clearly distinguished from one another by examination of associated proteins: subdomains of the small GTPases rab4 and rab5 are found on early endosomes, while recycling endosomes are labeled by rab4 and rab11 (Sönnichsen et al., 2000). Although our understanding of the functions of these different compartments is not complete, the identification of molecules that follow different pathways within the endosomal system, and of molecules that regulate this trafficking, is providing a more complete picture of the role of endosomes in protein sorting.

1-3.3b Endosomes in Neurons

Little is known about the endocytic sorting machinery in neurons, although the localization and function of several endosomal markers has been studied, and there are some similarities to endosomes in epithelial cells. Proteins such as rabs, which mediate vesicle docking, and SNAREs, which mediate vesicle fusion, are thought to contribute to the organization of specific trafficking steps in the endocytic pathway in neurons, as they do in other cells. Among the endosomal markers studied in neurons are rab5 and EEA1, two early endosome proteins that contribute to homotypic fusion, rab11, which is present

on recycling endosomes or the apical recycling endosome, and Syntaxin13, a t-SNARE necessary for proper recycling (Prekeris et al., 1998). It is not clear which of these participate in polarized recycling to the dendrites or the axon, though well characterized endosomal proteins, such as rab5 and Transferrin, have similar functions in neurons when compared to their function in epithelial cells (Kanaani et al., 2004; Prekeris et al., 1999). Some markers such as rab5 and Syntaxin13 are present in both axons and dendrites, while others, such as EEA1 and rab11 are restricted to dendrites (Kanaani et al., 2004; Prekeris et al., 1999; Steiner et al., 2002; Wilson et al., 2000). In addition, neuron-specific endosomal markers are also being identified, such as the Syntaxin13 interacting protein Neuron-Enriched Early Endosomal Protein of 21 kd, NEEP21 (Steiner et al., 2002). Such proteins may be important for regulating multiple aspects of neuronal function. For example, the quantity of AMPA receptors at postsynaptic sites is regulated by endocytosis into a Transferrin-positive compartment; LTP-inducing stimuli increase trafficking of AMPA receptors from recycling endosomes to the cell surface (Lee et al., 2001; Park et al., 2004). Both NEEP21 and rab11 have been shown to regulate both AMPA receptor recycling and Transferrin recycling (Park et al., 2004; Steiner et al., 2002).

While the initial delivery of newly synthesized synaptic vesicle proteins to the axon is thought to be mediated by tubules and vesicles of the biosynthetic pathway (Tsukita and Ishikawa, 1980), early endosomes near presynaptic terminals in the axon are involved in synaptic vesicle recycling. These endosomes are rab5-positive; rab5 is thought to mediate recycling at the synapse (de Hoop et al., 1994; Hannah et al., 1999;

Rizzoli and Betz, 2005). This is only one proposed recycling route for synaptic vesicles— synaptic vesicles are also thought to cycle by a fast pathway that does not involve endosomes (Rizzoli and Betz, 2005).

Axonal and dendritic endosomal pathways are thought to function somewhat independently, though they may intersect in a common degradation pathway (Parton et al., 1992), and other as yet unidentified points of intersection may also exist. Understanding the organization of endosomal traffic in neurons will depend on the further identification of molecular regulators of endosomal traffic and examination of the recycling pathways of ligands and receptors. In Chapter 2, the endosomal pathways followed by the Transferrin receptor and the LDL receptor are examined. Their endosomal trafficking bears some similarity to that observed in other cell types.

### 1-3.3c Polarized Sorting Through Endosomes En Route to the Cell Surface

While the prevailing hypothesis of protein sorting revolves around protein segregation into distinct transport vesicles at the *trans*-Golgi network, there is growing evidence that at least some transmembrane proteins travel to endosomes *before* they reach their proper location on the cell surface. This presents the possibility that sorting in the biosynthetic pathway could occur at an endosome rather than at the Golgi. Alternatively, passing through the endosome could represent a secondary sorting step that would serve to increase the fidelity of Golgi sorting.

Orzech et al. (2000) used a novel assay to show that both the poly immunoglobulin receptor (pIgR) and TfR traverse endosomes on their way to the cell surface. Two very recent studies use GFP-based imaging to show that two basolaterally targeted proteins, VSV-G and E-Cadherin, also pass through endosomes on their way to the cell surface. In the case of E-Cadherin, two-color live cell imaging showed that Golgi-derived carriers containing GFP-tagged E-Cadherin seem to fuse with endosomes labeled by rab11-RFP before arriving at the plasma membrane (Lock and Stow, 2005). Similarly, after releasing ts045VSVG-GFP from a 20° C block, Golgi-derived carriers were observed transiently colocalizing with Transferrin in a perinuclear recycling endosome (Ang et al., 2004). In addition, these three studies examined sorting mutant versions of each marker to ask if a missorted version also travels through endosomes. The apically missorted version of each marker tested (pIgR, VSV-G and E-cadherin) was also found in endosomes shortly after exit from the Golgi, indicating that both basolateral and apical proteins may traffic from the Golgi to the endosome before moving on to the plasma membrane. These studies and others (such as (Futter et al., 1995)) are giving more stock to the possibility that alternate, non-Golgi-based sorting mechanisms also function in the biosynthetic pathway.

### 1-3.3d Polarized Sorting After Initial Arrival at the Cell Surface

While endosomes may contribute to the initial biosynthetic sorting of some polarized proteins, they are more widely recognized as a sorting station for proteins internalized from the cell surface. There are two general types of polarized sorting that

occur after internalization. One, transcytosis, involves internalization from one surface domain, followed by delivery to a different surface domain. For example, transcytosis is the main pathway for delivery of membrane proteins to the apical domain in polarized hepatocytes. First, newly synthesized proteins are targeted to the basolateral domain, followed by internalization and targeting to the apical domain (Bastaki et al., 2002). The second type of sorting downstream of plasma membrane delivery recycles proteins to the same surface domain following internalization. Many basolateral receptors are resorted back to the basolateral domain after being endocytosed into the endosomal system. Evidence for specific machinery responsible for polarized recycling has been discovered in epithelial cells, and some recycling proteins have separate sorting signals for the biosynthetic and recycling pathways (Gan et al., 2002; Odorizzi and Trowbridge, 1997).

There is an ongoing debate about what role, if any, transcytosis plays in the final localization of polarized membrane proteins. The experiments in Chapter 2 are part of this debate. While transcytosis seems to be very important for separating basolateral and apical proteins in hepatocyes, this cell type is usually considered to be an exception to the rule (although transcytosis is an essential part of the function of some proteins (Hunziker and Kraehenbuhl, 1998). In non-hepatocyte epithelial cell lines and in unpolarized cells, apical and basolateral proteins are thought to be segregated into separate vesicles at the Golgi and delivered to separate domains (Keller et al., 2001; Kreitzer et al., 2003; Musch et al., 1996; Rustom et al., 2002; Wandinger-Ness et al., 1990; Yoshimori et al., 1996). In neurons, differences between the behavior of vesicles labeled by dendritic or axonal

proteins have been demonstrated (Burack et al., 2000; Kaether et al., 2000), so the epithelial model has been favored for sorting of axonal and dendritic proteins as well.

Recently, however, additional studies have given attention to the transcytosis model. The contribution of transcytosis to polarized sorting of axonal and apical proteins is currently being studied in both MDCK epithelial cells and in neurons (Anderson et al., 2005; Polishchuk et al., 2004; Wisco et al., 2003). Earlier studies provided evidence in support of sorting at the Golgi; these results were confirmed by Keller et al. 2001 and Rustom et al. 2002, who presented the first direct evidence that apical and basolateral markers are sorted into separate carriers at the Golgi. However, shortly after the publication of these studies, another study used similar methods but arrived at a different conclusion (Polishchuk et al., 2004). This study shows, also very clearly, that the apical and basolateral markers examined in Keller et al 2001 exit the Golgi in *the same* population of carriers. This study goes on to show that, in polarized MDCK cells, the apical marker GPI-GFP appears first on the basolateral surface after leaving the Golgi, even though the steady-state localization of this marker is predominantly apical. The appearance of GPI-GFP on the apical surface can be blocked by addition of a mild fixative, tannic acid, to the basolateral domain, indicating that basolateral-to-apical transcytosis of the GPI marker occurs after it is delivered to the basolateral domain, presumably in the same vesicle as VSV-G. The contradictory results of these two studies remain unresolved.

Another study, in hippocampal neurons, also favors the existence of a transcytotic pathway for axonal (rather than apical) protein localization (Wisco et al., 2003).

Compared to Polischuk et al. 2004, this study is far less definitive, but it does provide a testable hypothesis. This study showed that some proportion of the axonal marker Neuron-glia Cell Adhesion Molecule (NgCAM) could be detected on the dendritic surface after disrupting protein trafficking with brefeldin A (BFA), then allowing trafficking to proceed through the biosynthetic pathway. Under equilibrium conditions, however, NgCAM was polarized to the axon, in agreement with previous studies (Jareb and Banker, 1998; Sampo et al., 2003). In addition, some degree of colocalization between NgCAM and Transferrin, a well-known marker of the endosomal/recycling system in many cell types, was observed near the cell body. The authors conclude that two pathways from the Golgi to the axon coexist. In one pathway, NgCAM is transported from the Golgi to the dendritic surface, then endocytosed into a Transferrin-positive endosome and subsequently delivered to the axon. In the second pathway, NgCAM exits the Golgi in vesicles that do not fuse with the dendritic plasma membrane, but instead find their way into the axon and fuse with the axonal plasma membrane.

This study is intriguing, but some technical issues should be mentioned, especially since their results are not consistent with our observations (Chapter 2, and (Sampo et al., 2003). First, BFA, a fungal metabolite, blocks many vesicular trafficking steps by inhibiting the Arf1 family GTPases. BFA treatment causes endosomes to tubulate and causes the Golgi to collapse into the ER in a reversible fashion, causing a block in forward traffic through the biosynthetic pathway and in the endosomal/recycling system (Chardin and McCormick, 1999). Some studies also show that BFA treatment disrupts protein polarity, a side effect that would severely complicate interpretation of the

results with NgCAM (Low et al., 1992; Shitara et al., 1998). To address the possible problems associated with BFA, Wisco et al. also used a 20 °C block for 48 hours to arrest biosynthetic traffic in the Golgi. This method is also somewhat suspect, since the 20 °C block is known to slow exit from the Golgi but not completely block it (Kuismanen and Saraste, 1989), and it can also arrest recycling through the endosomal pathway (Gibson et al., 1998). It is preferable to use a shorter duration for a 20 °C block; 1-2 hours is more accepted in the field (Hirschberg et al., 1998; Keller, 2001; Polishchuk et al., 2003; Puertollano et al., 2003; Rustom et al., 2002).

The contribution of transcytosis to polarized sorting of axonal and apical proteins is thus a current topic of study in both MDCK epithelial cells and in neurons (Polishchuk et al., 2004; Wisco et al., 2003). In Chapter 2, experiments that address this question are presented, with protocols that allow direct observation of vesicles labeled by either dendritic (LDL receptor, Transferrin or Transferrin receptor) or axonal (NgCAM) markers in two colors. My results favor the classical model, supporting a mechanism in which axonal and dendritic proteins are sorted into different carriers at the Golgi and don't appear to share an endosome during their trafficking.

## 1-4 Sorting Signals

To transport a protein to a specific destination, there must be some sorting information present within the protein sequence itself that acts as a signal. The first sorting signal was identified in lysosomal hydrolases. These enzymes require a phosphorylated mannose residue (M-6-$PO_4$) to be sorted correctly to the lysosome. A

receptor in the TGN (the M-6-$PO_4$ receptor) binds enzymes with the proper phosphorylated residue and mediates their incorporation into clathrin-coated vesicles (Farquhar and Palade, 1998). The receptor with its bound cargo recruits an adaptor protein complex (AP-1 in this case). The adaptor complex facilitates the formation of a clathrin coat; assembly of this coat is thought to drive distention of the membrane to form a budding vesicle. The contents of this vesicle, through a series of additional steps, are eventually delivered to the lysosome (Kirchhausen, 1999). A similar mechanism is also responsible for receptor-mediated endocytosis at the cell surface. In this case, AP-2 binds both clathrin and peptide internalization signals in the cytoplasmic tails of plasma membrane proteins (Kirchhausen, 1999). These endocytosis motifs are of two general types: tyrosine-based (NPXY or YXXΦ, a tyrosine and a hydrophobic residue separated by two polar residues) or di-hydrophobic, usually di-leucine-based (Bonifacino and Traub, 2003).

These two examples illustrate the general model for the mechanism by which sorting signals are thought to govern protein localization. Many other proteins also contain cytoplasmic peptide motifs that have been found to be necessary for proper localization. When these peptide signals are mutated or deleted, the protein's localization is disrupted. In addition to targeting to the lysosome or to endocytic vesicles, polarized protein targeting also relies on such cytoplasmic motifs in many cases. In particular, most basolateral and dendritic proteins contain cytoplasmic motifs that, when mutated, result in mislocalization at the surface. Sorting signals, especially those involved in apical and axonal sorting, have also been localized to other protein regions, such as the

ectodomain and the transmembrane domain; even lipid anchors and glycosylation sites can serve as sorting signals. Less is understood about the mechanism by which these various motifs may act. Since all the experiments in this dissertation involve dendritic rather than axonal sorting signals, emphasis will be given to review of cytoplasmic sorting signals, although other types of sorting signals will also be briefly reviewed.

### 1-4.1 Basolateral Sorting Signals

The mechanism by which proteins are sorted into constitutive exocytic vesicles is still not completely understood; however, many basolateral proteins contain sorting signals that are similar to those that act in endocytosis and lysosomal targeting. For example, di-leucine-based motifs in FcRγII-B2 and CD44 that are responsible for their basolateral targeting are related to di-leucine motifs that direct endocytosis and lysosmal targeting (Bonifacino and Traub, 2003). When such basolateral sorting signals are mutated, the mutant proteins are mis-sorted to the apical domain or, in some cases, to both domains (Matter et al., 1992; Matter et al., 1994; Odorizzi and Trowbridge, 1997).

Other basolateral proteins contain cytoplasmic motifs that do not conform to canonical tyrosine or di-leucine motifs involved in endocytosis or lysosomal targeting. For example, the basolateral sorting signal for TfR is distinct from its NPXY internalization signal; mutating the tyrosine to alanine blocks endocytosis but has no affect on polarity (Odorizzi and Trowbridge, 1997). In VSV-G, perhaps the most studied basolateral protein, a tyrosine-based motif is important for polarity, but does not mediate endocytosis from the cell surface (Thomas et al., 1993).

The cytoplasmic tail of LDLR contains two tyrosine-based motifs (Matter et al., 1992; Matter et al., 1994), each of which appear to be sufficient for basolateral polarity. This marker was chosen as the main dendritic marker for studies in Chapter 2 because its sorting signal is very well characterized. The membrane-proximal tyrosine motif of LDLR overlaps with, but is distinct from, an NPXY endocytosis motif. The distal tyrosine motif contains a tyrosine, but does not conform to NPXY or YXXΦ. Both motifs depend on a downstream acidic cluster. More recently, a naturally occurring mutation in the glycine residue immediately upstream of the distal sorting signal has been shown to disrupt basolateral polarity of LDLR, leading to hypercholesterolemia (Koivisto et al., 2001).

Other basolateral motifs have been identified that are not dependant on tyrosine or di-hydrophobic residues. One example, studied in Chapter 4, is the Epidermal Growth Factor receptor (EGFR). EGFR contains a novel proline-based basolateral motif, although nearby di-hydrophibic motifs also contribute to its polarity (He et al., 2002; Kil et al., 1999); other motifs that direct endocytosis and lysosomal targeting are also present in the EGFR cytoplasmic domain (Kil et al., 1999; Warren et al., 1998).

### 1-4.2 Apical Sorting Signals

The sorting of apical proteins is not as well characterized as basolateral sorting. Apical sorting signals are most commonly found in the lumenal (extracellular) and transmembrane domains (Keller and Simons, 1998); however, cytoplasmic apical signals have been reported in several proteins (Cheng et al., 2002; Chuang and Sung, 1998;

Poyatos et al., 2000; Shayakul et al., 1997). Instead of adaptor-like proteins, glycolipids and cholesterol have been suggested as the primary mediators of apical sorting by inducing clustering in the plane of the Golgi membrane. These membrane microdomains, or "rafts," can be disrupted using drugs that either deplete cholesterol or inhibit its synthesis (Mays et al., 1995; Scheiffele et al., 1997). This disruption causes mis-sorting of many (but not all) apical proteins (Keller and Simons, 1997; Keller and Simons, 1998). Mis-sorting by cholesterol depletion may not always be related to association with rafts; in the case of the apical protein Neuraminidase, the amino acids necessary for raft association and those sufficient for apical targeting do not overlap (Barman and Nayak, 2000).

### 1-4.3 Sorting Signals in Neurons: A Parallel With Epithelial Cells?

It has been proposed that the molecular mechanisms used to sort axonal and dendritic proteins in neurons parallel those used to sort apical and basolateral proteins in MDCK epithelial cells. While this parallel holds true in some cases, it is not true in many other cases (Table 1). Even in cases where a protein does follow this parallel, there are often subtle differences between the residues involved in basolateral and dendritic sorting. For example, TfR depends on different, non-overlapping peptide sorting signals for basolateral and dendritic localization (Jareb and Banker, 1998; Odorizzi and Trowbridge, 1997). The LDLR sorting signal is also slightly different in neurons and epithelia. Mutating the tyrosine residues in LDLR disrupts its dendritic localization, but the naturally occurring glycine mutation (G34D) has no effect on dendritic polarity, while

it causes mistargeting in epithelia (Jareb and Banker 1998, our unpub. obs.). In Chapter 4, two proteins that use a di-leucine based sorting motif for targeting to the basolateral domain, FcRγII-B2 and CD44, are unpolarized when expressed in neurons (Hunziker and Fumey, 1994; Sheikh and Isacke, 1996; Silverman et al., 2005). Many proteins are apical in MDCK cells but uniform in hippocampal neurons, e.g., HA and many GPI-linked proteins (Hammerton et al., 1991; Jareb and Banker, 1998; Pietrini et al., 1992). Still other proteins are apical in MDCK cells but dendritic in neurons, such as EAAT3, the protein under investigation in Chapter 3 (Cheng et al., 2002). It has become clear that, although similar sorting machinery probably exists in the two cell types, a simplistic parallel is not a sufficient explanation.

Table 1. Comparison of Polarity: MDCK Epithelia vs. Neurons

| Protein | Polarity in Epithelia | Polarity in Neurons | Reference |
|---|---|---|---|
| **TfR** | B | D | (Odorizzi and Trowbridge, 1997; West et al., 1997) |
| **LDLR** | B | D | (Jareb and Banker, 1998; Matter et al., 1992) |
| **$GABA_A\alpha1$** | B | D | (Killisch et al., 1991; Perez-Velazquez and Angelides, 1993) |
| **FcRγII-B2** | B | U | (Hunziker and Fumey, 1994; Silverman et al., 2005) |
| **CD44** | B | U | (Sheikh and Isacke, 1996; Silverman et al., 2005) |
| **EGFR** | B | D | (Silverman et al., 2005) |
| **Glyt1b** | B | D | (Poyatos et al., 2000) |
| **TrKB** | B | U | (Kryl et al., 1999) |
| **NCAM180** | B | D | (Persohn and Schachner, 1990; Powell et al., 1991) |
| **LRP** | B | D | (Brown et al., 1997; Marzolo et al., 2003) |
| **pIgR** | B-transcytosed to A | D | (Casanova et al., 1991; Jareb and Banker, 1998; Reich et al., 1996) |
| **NgCAM** | B-transcytosed to A | A | (Anderson et al., 2005; Sampo et al., 2003) |
| **EAAT2** | U | U | (Cheng et al., 2002) |
| **Glyt1a** | U | D | (Poyatos et al., 2000) |
| **TrKC** | U | U | (Kryl et al., 1999) |
| **Influenza HA** | A | U | (Jareb and Banker, 1998; Rodriguez-Boulan and Sabatini, 1978) |
| **EAAT3** | A | D | (Cheng et al., 2002) |
| **GAT** | A | A | (Pietrini et al., 1994) |
| **CD8** | A | U | (Migliaccio et al., 1990; Sampo et al., 2003) |
| **$Na^+/K^+$ ATPase** | A | U | (Caplan et al., 1986; Pietrini et al., 1992) |

B=basolateral, A=apical (epithelia) or axonal (neurons), U=unpolarized

### 1-4.4 Studying Polarized Targeting in Neurons

The enveloped RNA viruses that were originally used to characterize basolateral and apical targeting in MDCK cells were also among the first types of proteins used to study polarized protein targeting in neurons. When Dotti and Simons (1990) infected hippocampal neurons with VSV or Fowl Plague Virus (avian influenza), they concluded that VSV-G was dendritic and the HA protein from influenza was more concentrated in the axon than the dendrites. To support their conclusions, images of cells immunostained for HA or VSV-G were presented. The staining in this study was difficult to interpret; many cells showed beaded processes characteristic of necrotic neurons, and the axon origin was not visible in any of the images. In addition, the authors did not try to quantify the degree to which either protein was enriched in the dendrites or axon.

Since this study, a protocol for quantifying fluorescence in axons and dendrites has been developed in the Banker lab. The measurement of the ratio of fluorescence in the axon to that in the dendrites can be used as a measure of polarity. In brief, a protein of interest is transfected into polarized cultured hippocampal neurons along with a soluble marker (such as CFP) that serves to outline the transfected cell's morphhology. This CFP fill is then used to identify regions of axon and dendrite that do not cross over one another, where it is appropriate to quantify fluorescence (this allows regions of the axons and dendrites to be chosen at random). The average brightness from the protein of interest (detected either by cell surface immunostain or by fluorescence of a YFP tag) is then quantified in these regions, giving a ratio of average fluorescence in the two regions.

The precursor to this method originated with Jareb and Banker (1998), a study in which total fluorescence on the axonal and dendritic surface was quantified. Subsequently, Sampo et al. (2003) used the average fluorescence on the axon and dendrites to quantify polarity of NgCAM. Adaptations of Sampo's method are used in Chapters 3 and 4 (Cheng et al., 2002; Silverman et al., 2005), and will be described in detail in those chapters; this method has also been used to study the polarity of expressed mGluR1α in our lab (Das and Banker, ms. in prep.). Other labs have also adopted similar methods as a non-biased tool for quantifying protein polarity in neurons (El-Husseini Ael et al., 2001; Garrido et al., 2001; Gu et al., 2003; Rivera et al., 2003; Rivera et al., 2005; Rosales et al., 2005). This method enables assessment of the polarity of various markers using quantitative methods that can be compared across labs as long as similar protocols are used for analysis. This method also provides a more rigorous way to identify dendritic or axonal localization signals by quantitatively comparing the polarity of wild type and mutant versions of the same protein.

Several neuronal localization signals have been characterized in this way. In most cases, only the equilibrium distribution of the protein of interest has been quantified. Therefore, events that determine sorting into the right vesicle in the biosynthetic pathway have not yet been distinguished from downstream factors that could also contribute to steady-state localization (such as stability in the plasma membrane). In order to address all the steps involved in determining protein localization, it is necessary to take timing into account, and assess localization on the surface soon after proteins leave the Golgi, as well as later on, once events such as transcytosis or selective retention at the surface

could have occurred. Assessment of polarity early after transfection was performed in Chapter 4 for EGFR, CD44 and FcRγII-B2. For these proteins, equilibrium localization was similar to initial localization, although not identical (see Chapter 5). Nearly all studies of axonal or dendritic localization signals to date identify motifs involved in equilibrium localization only. The motifs or protein regions associated with such steady-state axonal or dendritic localization are summarized in Tables 2 and 3. In some studies, only deletion or alanine substitution of the sorting signal was performed, indicating that the signal is necessary for proper targeting. In other studies, the signal was shown to be both necessary (by deletional/mutational analysis) and sufficient (by addition of the signal to an unpolarized reporter protein). The methods used for each protein are reported in the tables; most of these studies were performed in hippocampal neurons except where noted. Further studies assessing the initial localization of these markers compared to the equilibrium distribution will allow motifs involved in sorting into biosynthetic vesicles to be distinguished from motifs involved in plasma membrane fusion or retention.

### 1-4.5 Sorting to Dendrites

One aspect of the epithelial/neuronal parallel that has held up is that dendritic and basolateral proteins both contain peptide signals in their cytoplasmic domains that are necessary for dendritic polarity at the cell surface. For dendritic proteins, mutations that lead to loss of dendritic polarity always seem to change the localization of the mutant protein from polarized to unpolarized (Cheng et al., 2002; Lim et al., 2000; Mitsui et al.,

2005; Rosales et al., 2005; West et al., 1997). This equal distribution between domains is more rarely observed in epithelial cells, in which mutated basolateral proteins are often found at the apical surface only (Casanova et al., 1991; Deora et al., 2004; Matter et al., 1992; Matter et al., 1993; Sheikh and Isacke, 1996). While this generalization is quite reliable, it should be noted that polarity is usually not a black and white phenomenon. A protein is typically considered polarized if at least 80% of the total protein amount is restricted to one surface domain or the other. Mutations in a sorting signal can disrupt a protein's distribution only slightly (see EGR in Chapter 4), or can change a protein's localization completely (as above). Subtle differences in quantification techniques between labs can also contribute to gray areas when quantifying polarity and identifying sorting signals. These factors need to be considered when interpreting results from different studies.

While many different proteins are polarized to dendrites, the amino acids that mediate this localization have only been identified in a handful of proteins (shown in Table 2). Many dendritic sorting signals resemble tyrosine- and di-leucine-based signals that are thought to interact with soluble factors such as adaptor complexes. These include the motifs in TfR, LDLR, Delta-Notch-like EGF receptor (DNER), and Kv4.2. The dendritic targeting motifs in EGFR and pIgR have been studied extensively in epithelial cells (where they mediate basolateral targeting); their sorting signals resemble classic motifs in some ways. A few dendritic sorting signals do not resemble other known sorting signals, such as the motifs in EAAT3, Telencephalin and Kv2.1.

These three proteins are all localized to the dendritic domain, but within the dendrites they each have a unique distribution. Telencephalin is present throughout the dendritic membrane (Benson et al., 1998); most of the other dendritic proteins in Table 2 also have this broad dendritic localization. For Telencephalin, a point mutation in a phenylalanine residue causes the protein to be unpolarized. Wild type EAAT3 has a more specific localization within dendrites. It is present in synaptic-like clusters in dendritic spines when transfected into cultured hippocampal neurons (Chapter 3), and is known to be perisynaptic by immuno-EM localization in entorhinal cortex (He et al., 2001). Such clusters in dendritic spines are also observed for many neurotransmitter receptors, for example GABA, AMPA and NMDA receptors (Craig et al., 1994; Rao et al., 1998). For EAAT3, disrupting the dendritic sorting signal shown in Table 2 causes the protein to be unpolarized. The fraction of EAAT3 mutant still localized to dendrites remains clustered in dendritic spines, indicating that separate motifs control dendritic and peri-synaptic localization (Chapter 3); a similar observation has also been made for the dendritic sorting signals in Neuroligin and mGluR1α (Das and Banker, ms. in prep.; Rosales et al., 2005). The delayed rectifier potassium channel Kv2.1 is localized to large (1-2um) clusters in the proximal dendrites only (Antonucci et al., 2001). In Kv2.1, four different point mutations (three serines, one phenylalanine) each cause the loss of proximal dendritic clusters and an unpolarized distribution. For Kv2.1, it is possible that these motifs act at the vesicle formation step, although recent work has identified activity-induced phosphoregulation as a mediator of clustering (Misonou et al., 2004). It

is not clear which serine residues are involved in phosphorylation, nor if the loss of clustering is accompanied by a loss in dendritic polarity (Misonou et al., 2005).

Determining where these various motifs act (i.e. in vesicle formation at the Golgi, in retention at the plasma membrane, etc…) will lead to the development of a clear picture of all of the protein interactions that contribute to the final localization of a particular protein. By performing two-color live cell imaging studies of these markers, as has been done for LDLR in Chapter 2, the importance of these motifs in sorting into vesicles can be directly examined.

This type of experiment may be technically challenging for complex proteins; receptors and channels are usually multimers, and assembly of the various subunits can make live cell imaging studies difficult. One issue is that channel assembly is often coupled to folding and ER export (Heusser and Schwappach, 2005). Obtaining the correct subunit stoichiometry may involve transfecting cells with multiple subunits and hoping that they will all fold and assemble normally. In addition, prolonged subunit assembly can make it difficult to synchronize a population of proteins in any one trafficking step, which is necessary if different trafficking steps are to be analyzed independently. One other technical issue arises when residence in the ER is prolonged. For GFP-tagged constructs, an excess of fluorescence in the ER, which is present throughout the dendrites, can obscure the view of vesicle trafficking. These problems will no doubt make studying sorting signals somewhat difficult in such proteins.

Table 2. Dendritic Sorting Signals

| Dendritic Protein | Important Residues (in bold) | Method | Reference |
|---|---|---|---|
| **DNER** | -RPA**Y**EEFYNCR- | Alanine Substitution | Eiraku et al. 2002 |
| **EAAT3** | -KKSY**VNGGFA**VDKS- | Alanine Substitution/ Redirect Reporter | Cheng et al. 2002 (Ch. 3) |
| **EGFR** | -R**LL**QERE**LVEP**LT**P**SGEA- | Alanine Substitution | Silverman et al. 2005 (Ch. 4) |
| **LDLR** | -DNPV**Y**QKTTEDEVHIC HNQDG**Y**S**Y**PSRQMVSLEDD- | Alanine Substitution/ Deletion | Jareb and Banker 1998 |
| **Kv4.2** | -FETQHHH**LL**HCLEKTT- | Alanine Substitution/ Deletion/Redirect Reporter | Rivera et al. 2003 |
| **TfR** | -FGGE**PLSYTRFSLAR**QVD- | Deletion | West et al. 1997 |
| **Telencephalin*** | -AESPADGEV**F**AIQLTSS | Alanine Substitution/ Deletion/Redirect Reporter | Mitsui et al. 2005 |
| **pIgR** | -RHRRNVDRVSICSY- | Deletion | Jareb and Banker 1998 |
| **Kv2.1** | -MRSMS**S**ID**SF**I**S**CATD- | Deletion/Alanine Substitution/Redirect Reporter (60AA redirects Kv1.5, not others) | Lim et al. 2000 |
| **neuroligin** | **-VVLRTACPPDYTLAMRRS** PDDVPLMTPNTITM- | Deletion/Redirect Reporter | Rosales et al. 2005 |

* performed in transgenic mice, cerebellar Purkinje neurons

## 1-4.6 Sorting to Axons

Axonally polarized proteins are also thought to have sorting signals, but these signals have been found in the ectodomain, in the transmembrane anchor, or in cytoplasmic domains. When comparing axonal sorting signals, no obvious commonalities emerge (Table 3). In addition, many of the protein regions identified as important for axonal localization are also important other aspects of the protein's function. For example, in the axonal protein NgCAM, the extracellular fibronectin domains are important for axonal polarization, whereas the cytoplasmic domain is unecessary (Sampo et al., 2003). The extracellular domain is also critical for homotypic binding, so deleting the fibronectin domains could also disrupt retention in the plasma

membrane (Kadmon and Altevogt, 1997). In two shaker family potassium channels, Kv1.2 and Kv1.3, the tetramerization domain of the intracellular N-terminus has been found to be important for axonal localization (Gu et al., 2003; Rivera et al., 2005). Unfortunately, it is difficult to separate the importance of tetramerization from the mechanism behind polarized sorting, and the two studies of the shaker channels do not address these issues very well.

Other axonal protein localization signals point to a role for endocytosis from an inappropriate surface domain as a factor in their polarized distribution. At least two axonal proteins contain endocytosis signals that, when mutated, disrupt proper axonal localization: VAMP2 and the $Na^+$ channel subunit $Na_v1.2$. In the case of VAMP2, mutation of a cytoplasmic methionine residue known to be necessary for VAMP2 endocytosis is sufficient to disrupt its axonal localization (Sampo et al., 2003). The initial segment localization of the Na channel subunit $Na_v1.2$ has been studied in some detail in recent years (Fache et al., 2004; Garrido et al., 2001; Garrido et al., 2003a; Garrido et al., 2003b). Unfortunately, full-length $Na_v1.2$ does not reach the surface when exogenously expressed. Instead, these studies use a chimera of the single-transmembrane unpolarized protein CD4 and various subregions of the $Na_v1.2$ subunit to study protein regions involved in localization to the axon initial segment. They find three separate regions, two in a cytoplasmic transmembrane linker region and one in the cytoplasmic c-terminus, that play a role in the localization of $Na_v1.2$. They propose that a combination of retention and endocytosis are responsible for proper $Na^+$ channel localization.

Membrane-association motifs like palmitoylation sites have also been found to be important for axonal targeting. The palmitoylation of GAP-43 is critical to its preferentially axonal distribution, but disrupting palmitoylation also disrupts membrane association, so it is no surprise that the localization is altered. However, when the palmitoylation site in the dendritic protein PSD-95 is replaced with that of GAP-43, the chimera is redirected to the axon, implying that there is an axonal sorting determinant present in the GAP-43 sequence (El-Husseini Ael et al., 2001). A similar dependence on palmitoylation is found for the GABA synthesizing enzyme GAD-65. Its localization to axonal endosomes requires an intact palmitoylation site (Kanaani et al., 2004; Kanaani et al., 2002). In summary, axonal sorting motifs have been difficult to identify compared to dendritic motifs. Although common themes in axonal protein targeting have yet to emerge, the motifs identified to date point to stability in the plasma membrane as a determining factor for axonal steady-state localization.

Table 3. Axonal Sorting Signals

| Axonal Protein | Important Domain | Protein Region | Method | Reference |
|---|---|---|---|---|
| **Kv1.3** | T1 tetramerization | Intracellular N-terminus | Deletion/AlanineSubstitution/ Redirects Reporter | Rivera et al. 2005 |
| **$Na_v1.2$** | di-leucine (endocytosis)<br><br>2 regions of cytoplasmic transmembrane linker (endocytosis and retention) | C-terminus<br><br>Intracellular loop between tm12 and 13 | Deletion/AlanineSubstitution/ Redirects reporter (all in CD-4 chimera) | Garrido et al. 2001; Garrido et al. 2003; Fache et al. 2004 |
| **NgCAM** | Fibronectin domains 1-5 | Extracellular N-terminus | Deletion/Redirects Reporter | Sampo et al. 2003 |
| **VAMP** | M46 (endocytosis) | Cytoplasmic C-terminus | Alanine Substitution | Sampo et al. 2003 |
| **Kv1.2** | T1 tetramerization | Intracellular N-terminus | Deletion/Redirects reporter | Gu et al. 2003 |
| **GAP-43** (not a transmembrane protein- lipid anchor) | Palmitoylation | N-terminus (inner leaflet membrane anchor) | Substitution/Redirects Reporter | El-Husseini Al et al 2001 |

## 1-5 Mechanism of Sorting Signal Action

One purpose of the studies in this dissertation is to provide information that will ultimately allow the identification of the protein-protein or protein-lipid interactions responsible for governing cargo sequestration into different vesicle populations. The identification of cytosolic proteins that interact with sorting signals, and the study of the order and timing of these interactions, will be necessary to reach an understanding of the molecular events that occur when a protein is selected for incorporation into a forming vesicle. The identification of sorting signal interaction partners in neurons is a likely direction for future experiments following this dissertation. For this reason, the next section will spotlight the most likely candidates for mediating dendritic sorting, the adaptors. In addition, a couple of examples of known sorting mechanisms will be given. Even though these examples are not necessarily related to polarized sorting, they involve

accessory proteins whose actions may be similar to those involved in polarized vesicle formation.

### 1-5.1 Adaptors

The most thoroughly characterized proteins that act as sorting signal receptors are a group of protein complexes called adaptors. These are currently the best candidate proteins for interacting with dendritic sorting signals and mediating their incorporation into specific dendritic vesicles. There are four adaptor complexes: AP-1, AP-2, AP-3 and AP-4. Each is composed of four subunits, which are referred to as adaptins. Some of these subunits exist in tissue-specific isoforms. AP-2 is localized to the plasma membrane and is important in clathrin-mediated endocytosis, while the other adaptors are localized to the Golgi and endosomal system, where they mediate sorting along specific intracellular trafficking pathways (Boehm and Bonifacino, 2002). Another group of adaptor-like proteins has also been identified; they are called GGAs (Golgi-localized, Gamma-adaptin containing, ARF-binding). GGAs are thought to be involved in lysosomal sorting, bind di-leucine motifs, and work in concert with AP-1 and clathrin (Boman, 2001; Puertollano et al., 2003). A second example of a protein that works with AP-1 is PACS-1 (phosphofurin acidic cluster sorting protein-1), which mediates localization of several proteins to the TGN (Thomas, 2002). Of the adaptors that localize to the Golgi and endosomes, AP-4 and AP-1 have been shown to play roles in basolateral targeting, while AP-1 is also required for a type of dendritic sorting in *C. elegans*. These

two adaptor complexes may therefore play a role in dendritic targeting in mammalian neurons.

First, the AP-1 adaptor has two alternate μ subunits (the subunit that commonly binds tyrosine-based sorting signals). The μ1A subunit is expressed in all tissues, while μ1B is expressed only in epithelial cells. The epithelial-specific μ subunit binds to the cytoplasmic tail of LDLR and TfR in a surface plasmon resonance (SPR) binding assay, but this binding is lost when mutant versions of the tails are used. In addition, in an epithelial cell line that only expresses μ1A, LDLR is mistargeted to the apical domain, while TfR is unpolarized. This missorting can be rescued by transfecting cells with μ1B. Surprisingly, neurons do not express the isoform, so μ1B cannot contribute to TfR or LDLR polarity in neurons (Folsch et al., 1999). It is possible that μ1A is substituting for μ1B in neurons, even though in other mammalian cell types, μ1A is known to be involved in sorting from the Golgi to the endosome/lysosome system (Boehm and Bonifacino, 2002). In *C. elegans* neurons, which express only one μ1 isoform (unc101), mutation of unc101 disrupts the localization of odorant receptors that are usually localized to the tip of the dendrite (Dwyer et al., 2001). The μ1A subunit did not bind the LDLR tail in the SPR assay discussed above. Nevertheless, μ1A could be involved in binding to dendritic sorting signals other than LDLR. Possible low levels of expression of μ1B in mammalian neurons is unlikely, since *in situ* hybridization of postnatal day 3 rats clearly showed no μ1B reactivity in the nervous system (Folsch et al., 1999).

The μ4 subunit of AP-4 interacts with basolateral sorting signals (such as LDLR and TfR), but not with sorting signal mutants of these proteins. AP-4 is also necessary

for proper basolateral localization of some proteins; MDCK cells expressing antisense μ4 lose the ability to polarize LDLR and two other basolateral proteins (Simmen et al., 2002). Curiously, the basolateral polarity of TfR is only slightly affected in cells expressing antisense μ4, despite the fact that its sorting signal binds μ4 *in vitro*. The AP-4 adaptor is expressed at low levels in all tissues (Hirst et al., 1999), so this adaptor complex may be a likely candidate for involvement with dendritic sorting. A recent study confirmed that AP-4 is expressed in CNS neurons, and also showed that it binds to the δ2 Glutamate receptor, further implicating AP-4 in dendritic targeting (Yap et al., 2003).

AP-3 is involved in transport of cargo to lysosomes and lysosome-related organelles (Bonifacino and Traub, 2003). Mammalian AP-3 has two neuron-specific subunits, β3B and μ3B. In an *in vitro* budding assay, decreased budding of synaptic vesicles from PC12 membranes was observed in the presence of β3B-depleted cytosol (Blumstein et al., 2001). Mice that competely lack the AP-3 complex due to disruption of the δ subunit gene display increased seizures and hyperactivity, as well as inner ear degeneration; however, the nervous system is relatively normal (Kantheti et al., 1998). It was recently reported that the δ3 subunit is able to bind the cytoplasmic domain of VSV-G *in vitro*, and overexpression of the VSV-G-binding region of δ3 slows the rate at which VSV-G is transported to the plasma membrane in BHK cells (Nishimura et al., 2002). This indicates that AP-3 could be involved in transporting proteins to the cell surface. When VSV-G-GFP, which is basolateral in epithelial cells, is expressed in neurons, it is uniformly distributed in axons and dendrites (our unpub. obs). This, coupled with the

relatively mild neuronal phenotype of the AP-3 knockout, indicates that AP-3 is not a likely candidate for involvement in polarized sorting in neurons.

The existence of various dissimilar basolateral sorting signals raises questions about the rules of cargo-adaptor binding, as well as the number of different vesicles that can transport proteins along any one path. One possibility is that there are multiple binding sites on adaptors. If this were the case, many different proteins destined for the basolateral domain could bind different sites on the same sorting receptor and get recruited into a single vesicle, which would then be transported to the basolateral membrane. This would be more efficient than having each cargo molecule compete for a single binding site on an adaptor. Evidence in support of this notion has been found for the NPXY and YXXΦ endocytosis signals, which appear to bind different sites on the AP-2 adaptor subunit μ2 (Boll et al., 2002), as well as for the adaptor complex AP-1, whose μ subunit binds Y-based signals, while the β subunit binds di-leucine signals. Alternatively, multiple adaptors could sort basolateral cargo into more than one vesicle population bound for the basolateral membrane. Precedence for this theory is found in yeast, which have two pathways to the vacuole, each dependent on a different set of adaptors (Boehm and Bonifacino, 2002), and also in certain epithelial cell lines, which have two pathways to the basolateral membrane (Folsch et al., 1999; Le Maout et al., 2001).

While adaptor proteins are critical for polarized sorting in many cases, it is likely that additional adaptor-like molecules exist and function by interacting with sorting signals to play an important role in polarized sorting. Among these additional factors

for polarized sorting are the interacting partners of apical proteins. A sorting receptor, PI(4)P adaptor protein 2 (FAPP2), has recently been proposed to act as an apical sorting receptor (Vieira et al., 2005). Other proteins are also being identified as key players in various sorting steps. Some of these, such as GGAs and PACS-1, may to work together with adaptors, while others may function independently.

### 1-5.2 COPII- The Role of GTPases in Vesicle Formation

COPII is the coat complex known to regulate vesicle formation as proteins are exported from the ER. *In vitro* budding assays in yeast have been valuable for determining which molecules are involved in vesicle formation at the ER. Results from this system have shaped the current model for the order and timing of protein-protein and protein-lipid interactions that cause vesicle formation. The model emerging from these studies emphasizes the role of GTP exchange and hydrolysis in vesicle formation; GTPases are also known to function at other sites of vesicle formation. As an example of a particularly well-studied series of events leading to vesicle formation, the molecular interactions necessary for COPII-mediated vesicle formation will be described in some detail here.

Soluble and transmembrane proteins migrate from their site of synthesis and folding on the rough ER to specialized ER export sites. Components of the coat protein complex COPII are stably associated with exit sites; new sites do not seem to form in response to increased protein secretion, and live cell imaging studies show that they do not move over time (Watson and Stephens, 2005). Cargo molecules are recruited into

vesicles by virtue of cytoplasmic sorting signals that are recognized by at least three different sites on the COPII subunit sec24. These ER-export signals are necessary for efficient export from the ER (Mancias and Goldberg, 2005). Sec12, a transmembrane protein present throughout the ER, acts as a GTP exchange factor to stimulate exchange of GDP for GTP on the small G-protein Sar1p. In the GTP-bound state, Sar1p becomes associated with a membrane anchor. Sar1p-GTP recruits the COPII subunits sec23 and sec24. Sec24 contains several cargo binding sites. Sec13/31 is then recruited, possibly aiding in curvature of the membrane since it has an elongated curved structure. Shortly after the sec23/24 complex associates with Sar1p-GTP, it hydrolyzes GTP to GDP, destabilizing the membrane budding complex. It is thought that the GAP activity of sec12 and the GEF activity of sec23/24 compete to help determine the nucleotide state, and thus membrane association, of Sar1p. It has been shown *in vitro* that interaction of sec23/24 with cargo sorting motifs can diminish the GAP activity of sec23/24, thus prolonging the interaction of Sar1p with the membrane, and potentially favoring formation of budding profiles in the presence of cargo (Mancias and Goldberg 2005, Goldberg 2000). Similar GTP "switches" operate at the Golgi and in endosomes, where Arf1 GTPases recruit adaptor complexes to the membrane, and are regulated by their own set of GTP exchange factors and GTPase-activating proteins (Chavrier and Goud, 1999). The possibility that specific sorting signals can affect the rate of GTP hydrolysis of small GTPases is an intriguing idea. If the presence of a sorting signal were to reduce the rate of GTPase activity on Arf1, it could effectively stabilize cargo recognition and vesicle formation by allowing coat components to remain membrane associated.

1-5.3 Sorting Nexin 1: A Detector of Membrane Curvature and Composition

Another interesting model for vesicle formation involves lipid domains and membrane curvature as determinants for sorting sites. While this example of vesicle formation is less studied that the previous COPII model, it touches on a growing theme in studies of vesicle formation: that phophoinositides are recognized by sorting-signal binding partners, and that they recruit both cargo and adaptors to budding sites (Roth, 2004). In addition, it has been found that different phosphoinisitides are present on different organelles, indicating that they could contribute to specificity in trafficking.

One sorting receptor that has been shown to bind to phosphoinositides is Sorting Nexin 1 (SNX1). Sorting Nexins are a relatively uncharacterized family of at least 28 proteins (Teasdale et al., 2001). SNX1 has been shown to bind directly to the EGFR cytoplasmic tail and regulate its trafficking; overexpressing SNX1 causes increased downregulation of the receptor-ligand complex (Kurten et al., 1996). SNX1 has two domains that could be important for its proposed role in sorting at early endosomes. First, it has a PX (PHOX homology) domain that binds to the phosphatidyinositol lipid PI(3)P (phosphatidylinositol-3-phosphate), second it has a BAR domain (Bin, Amphiphysin, Rvs) that binds to curved membranes. It has been hypothesized that these two domains function together to recognize lipid domains on endosomes and to participate in sorting cargo into vesicles since mutation of either domain results in loss of SNX1 localization to early endosome tubules (Carlton et al., 2004; Carlton et al., 2005).

## 1-5.4 Phosphoregulation of Sorting

Phosphorylation can modulate the trafficking of various cargo proteins by affecting specific protein-protein interactions between cargoes and their adaptors. This form of regulation adds another layer of complexity to the mechanism by which cargo is thought to be recruited into budding vesicles. Phosphoregulation of trafficking has been particularly well studied in the transmembrane protein Furin (Schapiro et al., 2004; Scott et al., 2003; Thomas, 2002), though it is involved in the trafficking of other proteins as well (Hirt et al., 1993; Kametaka et al., 2005; von Essen et al., 2002). Furin is predominantly localized to the TGN, but it trafficks from the TGN to endosomes and also to the cell surface— the basolateral surface in epithelial cells (Gu et al., 2001). A pair of serine residues that lie in Furin's cytoplasmic acidic cluster motif are phosphorylated by Casein Kinase 2, and dephosphorylated by Protein Phosphatase 2A (Craig et al., 2000; Jones et al., 1995; Molloy et al., 1998). When phosphorylated, Furin binds the adaptor PACS-1 and localizes preferentially to the TGN; when dephosphorylated, Furin localizes preferentially to endosomes (Crump et al., 2001; Molloy et al., 1998; Wan et al., 1998). PACS-1 also contains an acidic motif that is phosphorylated by Casein Kinase2; phosphorylation of this region is thought to release PACS-1 autoinhibition, allowing PACS-1 binding to Furin or other cargo (Scott et al., 2003). These studies nicely illustrate a mechanism by which phosphorylation is able to influence protein sorting and trafficking pathways.

## 1-6 Events Downstream of Sorting: Transport, Fusion and Retention

Once polarized proteins are sorted into transport vesicles, they travel along the cytoskeleton in a process dependent on molecular motors (Goldstein and Yang, 2000; Terada and Hirokawa, 2000). In neurons, dendritic proteins are transported in vesicles that are unable to enter the axon (Burack et al., 2000). Dendritic polarity could thus be mediated by specific motor proteins that are only able to move vesicles in dendrites. In contrast, axonal proteins are transported in both dendrites and axons; their transport is not selective (Burack et al., 2000). Axonal proteins are transported with a slight bias into the axon, but this alone is not enough to account for axonal polarity. It is likely that preferential fusion with the axonal plasma membrane and/or retention also contribute to axonal polarity. Transport, fusion and retention as they might pertain to axonal or dendritic polarity will be discussed briefly below.

### 1-6.1 Transport

In mature neurons, microtubule orientation is different in axons and dendrites. In axons, microtubules are oriented with their plus ends toward the distal axon, while in dendrites microtubule orientation is mixed (Baas et al., 1988; Stepanova et al., 2003). Studies using GFP-tagged constructs to visualize transport carriers in living neurons show that dendritic vesicles (labeled with TfR-GFP, Tf, or LDLR) are excluded from the axon, whereas axonal vesicles (labeled with NgCAM-GFP) are conveyed into both membrane domains (Burack et al., 2000; Prekeris et al., 1999; Sampo et al., 2003;

Silverman et al., 2001). One explanation for this observation could be that dendritic vesicles use a minus end-directed motor exclusively, allowing them to move bidirectionally in the dendrites, but not allowing their entry into the axon. Meanwhile, carriers containing axonal proteins may use both minus and plus end-directed motors, explaining their bidirectional transport in both axons and dendrites (Burack et al., 2000; Goldstein and Yang, 2000). A problem with this model was pointed out by Silverman et al. (2001), who showed that even in immature neurons, where 90% of dendritic microtubules are oriented plus end out (Baas et al., 1989; Stepanova et al., 2003), carriers containing the dendritic protein TfR move in both directions, indicating that they are capable of using both plus end and minus end-directed motors.

Despite this finding, it is still possible that motor-cargo specificity is important for establishing polarity, and a special motor may carry only vesicles containing dendritic cargo. Perhaps something about the microtubules in dendrites allows only certain motor proteins to translocate and contributes to dendritic delivery of cargoes. Visualizing the transport of different GFP-tagged motors could help identify candidates for polarized transport. Very few studies of this nature have been published despite the recent surge in live cell imaging of microtubule-based transport. Recent reports characterizing the transport of a GFP-tagged motor in neurons came from the Scholey lab (Zhou et al. 2001), which showed *in vivo* transport characteristics of GFP-UNC104 (a microtubule-based motor) in *C. elegans* neurons, and the Kim lab (Lee et al. 2002), which showed that, like its homolog UNC104, KIF1A-GFP particles move bidirectionally in both dendrites and axons of cultured hippocampal neurons, albeit with a heavy anterograde

bias (only 17% of KIF1A-GFP particles moved retrogradely). Hirokawa's group (Guillaud et al. 2003) also reported vesicle-like movement of the neuron-specific YFP-tagged kif17, although the number of transport events observed was more than two orders of magnitude lower than those reported by either Scholey's or Kim's work (2 events compared to 300-400 events).

Another approach to study cargo-motor relationships in cells is to specifically disrupt motor function and look for a change in behavior of transport carriers labeled by GFP-tagged cargo proteins. Using this method, Kaether et al. (2000) reported that overexpressing an antisense kinesin heavy chain construct caused carriers containing GFP-tagged Amyloid Precursor Protein to change direction more often, and also decreased excursion length. No studies to date have determined which motors, if any, are responsible for carrying exclusively dendritic (or axonal) cargo, though many motors have yet to be examined.

### 1-6.2 Fusion

After being transported along cytoskeletal tracks, vesicles must fuse with their target membrane to deliver their contents. Two large families of proteins, rabs (small GTPases of the Ras superfamily) and SNAREs (Soluble N-ethyl-maleimide sensitive factor Attachment protein REceptor) have distinct subcellular localizations and are thought to mediate specificity in fusion (Pfeffer, 1999; Pfeffer and Aivazian, 2004; Zerial

and McBride, 2001). SNAREs are important for actual fusion, while rabs mediate the initial docking or tethering of a vesicle to its target membrane.

The fusion apparatus for most fusion events in cells is formed by a complex of NSF, SNAP (Soluble NSF-Attachment Protein), and two SNAREs, one each from the donor membrane and the acceptor membrane. The SNAREs and SNAP proteins interact to assemble into a four-helical bundle that drives fusion between two membranes, while NSF is thought to regulate the disassembly if the complex (Rothman, 1994). Since different members of the SNARE family are differentially distributed in subcellular organelles, it was hypothesized that specificity in fusion between a vesicle and its target could be achieved by specificity between SNARE isoforms present on each membrane. Evidence for this idea is found in epithelial cells, where the SNARE protein Syntaxin 3 is found on the apical plasma membrane, while a different SNARE, Syntaxin 4, is found on the basolateral membrane. In MDCK cells, a chimera between the N-terminus of Syntaxin 4 and Syntaxin 3 was localized to the basolateral domain. Overexpression of this chimera, along with an interacting partner Munc18b, caused normally apical proteins to be mislocalized to the basolateral surface (Ter Beest et al., 2005). Another study showed that injecting MDCK cells with an antibody to Syntaxin 3 prevented fusion of vesicles containing the apical protein p75 (Kreitzer et al., 2003) . In neurons, such distinct plasma membrane distributions of SNARE proteins has not been found (Tang, 2001).

The association between specific SNARE isoforms is probably only part of the mechanism for fusion specificity. Rab proteins are thought to mediate vesicle docking and tethering steps that occur before actual fusion, and therefore are likely contribute to fusion specificity. Rab proteins were first identified as mediators of vesicle docking/tethering in yeast, where mutations in rab proteins often resulted in the accumulation of vesicles in the cytoplasm (Olkkonen and Stenmark, 1997). Rabs function as molecular switches. They exist in GTP- or GDP-bound states, and their nucleotide association is regulated by many interacting proteins. In the GTP-bound state, they are typically active, increasing fusion between membranes; in the GDP-bound state, fusion is inhibited (Gorvel et al., 1991; Pfeffer, 2005).

It has been shown that some rabs, along with their effectors, form a membrane subdomain that might be specialized for fusion. For example rab5 is found on early endosome membranes enriched in PI(3)P (Shin et al., 2005). Its presence on early endosomes is regulated by association with the rabaptin5-rabex5 complex, which catalyzes GTP exchange onto rab5 and associates with membranes, and by EEA1, which has binding sites for both rab5 and PI(3)P (Zerial and McBride, 2001). These proteins are thought to form an oligomeric complex with the help of NSF, the regulator of SNARE complex association (McBride et al., 1999). EEA1 also binds directly to the SNARE proteins, Syntaxin 6 and Syntaxin 13 (McBride et al., 1999; Simonsen et al., 1999). The membrane domain containing rab5, EEA1, and the rabaptin5-rabex5 complex could function as a docking site for incoming vesicles.

Proteins in this putative docking domain also have connections to coat proteins; rabaptin5-rabex5 binds to GGAs, AP-1 and AP-2 (Hirst et al., 2000; Mattera et al., 2003). In addition to roles in docking/tethering, rabs may also contribute to other steps in vesicle traffic such as transport. Rab5 has been shown to regulate transport of early endosomes by interacting with the plus end-directed motor KIF16B (Hoepfner et al., 2005). While some of the functions of rab proteins such as rab5 are relatively well-characterized, their role in vesicle trafficking is only partially understood; rab5 alone has over 20 interacting proteins, only a few of which have been studied extensivley (Christoforidis et al., 1999). The role for rabs in polarized trafficking has not been characterized in neurons, although rab11 and EEA1 are polarized to dendrites, as mentioned in the section on endosomes in neurons (1-3.3b) above.

1-6.3 Retention

Once proteins are successfully delivered to the correct destination, they must be prevented from diffusing away from their intended localization. In the case of polarized cells like neurons and epithelia, diffusion barriers are in place between the two main surface subdomains of the cell. In epithelia, the basolateral and apical domains are separated by tight junctions (Drubin and Nelson, 1996); in neurons, the axon initial segment functions as a barrier to diffusion of lipids and proteins between the axon and the somatodendritic domain (Kobayashi et al., 1992; Nakada et al., 2003; Winckler et al., 1999).

In addition to general diffusion barriers like these, membrane proteins are also often anchored to the cytoskeleton or to scaffolding complexes to maintain a particular distribution in the membrane. Glutamate receptors are first inserted in a diffuse pattern in the dendritic plasma membrane, then later become clustered and retained at postsynaptic sites (Rao et al., 1998). Many of the axonal proteins discussed earlier, such as the $Na^+$ channel, are thought to participate in specific protein-protein interactions that contribute to retention in a particular domain (Fache et al., 2004; Garrido et al., 2003a). As a complement to retention, selective instability in the wrong domain can contribute to post-fusion localization. The selective endocytosis of VAMP2 from the dendritic domain is an example of this type of regulation (Sampo et al., 2003).

Discussion of the details of vesicle trafficking in this chapter was intended to give the reader a perspective on the current and past literature pertaining to the studies in this dissertation. The remainder of the thesis will be devoted to reporting the results of three different studies. In the first study (Chapter 2), fluorescence microscopy is used in conjunction with hippocampal cell culture to examine transport vesicles that are involved in the trafficking of axonal and dendritic markers. A combination of high-resolution quantitative light microscopy and live-cell imaging provide complementary sets of data that describe the sorting of the axonal marker NgCAM, the dendritic markers TfR and LDLR, and an unpolarized mutant of LDLR. In the second and third studies (Chapters 3 and 4), quantitative fluorescence microscopy allows the analysis of dendritic sorting signals in several different plasma membrane proteins. The rational for each study and a

discussion of the results are provided in the corresponding chapter; additional discussion of some aspects of these studies and suggestions for further experiments are presented in the final chapter.

**Chapter 2**

# Polarized Protein Sorting in Hippocampal Neurons Analyzed by Two-color Microscopy

Greta Glover, Stefanie Kaech and Gary Banker
Center for Research on Occupational and Environmental Toxicology, Oregon Health and Science University, Portland, Oregon 97239

Manuscript in Preparation

In this chapter, I performed all experiments, Stefanie Kaech assisted in developing methods for quantifying colocalization, Julie Luisi Harp made the FP-tagged LDLR constructs and Barbara Smoody prepared hippocampal cultures.

**Abstract**

To examine the sorting of polarized membrane proteins in neurons, we coexpressed pairs of CFP- and YFP-tagged marker proteins and compared their localization in intracellular vesicles by both live-cell imaging and deconvolution microscopy. The dendritic markers Low Density Lipoprotein Receptor (LDLR) and Transferrin receptor (TfR) labeled similar endosomal populations, while the axonal marker NgCAM was not present in these endosomes. When vesicles in the biosynthetic pathway were examined, NgCAM and LDLR were found to be sorted into different transport vesicle populations. Mutating the dendritic sorting signal in LDLR caused a disruption of this sorting, shifting the mutant LDLR into NgCAM-containing transport vesicles. These observations support the hypothesis that axonal (NgCAM) and dendritic (LDLR) proteins are sorted into different vesicle populations as they exit the Golgi apparatus, and that an intact dendritic sorting signal is necessary for this sorting.

## Introduction

Axons and dendrites maintain distinct populations of resident plasma membrane proteins, consistent with their different roles in electrochemical signal processing. Neurotransmitter receptors and other postsynaptic proteins are restricted to dendrites, while presynaptic machinery and axonal guidance proteins are polarized to the surface of the axon (Horton and Ehlers, 2002; Marchand and Cartaud, 2002). Proper protein polarity is critical for all aspects of neuronal function; therefore, definition of the underlying mechanisms of protein targeting is central to understanding neuronal cell biology.

Vesicles or tubules mediate the transport of transmembrane proteins between various intracellular compartments and the plasma membrane. Polarized proteins are thought to be actively sorted into these forming vesicles. A targeting signal within a membrane protein's sequence drives interactions with appropriate protein and/or lipid factors (Gu et al. 2001), directing incorporation into nascent vesicles, which will eventually deliver their cargo to particular cellular destinations. Most of the data that have contributed to the formation of this model have been indirect. Fluorescence microscopy of living cells can be used to directly visualize and characterize these sorting steps, allowing the trafficking pathways taken by various proteins to be compared. These methods are now being employed in unpolarized cells with some success, but the visualization of vesicle populations that mediate polarized sorting in a polarized cell has not been reported.

In epithelial cells, biochemical and live-cell imaging studies suggest that proteins localized to the basolateral or apical plasma membrane bud from the Golgi in separate vesicle populations, and are then transported to the appropriate surface domain (Musch et al., 1996; Wandinger-Ness et al., 1990). While this is the dominant model in the field, there is also evidence that apical and basolateral proteins are not sorted into separate vesicle populations at the Golgi, but instead are first delivered to the basolateral domain together, then sorted away from one another in a subsequent trafficking event (Polishchuk et al., 2004).

Less is known about the sorting of axonal and dendritic proteins in neurons. It has been proposed that axonal and dendritic targeting signals mediate sorting into different carrier vesicles (Craig and Banker, 1994), but this has not been demonstrated directly. Because neurons in culture are essentially two-dimensional, it is possible to visualize and track the transport of vesicles following expression of appropriate GFP-tagged proteins (Burack et al., 2000; Horton and Ehlers, 2003b; Kaether et al., 2000). Using this approach, it has been shown that vesicles containing a dendritic protein (Transferrin Receptor, TfR) are transported bidirectionally in dendrites but practically never enter the axon, while vesicles labeled by expression of a GFP-tagged axonal protein are transported into both axons and dendrites (Burack et al., 2000; Silverman et al., 2001). This implies that these two proteins must reside in separate vesicles, at least over part of their course. Whether this occurs as newly synthesized axonal and dendritic proteins leave the Golgi, or in a subsequent sorting step such as a sorting event in the dendrites, remains unknown.

In the present study, we use dual-color CFP/YFP imaging in living and fixed hippocampal neurons to establish fundamental rules of polarized protein sorting. By coexpressing pairs of proteins tagged with different fluorophores, it is possible to determine if two proteins are present in the same or different vesicle populations. Here we show that the axonal marker NgCAM and the dendritic marker LDLR are sorted into separate vesicles at the Golgi apparatus, and remain in separate vesicles throughout their trafficking pathways; NgCAM does not intersect with the dendritic markers LDLR or TfR in early/recycling endosomes. In addition, we examine the vesicles labeled by an unpolarized protein, a mutant form of LDLR in which the dendritic sorting signal has been disrupted. Unlike wild type LDLR, the mutated form of LDLR is not sorted away from NgCAM, instead it is found in an overlapping vesicle population with this axonal marker. While the results of this study do not necessarily represent the behavior of all axonal and dendritic markers, it does provide a framework upon which a more complete model can be built.

**Results**

To compare the sorting of axonal and dendritic proteins at the level of vesicle populations, we chose three representative marker proteins: two dendritic (TfR and LDLR) and one axonal (Neuron-glia Cell Adhesion Molecule, NgCAM). Each of these markers is a single-pass transmembrane protein whose neuronal targeting has been well-characterized (Jareb and Banker, 1998; Sampo et al., 2003). Previous studies have demonstrated that GFP chimeras of NgCAM (tagged at the cytoplasmic terminal) and

TfR (tagged in the ectodomain) are appropriately polarized when expressed in hippocampal neurons (Burack et al., 2000). In preliminary experiments, we found that LDLR tagged with GFP at the C-terminal was unpolarized when expressed in hippocampal neurons. The mistargeting was presumably due to the proximity of the GFP tag to the sorting signal, which lies in the cytoplasmic C-terminus. When we instead tagged LDLR in the ectodomain (immediately after the signal sequence), the chimera was polarized to dendrites, like untagged LDLR (Figure 1A, green). The N-terminally tagged construct was used for all further experiments.

To evaluate the sorting of polarized proteins, we coexpressed pairs of proteins and determined the extent of their overlap in intracellular vesicles. Figure 1 illustrates that the axonal and dendritic markers used in this study, one tagged with CFP, one with YFP, are correctly polarized upon coexpression in neurons. The axonal marker, NgCAM, was restricted to the surface of the axon, as visualized by live-cell immunostaining against an extracellular epitope (Figure 1A, red), but the signal from the FP tag (Figure 1B, yellow) labeled intracellular tubulovesicular structures throughout the dendrites as well as the axon. In contrast, the tubulovesicular structures labeled with FP-tagged dendritic markers were restricted to the dendrites (shown for TfR in Figure 1B, blue), as was the cell surface immunostaining (shown for LDLR in Figure 1A, green). This is consistent with previous results based on expression of individual markers, which show that vesicles containing dendritic membrane proteins are excluded from the axon while vesicles containing axonal proteins are transported into both axons and dendrites (Burack et al., 2000; Silverman et al., 2001).

Two methods for Analyzing Colocalization

To determine the extent to which various pairs of CFP- and YFP-tagged proteins were sorted into an overlapping population of intracellular vesicles, we used two complementary methods. The first method, based on deconvolution analysis of fixed cells, offers optimal sensitivity and resolution. This method uses correlation analysis to determine overlap based on both position and intensity of fluorescence. In this way, both the location and the concentration of each protein in a given spot are included in the colocalization measurement. This first method does not distinguish moving vesicles from stationary structures; a coated pit on the plasma membrane would be treated in the same way as an intracellular organelle.

The second method is based on analysis of organelle transport in live-cell recordings. This method provides more definitive evidence that two markers reside in the same organelle because they move in concert. Investigating the behavior of moving vesicles also allows only the primary mediators of sorting—the transport vesicles—to be analyzed. However, fainter vesicles in these movies are more difficult to detect due to out-of-focus fluorescence and a decreased signal-to-noise ratio. In addition, since the resolution of light microscopy is not fine enough to distinguish between one and two small vesicles, it is possible that vesicles labeled by two different markers are actually two separate vesicles moving coordinately. This is unlikely, however, since correlative light-electron microscopy studies have shown that post-Golgi vesicles of the constitutive

secretory pathway are single tubular compartments, not multiple vesicles linked together (Polishchuk et al., 2000).

Both of these methods allowed quantitative analysis of colocalization, though there were advantages and disadvantages of each. These issues are discussed briefly here, and more extensively in the Data Supplement, Supplementary Figures 1 and 2, the Experimental Procedures of this chapter, as well as in Chapter 5. In experiments in which endosomes in dendrites were being examined, it may be preferable to quantify colocalization using the method in fixed cells. Our results indicate that most endosomes are stationary, although a subset is transported rapidly. Analyzing only moving structures may eliminate the great majority of endosomes. In addition, the increased signal-to-noise ratio allowed by imaging in fixed cells was also a distinct advantage. We supplemented these data with parallel experiments using two-color live cell imaging to compare colocalization in moving vesicles to that observed in analysis of fixed cells.

In experiments examining sorting in Golgi-derived vesicles, we focused on analysis of moving vesicles. By combining two-color live cell imaging of proteins expressed for short times with a low-temperature incubation to block protein exit from the Golgi, it was possible to examine colocalization in transport vesicles that were very likely to be carrying sorted proteins along the biosynthetic pathway. Such two-color live-cell experiments are extremely powerful because there is little ambiguity concerning the identity of the moving fluorescent puncta. One limitation of this technique is that colocalization in a vesicle was recorded as either present or absent, and no measure of concentration *within* the vesicle was provided. This was due to a low signal-to-noise

ratio of fluorescence in vesicles, and therefore poor ability to accurately detect differences in intensity between channels. Because of this, if one protein were two times more concentrated in a particular vesicle than a second protein, we would be unable to detect this difference. In addition, the vesicles move rapidly, so exposure times had to be limited to no longer than 800msec with essentially no inter-image delay. This limits the signal-to-noise ratio significantly, so we could be unable to detect very dim vesicles. The potential impact of these caveats on the results presented here will be included in the Discussion section of this chapter and in Chapter 5.

Sorting of Axonal and Dendritic Markers After 18-24h Expression

Previous studies of NgCAM and TfR in neurons examined their expression 18-36h after transduction with virus or transfection with lipid-mediated reagents (Burack et al., 2000; Sampo et al., 2003; Wisco et al., 2003). In order for our results to be comparable to those from previous studies, we used this timepoint for initial studies of vesicle populations labeled by NgCAM, TfR and LDLR. After these initial studies, we determined that it was necessary to repeat these experiments at an earlier timepoint. The results of experiments performed at earlier times will be discussed in the second half of this section.

Rapidly endocytosed proteins such as TfR are known to be present in a mixture of endosomes (labeled by transferrin) and biosynthetic vesicles at 18-24h expression by herpes virus transduction (Burack et al., 2000). Using lipid-mediated transfection, NgCAM has also been reported to be present in some proportion of transferrin-positive

endosomes at this time (Wisco et al., 2003). We further investigated the approximate proportion of TfR that was present in the endocytic pathway at this timepoint using lipid-mediated transfection, and also determined whether or not LDLR and NgCAM were present in these endosomes. We used a fluorescently labeled version of the TfR ligand Transferrin to label the early/recycling endosome pathway. This marker is commonly used as the defining label for the endosomal recycling pathway in many cell types, including neurons (Ang et al., 2004; Brown et al., 2000; Haft et al., 1998; Lee et al., 2001; Leung et al., 2000; Prekeris et al., 1999). We incubated cells expressing TfR or LDLR with Alexa568 Transferrin (A568Tf) for 45 minutes, long enough to label the entire recycling pathway (Sönnichsen et al., 2000), and we observed that most, but not all, of the TfR- or LDLR-labeled puncta were also Tf-positive (Supplementary Figure 3A,B). This indicated that very few biosynthetic carriers were labeled with LDLR and TfR at this timepoint. In contrast, puncta labeled by both NgCAM and Tf were practically never observed (Supplementary Figure 3C). Thus, little or no NgCAM-GFP was present in early/recycling endosomes 18-24h after transfection. The existence of a Tf-free endosome population in dendrites that contains NgCAM cannot be ruled out.

We also examined colocalization between NgCAM, TfR and LDLR at this timepoint. We examined the extent of colocalization in fixed cells by deconvolution analysis and in two-color movies of vesicle transport. In cells analyzed following deconvolution, neither of the dendritic markers colocalized with NgCAM-containing structures (Figure 2A, B). High magnification images reveal few, if any, structures labeled with both NgCAM and a dendritic marker. Correlation plots confirm this: the

average correlation coefficient for cells cotransfected with NgCAM and TfR was 0.14±.07, for NgCAM and LDLR, the average correlation coefficient was 0.14±.13 (Figure 2D). These data indicate that NgCAM is present in a different vesicle population than TfR and LDLR. When TfR and LDLR were coexpressed, the majority of labeled structures contained both markers (Figure 2C), consistent with the fact that they both overlapped extensively with A568Tf (Supplementary Figure 3A, B). A few organelles were brightly labeled with one, but not the other marker. Correlation analysis confirmed a significant colocalization of the two proteins (r= .53± .14, Figure 2D), although the degree of their overlap was not quite as high as observed following coexpression of TfR-CFP and TfR-YFP. From these data it seems likely that TfR and LDLR largely follow a common recycling pathway in neurons, as they do in other cell types (Brown et al., 2000; Warren et al., 1998).

We examined the colocalization of these marker proteins in two-color movies (Figure 3). Each construct labeled vesicles moving in both the anterograde and retrograde directions with about equal frequency; their average velocities ranged from 0.1 to 1.5 μm/sec. Figure 3A and B illustrate a cell coexpressing NgCAM-YFP and CFP-LDLR. The two kymographs illustrated, taken from short segments of dendrites, show moving vesicles that contained LDLR or NgCAM, but not both markers. Based on an analysis of 7 cells, which exhibited 278 transport events, only 12±9% of vesicles containing YFP-LDLR were also labeled by NgCAM-CFP, while 10±7% of NgCAM-CFP vesicles contained YFP-LDLR (Fig. 3E). A movie illustrating transport in a cell expressing YFP-LDLR and NgCAM-CFP is provided in the Data Supplement (Movie 1).

Similar results were observed in cells coexpressing TfR-CFP and NgCAM-YFP (not shown). In cells coexpressing the two dendritic markers (TfR and LDLR), many vesicles contained both markers (Figure 3C, D). For example, in the kymographs shown, 5 moving vesicles contained both LDLR and TfR and 1 was labeled only with TfR. (A movie illustrating the transport in this cell is provided in the Supplement, Movie 2). Based on analysis of 8 cells, 74+13% of TfR-CFP-labeled vesicles contained YFP-LDLR, and 66+13% of YFP-LDLR-labeled vesicles contained TfR-CFP (Fig. 3E). This is somewhat less than the overlap in live cells observed following coexpression of CFP- and YFP-tagged TfR (about 90%, Figure 3E), but much greater than that observed following coexpression of an axonal and a dendritic protein. Taken together, the results of these experiments show that the axonal marker NgCAM does not enter the largely endocytic pathway labeled by TfR or LDLR at this timepoint. This argues against the existence of a significant role for either NgCAM transcytosis via Tf-positive endosomes or for a post-Golgi sorting step for NgCAM in dendritic endosomal compartments.

Sorting of Axonal and Dendritic Markers in the Biosynthetic Pathway

We next wanted to examine sorting of these markers upon exit from the Golgi complex, long considered the first place where proteins going to different subcellular domains can be separated from one another (Farquhar, 1985; Keller and Simons, 1997; Rodriguez-Boulan and Musch, 2005). To enrich for Golgi-derived vesicles, we developed a protocol for making two-color CFP/YFP movies at early times after transfection.

To determine when after transfection markers could first be detected on the cell surface, neurons were transfected with GFP-tagged versions of each of the markers, then live cells were incubated with Cy3-conjugated antibodies directed against extracellular epitopes specific for each (Supplementary Figure 4). Imaging GFP antibody signals starting at 3.75h after transfection showed that markers could be detected on the cell surface in a few cells by four hours after transfection. By 5-6 hours, more cells showed GFP fluorescence and surface staining was brighter. For LDLR and TfR, surface staining was always punctate. These puncta likely corresponded to coated pits or endosomes, since LDLR and TfR both spend the majority of their time in coated pits when they are at the surface, and are both rapidly endocytosed (van Deurs et al., 1989). NgCAM staining was more uniform, and appeared first at the initial segment and distal tip of the axon. In addition, a brightly stained Golgi complex was evident for all constructs by 4h (Supplementary Figure 4).

To further enrich for Golgi-derived vesicles, and to help synchronize expression of markers within the transfected cells on the coverslip, cells were incubated at 19° C for 1-2h after 3.5h expression at 37° C. After the Golgi block, cells were warmed to 29° C to release the block (while still slowing transport relative to 37 ° C). Slowing transport slightly was desirable because a slightly higher fluorescence signal could be obtained in the same amount of time if vesicles were moving slower. Movies made at this time revealed very bright Golgi labeling for all constructs as well as many moving vesicles.

To ensure that this Golgi block protocol did not allow TfR and LDLR to become enriched in endosomes, cells were incubated in media containing A568Tf starting at 1.5h

after transfection, and two-color movies of TfR-GFP, GFP-LDLR or NgCAM and A568Tf were made. Cells were exposed to A568Tf for 2h preceding the 19° C block, as well as during and after release of the block, including the entire period of live-cell imaging. Movies were made between 2 and 20 minutes after warming the cells to 29° C or 35° C. These experiments were only possible using a confocal microscope due to fluorescence from A568Tf in the bath. Figure 4A and B illustrate a cell expressing GFP-LDLR and labeled by fluorescent Tf. The two kymographs illustrated in figure 4C are taken from the boxed regions. They show moving vesicles that contained GFP-LDLR or A568Tf, but not both markers (A movie illustrating transport in this cell is shown in the Data Supplement, Movie 4). Practically no Tf-positive vesicles were observed at this timepoint for GFP-LDLR or NgCAM-GFP, indicating that under these conditions the biosynthetic pathway was preferentially labeled. Suprisingly, even 15 minutes after release from the Golgi block,10-40% of moving TfR-GFP-positive vesicles were also Tf-positive (Figure 4D). These results may indicate that TfR is endocytosed very efficiently: even under expression conditions where very little cell-surface TfR can be detected with antibody, a minor but significant percentage of vesicles are already cell-surface derived. An alternative possibility is that TfR passes through endosomes on its way to the cell surface, a phenomenon that also has been observed in other cell types (Ang et al., 2004; Futter et al., 1995; Lock and Stow, 2005; Orzech et al., 2000). We attempted to differentiate between these possibilities by repeating this control experiment using an antibody to the extracellular GFP tag in place of the fluorescent Transferrin. That way, only receptors that had actually arrived at the cell surface and been endocytosed would be

labeled. Unfortunately, we detected puncta that were labeled by antibody only, indicating that the antibody could be released from TfR-GFP. In addition, we noticed more stationary structures in cells that were labeled by antibody compared to fluorescent Transferrin, which could possibly reflect an antibody-induced block in TfR recycling (Killisch et al., 1992). In summary, it was not possible to define conditions in which expressed TfR labeled post-Golgi carriers exclusively, and not endosomes.

To determine if NgCAM and LDLR were sorted into the same or different Golgi-derived vesicle, we used the timecourse worked out above to make two-color movies of NgCAM-CFP and YFP-LDLR. An illustration of vesicle traces from these movies is provided in Figure 5A, which shows examples of kymographs taken from dendrites of two different cells coexpressing NgCAM-CFP and YFP-LDLR. Almost all vesicles that contained one of the proteins did not contain the other. In 7 cells with a total of 199 transport events, LDLR and NgCAM were present in nearly completely separate vesicle populations; an average of 7±8% of NgCAM-CFP vesicles were labeled by YFP-LDLR, and 6±7% of YFP-LDLR vesicles contained NgCAM (Figure 6). This indicates that, at least for these two markers, axonal and dendritic proteins are segregated into separate vesicles early in the biosynthetic pathway.

## The Role of the Dendritic Sorting Signal in LDLR

Presumably the interaction between sorting signal and receptor during vesicle formation was responsible for the segregation of these markers into separate vesicles. We next used our Golgi-block protocol to test this commonly accepted model.

Previous studies have shown that mutating the basolateral sorting signal of LDLR disrupts its dendritic polarization in neurons (Jareb and Banker, 1998). To determine if mutation of the LDLR sorting signal altered the protein's sorting into the proper vesicle population, we mutated three crucial tyrosine residues to alanines in CFP-LDLR (as in Matter et al. 1992). The mutant protein was present on the surface of both axons and dendrites when expressed in hippocampal neurons, identical to the distribution observed by Jareb and Banker (1998). In addition, the timing of arrival on the cell surface was identical to that of wild type CFP-LDLR, and vesicles labeled by the mutant LDLR after release from Golgi block were not labeled by Tf uptake (not shown).

We expressed the mutant LDLR together with NgCAM to determine whether the sorting signal mutation in LDLR caused it to change vesicle populations. We could not directly compare the trafficking of LDLRmut and wild-type LDLR because when the two proteins were coexpressed, their localization on the cell surface was altered: wild type LDLR was not completely excluded from the axon and LDLRmut was slightly polarized to dendrites (not shown). This effect was most likely due to dimerization between wild type and mutant copies of LDLR (van Driel et al. 1987); since LDLR is expressed only at very low endogenous levels in neurons (Rebeck et al. 1993), expressing the LDLRmut on its own would not cause this problem. In contrast to wild type LDLR, LDLRmut was frequently present in vesicles labeled by wild type NgCAM. Figure 5B shows representative kymographs from two different cells expressing CFP-LDLRmut and NgCAM-YFP (movie 5 in the supplement). Many double-labeled vesicle traces can be observed in these kymographs, although a few vesicles are single-labeled by either

NgCAM or LDLRmut. On average, 76±19% of CFP-LDLRmut-labeled vesicles contained NgCAM-CFP, and 68±22% of moving vesicles containing NgCAM-CFP also contained YFP-LDLRmut. This is a much greater degree of overlap than between wild-type LDLR and NgCAM, but is not significantly different than the overlap observed when NgCAM-CFP and NgCAM-YFP were coexpressed as a control (Figure 6). These results directly demonstrate that the LDLR sorting signal is critical for proper LDLR sorting at the level of vesicle populations.

**Discussion**

The experiments in this study were designed to examine the rules governing the sorting of axonal and dendritic proteins into transport vesicles in neurons, and to determine the role of a previously identified dendritic targeting signal in cargo selection. By coexpressing pairs of CFP- and YFP-tagged membrane proteins, we were able to directly compare vesicle populations labeled by axonal and dendritic markers. Our results show that the dendritic markers are sorted into different transport vesicles than the axonal marker in the biosynthetic pathway, and that the axonal marker does not pass through endosomes labeled by the dendritic markers. In addition, mutating a dendritic sorting signal causes missorting of the dendritic protein into an NgCAM-positive vesicle population in the biosynthetic pathway.

Using Coexpression to Analyze Protein Sorting

We describe two complementary methods for assessing whether pairs of coexpressed proteins reside in the same or different organelles. Both represent significant advances because they permit quantitative assessment of protein sorting in neurons. The first method employs deconvolution analysis of a through-focal series of images to enhance the signal to noise ratio by reducing out-of-focus and cell-surface fluorescence. This enables analysis of faintly labeled structures that cannot be resolved in movies of living cells. At present, this method can only be applied to fixed cells, because organelles move far too fast to capture a z-series of images using cameras currently available. The second method—live-cell, two-color imaging—focuses specifically on moving vesicles. The purpose of protein sorting, whether it occurs at the Golgi complex, the plasma membrane, or an endosome, is to create transport vesicles that shuttle a subset of proteins from one location to another. Rather than assessing colocalization based on a single point in time, live-cell studies identify double-labeled organelles that start, stop, and move in unison, providing strong evidence that the two proteins reside in the same transport vesicle. Cultured neurons are an ideal model for applying this method because they are essentially two-dimensional, making it possible to visualize many transport vesicles and track them over long distances in a single z plane.

Despite the strengths of these methods, some caution is needed in interpreting the results of such coexpression experiments. Vesicles with only a few copies of GFP-tagged proteins may not have been detected, and organelles identified as containing only one

protein might have contained the other protein at levels too low to detect. This is of particular concern in live-cell imaging, because organelles move quickly and exposure times cannot be increased to compensate for faint labeling. In preliminary experiments we found that increasing the ratio of DNA encoding TfR vs. LDLR during transfection gave rise to a disproportionate expression of TfR and spuriously increased the proportion of single labeled TfR vesicles (data not shown). Although we took care to transfect amounts of DNA that gave comparable levels of expression, if anything, our results may have underestimated the extent of overlap between pairs of marker proteins.

When comparing CFP/YFP movies to GFP/A568Tf movies, we noticed a difference in the signal-to-noise ratio. CFP/YFP movies were dimmer than GFP/A568Tf. This was probably directly related to the brightness of the fluorophores- GFP and Alexa568 are both very bright and stable fluorophores that can be excited easily by many different light sources. In contrast, CFP is much dimmer, and YFP is easily photobleached. In all CFP/YFP movies, the CFP signal was very low, while the YFP signal was bright but tended to bleach quickly. This may have caused a decrease in the number of vesicles we were able to detect. These factors are likely to explain why the average number of moving vesicles detected per cell is lower in CFP/YFP movies compared to GFP/A568Tf movies (Figures 6 and 4d, respectively).

These issues related to signal-to-noise suggest that caution is warranted in interpreting the absolute percentages of overlap between markers. Instead, we use these values to compare different pairs to each other. Nevertheless, it is unlikely that the our

results were dramatically affected by the low signal-to-noise ratio—the percentage of overlap for a particular marker pair was quite consistent from cell to cell and experiment to experiment, and the high level of overlap in controls in which different colors of the same marker were compared showed that detection in CFP was similar to that in YFP.

Different Carrier Populations Transport Axonal and Dendritic Membrane Proteins

Two general models could explain the polarization of axonal and dendritic membrane proteins. In the first, polarized proteins are selectively added only to the appropriate domain of the plasma membrane. In the second, they are added equally to both domains, but retained on the cell surface only in the appropriate domain. These two models differ in terms of where protein sorting is predicted to occur. The selective addition model predicts that axonal and dendritic proteins are sorted into separate vesicles along the biosynthetic pathway; the selective retention model predicts that axonal and dendritic proteins reach the membrane in a common vesicle. Our data support the selective addition model. We found that axonal (NgCAM) and dendritic (LDLR) marker proteins are sorted into different populations of vesicles in the biosynthetic pathway. In two-color movies of NgCAM and LDLR made under conditions in which the biosynthetic pathway was preferentially labeled, less than 10% of moving vesicles contained both markers. In addition, we found that axonal and dendritic markers do not intersect in dendritic early/recycling/sorting endosomes labeled by the endosomal marker Transferrin. By deconvolution analysis, the correlation of labeling between NgCAM and TfR or LDLR was near zero. By live cell imaging, 90% of the moving vesicles labeled

with NgCAM did not contain a dendritic marker. From these data, it is likely that dendritic and axonal markers traverse predominantly separate vesicle populations along both biosynthetic and endocytic pathways. At most, only a small fraction of the NgCAM (less than 10%) may be co-transported in dendrites along with LDLR and TfR.

Some aspects of our results disagree with observations of Wisco and colleagues (2003). They presented evidence that most NgCAM first appears on the dendritic membrane, is endocytosed into a Transferrin-positive endosome, and then appears on the surface of the axon. In addition to this transcytotic pathway, they also described a pathway for direct addition of NgCAM to the axonal membrane. As discussed in Chapter 1, there are several technical issues that cast doubt on these conclusions. In our hands, we have been unable to detect the endocytosis of NgCAM from the dendritic membrane (Sampo et al., 2003), and in the present study we could not detect NgCAM vesicles in dendrites that were labeled by uptake of fluorescent Transferrin. Transferrin uptake should label the entire early and recycling endosome pathway, but does not label late endosomes or lysosomes. There could be other endosomal compartments, such as caveolae and GPI-anchored-protein-enriched endosomal compartments, that are unlabeled by Tf-uptake (Perret et al., 2005). These latter types of endosomes are thought to deliver their contents to the Golgi complex, to recycling endosomes, or to the ER (Perret et al., 2005). Therefore, we can't completely rule out the possibility that NgCAM vesicles in dendrites are endosomal in nature. With the exception of this possibility, these data, together with the finding that NgCAM vesicles seldom are labeled with dendritic markers, argue that NgCAM is predominantly polarized by selective addition.

This model of axonal sorting may not apply to all axonal markers. For instance, VAMP2 is initially inserted in both axonal and dendritic plasma membranes, but is subsequently removed from the dendritic surface via rab5-positive endosomes (Sampo et al., 2003). Studies of the intracellular domains of the Na+ channel subunit Nav1.2 have also indicated that endocytosis from the dendritic surface could be one of the trafficking steps taken by this protein, although analyzing different sections of this complex protein independently could introduce artifacts. By extending the methods used in our study to other marker pairs, general principles that govern polarized sorting will become clearer.

Signal-dependent sorting

Mutations that disrupt the interaction between the sorting signal and adaptor result in mispolarization on the cell surface (Matter et al., 1994; Simmen et al., 2002). Until now, it has not been possible to show how these mutations influence the protein's incorporation into transport vesicle populations, in neurons or in any other cell type. Is the mutated protein trafficked indiscriminately in all vesicles? Or is it instead packaged into a different vesicle that contains only unpolarized proteins? By expressing a mutant version of the dendritic protein LDLR in combination with NgCAM, we found that mutation of the sorting signal caused LDLR to be packaged in a vesicle containing the axonally polarized protein NgCAM. It was unexpected to find that NgCAM was packaged together with this unpolarized protein. This argues against the existence of a "default" vesicle population containing only unpolarized, or unsorted proteins. Could a subsequent sorting event segregate NgCAM from the unpolarized LDLRmut found in

these vesicles? Endosomes are known to contain subdomains that are thought to be important for cargo sorting (de Renzis et al., 2002; Sönnichsen et al., 2000); perhaps such a sorting event could occur within a vesicle containing NgCAM and LDLRmut.

An alternative possibility could be that LDLRmut is present in multiple vesicle populations that deliver their contents to both axonal and dendritic plasma membrane domains. Since technical factors prevented us from determining whether LDLRmut was also present in a vesicle population containing wild-type LDLR, or a different dendritic marker like TfR, we can't determine which of these two scenarios is correct at this time. Future experiments in which LDLRmut is compared to other dendritic and unpolarized markers will address this. Nevertheless, the experiments in the current study provide some of the clearest evidence to date that dendritic targeting signals act by governing the sorting of proteins into specific populations of transport vesicles. These methods also provide a clear readout for experimental manipulations to identify the molecular sorting machinery in neurons. For example, disrupting the function of proteins involved in the dendritic sorting of LDLR (such as specific adaptor subunits) could cause LDLR to be missorted into vesicles labeled by NgCAM in the same way that mutating the LDLR sorting signal did.

## A model for the sorting of axonal and dendritic membrane proteins

The formation of dendritic vesicles likely involves two crucial selectivity events that together can explain how dendritic membrane proteins become polarized. First, during the process of budding, a sorting mechanism recruits dendritic cargo proteins to

the forming vesicle, based on targeting motifs contained within their cytoplasmic domains. This form of selectivity begins in the biosynthetic pathway and also applies to endosomes. Second, specific microtubule motors are recruited to the newly formed dendritic vesicles. The motor proteins may bind directly to a dendritic cargo protein, may be linked to cargo proteins via a scaffolding complex, or may interact with specific lipids in the vesicle membrane (Gunawardena and Goldstein, 2004). Whatever the linkage, the motors associated with dendritic vesicles are "smart", in that they mediate the transport of vesicles along dendritic but not axonal microtubules (Burack et al., 2000; Goldstein and Yang, 2000; Shah and Goldstein, 2000). Selective sorting and selective transport ensure that dendritic proteins are selectively added to the dendritic membrane. The biosynthetic and endocytic vesicles we visualized using LDLR and TfR as markers are likely to contain many other dendritically polarized proteins. In addition, there may well be other populations of vesicles that share the same essential features as the vesicles we visualized, but that contain different sets of dendritic proteins (Cheng et al., 2002; Lim et al., 2000). For example, proteins such as neurotransmitter receptors are clustered at specific sites within the dendrites; it could be that such proteins are delivered to the dendritic membrane in a separate vesicle population, allowing separate regulation of the trafficking of synaptic proteins and non-synaptic proteins.

The sorting events that underlie polarization of axonal proteins are less clear. NgCAM is sorted into a biosynthetic vesicle population that does not contain a dendritic marker. This indicates that no downstream sorting event, such as one that might occur in a dendritic endosome, or at the dendritic cell surface, is necessary to separate proteins

going to different domains. The events that lead to the delivery of the contents of this vesicle to the axon (but not to the dendrites) are unknown. Why are NgCAM vesicles transported into dendrites if they do not deliver their cargo to the dendritic surface or to dendritic endosomes? It has been suggested previously that since the Golgi apparatus is localized to the soma and proximal dendrites, it would be more difficult to keep NgCAM vesicles out of the somatodendritic domain than to allow them in (Burack et al., 2000). Since the dendrites are much shorter than the axon, NgCAM vesicles are really not making too big a detour by traveling into and out of dendrites.

NgCAM is different from other axonal proteins like VAMP2 or the Na+ channel (Nav1.2) in that it does not seem to fuse readily with the dendritic membrane, even though NgCAM carriers are present in dendrites. Could there be separate vesicle populations for different axonal proteins? In one study, two-color movies of APP-YFP and synaptophysin-CFP showed that these markers were in separate vesicles (Kaether et al., 2000). Unfortunately, this study did not synchronize trafficking of the two markers, so it is possible that one marker was enriched in the biosynthetic pathway, while the other was enriched in endosomes. Applying the methods used in this study to comparisons between other axonal, dendritic and unpolarized markers will allow a generalized model of polarized protein sorting in neurons to emerge. The results of the experiments in this and future studies also provide a background for experiments that identify the molecules that participate in the selective recruitment of cargo into axonal and dendritic vesicle populations.

## Experimental Procedures

### DNA Constructs

All constructs were expressed from the plasmid vectors pJPA5 or pJPA7, which each contain a CMV promoter/enhancer and an artificial intron sequence upstream from the MCS, and differ only in the orientation of their MCS (J. Adelman, OHSU). NgCAM (P. Sonderregger, University of Zurich) and TfR (C. Enns, OHSU) were engineered to have a C-terminal CFP or YFP tag. LDLR (I. Mellman, Yale University) was initially tagged with GFP at the C-terminus, but due to apparent interference with proper dendritic targeting, an N-terminally tagged LDLR was constructed by insertion of the CFP or YFP sequence downstream of the signal sequence. The LDLR mutant construct was also tagged with CFP or YFP at the N-terminus, and contained three tyrosine-to-alanine substitutions at positions 18, 35 and 37 of the C-terminus. For a detailed description of cloning strategies, see the Data Supplement. All constructs were verified by sequencing.

### Expression of Chimeric Proteins in Neuronal Cultures

Primary hippocampal cultures with glial feeder layers were prepared from E18 embryonic rats as described previously (Banker and Goslin, 1998). Cells were plated at 250-500 cells/mm2 on polylysine-treated coverslips (4 per 6 cm dish) and maintained in neurobasal medium supplemented with B27 and Glutamax (Lifetech/Gibco-BRL, Gaithersburg, MD). 2 to 4 μg of plasmid DNA was introduced into cultures at 7-8 days

*in vitro* using either Effectene (Qiagen, Valencia, CA) or Lipofectamine2000 (Invitrogen, Carlsbad, CA). After various times of expression, cells were imaged live or fixed in 4% paraformaldehyde, 4% sucrose, 0.01% glutaraldehyde for 20 min, quenched with 0.5mg/ml NaBH4 in PBS (3x5 min), and permeabilized in 0.25% Triton X-100 for 5 min prior to mounting in elvanol (Banker and Goslin, 1998).

To detect the cell surface distribution of membrane protein markers, living cells were incubated with the appropriate primary antibodies for 5 min at 37° C, rinsed, fixed in 4% paraformaldehyde, 4% sucrose for 20 min, then incubated with Cy3- or Cy5-coupled secondary antibodies (Jackson ImmunoResearch Laboratories, West Grove, PA) for 45 min at 37°. After fixation and staining, coverslips were washed in PBS (3x5min) and mounted on slides with elvanol (Banker and Goslin, 1998). For experiments in which antibody labeling was followed in live cells, cells were incubated in primary antibody that had been pre-coupled to cy3 Fab fragments (Jackson ImmunoResearch Laboratories). Surface NgCAM was detected with monoclonal 8D9 (Developmental Studies Hybridoma Bank, Iowa City, IA); surface TfR, LDLR and mutant LDLR were detected with either monoclonal anti-GFP (Roche Diagnostics Corporation, Indianapolis, IN) or polyclonal anti-GFP (Molecular Probes, Eugene, OR).

In Transferrin uptake experiments, live cells were incubated in 250nM Alexa568 Transferrin (Molecular Probes) dissolved in imaging medium (see below), then fixed as described above.

Colocalization Analysis (Fixed cells)

To ensure that fixation does not alter organelle morphology, we compared individual transport vesicles before and after fixation. We added pre-warmed fixative (4% paraformaldehyde, 4% sucrose in PBS) to a cell transfected with NgCAM-YFP while making a movie of organelle transport. The morphology of moving vesicles was preserved after fixation (data not shown), consistent with published results for other GFP-tagged membrane proteins (Hirschberg et al., 1998; Polishchuk et al., 2000).

For colocalization analysis, fixed neurons expressing CFP/YFP pairs were analyzed by deconvolution. For thin specimens such as cultured neurons, wide-field microscopy coupled to constrained-iterative deconvolution produces a higher image quality than confocal microscopy (Swedlow et al., 2002). A through-focal series of images (32 planes, 0.2um apart) was acquired using a 63X, 1.32 N.A. Plan Apo objective, then processed by constrained-iterative deconvolution (15 iterations) using Deltavision SoftWoRx software (Applied Precision, Issaquah, WA). Single planes of deconvolved CFP and YFP images were then subjected to correlation analysis using the Correlation Plot function in Metamorph (Universal Imaging, Downingtown, PA). Fluorescence from cell bodies was not included in the analysis (due to double-labeling in the Golgi region), and thresholds were applied to eliminate background fluorescence in dendrites. These measures ensured that only fluorescence from tubulovesicular organelles was included for quantification of colocalization. We focused on dendrites for two reasons. First, dendritic markers are never found in the axon, so whenever one of the

two transfected proteins was a dendritic marker, comparisons could be made only in the dendrites. Second, the diameter of an axon is near the diameter of a transport vesicle, so it was more difficult to separate cell surface signal from intracellular vesicles. We addressed whether chance overlap could artificially increase the correlation coefficient by analyzing a digitally scrambled image. Statistical significance of differences in correlation between groups was determined by performing the Newman-Keuls multiple comparisons test for independent groups.

Transport Vesicle Analysis

Before acquiring movies, coverslips were sealed into a heated chamber (Warner instruments, Hamden, CT) containing imaging media (130mM Sodium Chloride, 2.8mM Potassium Chloride, 5mM Calcium Chloride, 1mM Magnesium Chloride, 10mM HEPES, 10mM glucose, pH7.4, 300 mosm (Taraska et al., 2003)). Immediately before acquiring movies, medium in the chamber was exchanged for imaging media in which 50mM NaCl was replaced by 50mM Ammonium Chloride. Cells were maintained at 29° C or 35° C for the duration of the recording. For movies made at 18-24h after transfection, a DG4 rapid wavelength switcher/Xenon light source (Sutter Instruments, Novato, CA) was used to capture sixty 800msec exposures (alternating between CFP and YFP illumination) essentially without inter-image delays with an interline Princeton Instruments MicroMax CCD camera (Photometrics, Tucson, AZ). For all other movies, images were captured with a spinning disk microscope setup custom built by Solamere Technology Group (Salt Lake City, Utah). Laser excitation wavelength for different

fluorophores was as follows: CFP at 457nm, YFP at 514nm, GFP at 488nm, and Cy3 or Alexa 568 at 568nm.

To perform colocalization analysis, we used the kymograph function in Metamorph. For each movie frame, the brightest pixel within a 2 μm corridor along the axis of a dendrite (or axon) is displayed at the corresponding location on a kymograph. The fluorescence patterns for all 30 movie frames are then displayed adjacent to one another. This produces a graph on which the x-axis represents time and the y-axis represents distance along the process. For two-color movies, we made two kymographs: one for YFP, one for CFP. We traced the diagonal lines on each kymograph individually, then overlayed the tracings from CFP and YFP kymographs and counted the number of tracings/moving vesicles present in one or both colors. All vesicles that moved more than 1 μm were included in our data. Statistical significance of differences between groups was determined by performing the Newman-Keuls multiple comparisons test for independent groups.

**Figure legends**

Figure 1. Cell surface and intracellular distribution of polarized markers coexpressed in cultured hippocampal neurons. **A** When coexpressed, NgCAM-CFP (pseudocolored red) and YFP-LDLR (pseudocolored green) were appropriately polarized to the axonal and dendritic plasma membrane, respectively (as revealed by live-cell immunostaining with antibodies that recognize extracellular epitopes). **B** The fluorescence signal from NgCAM-YFP (yellow) revealed tubulovesicular organelles in dendrites; in the axon, cell surface fluorescence largely obscured the tubulovesicular organelles (which were visible at higher magnification). In contrast, vesicles labeled with a dendritic marker (TfR-CFP, blue) were restricted to the dendrites. White arrows indicate stretches of the axon. Cells were transfected at 7-8 days *in vitro*, then stained, fixed and imaged 18-24h later. The cell in **A** appears to have two axons with a common origin; such multiple axons are observed occasionally in these cultures. Scale bar: 20 μm

Figure 2. Axonal and dendritic membrane proteins label separate organelles, whereas two dendritic proteins label an overlapping population of vesicles. Neurons expressing pairs of dendritic and axonal proteins labeled with YFP or CFP (**A** NgCAM-YFP/TfR-CFP, **B** YFP-LDLR/NgCAM-CFP) or with two different dendritic proteins (**C** CFP-LDLR/TfR-YFP) were fixed, imaged, and processed by deconvolution. The left panels show segments of the dendrites at high magnification (illustrating each marker

individually and in two-color overlays) and the right panels show correlation plots quantifying the degree of colocalization within the entire dendritic arbors of the same cells. The structures labeled with axonal and dendritic markers exhibit very little overlap (**A** and **B**, left), whereas the two dendritic makers are frequently found in the same organelles (**C**, left). Correlation analysis, shown in the right panels, confirmed that axonal and dendritic markers do not show significant colocalization, whereas the two dendritic markers are significantly correlated. Scale bar: 2 μm **D** Summary of correlation coefficient values. Bars represent correlation coefficient mean ± standard deviation of between 5 and 14 cells per pair from at least two independent experiments. Values for TfR vs TfR and TfR vs LDLR were each significantly different from all other groups ($p<0.05$), values for NgCAM vs TfR and NgCAM vs LDLR were not significantly different from each other.

Figure 3. The dendritic marker LDLR is in a separate transport vesicle population from the axonal marker NgCAM under conditions in which LDLR predominantly labels the dendritic sorting/recycling pathway. Living neurons expressing one dendritic and one axonal protein (**A,B**), or two dendritic proteins (**C,D**) were imaged sequentially in CFP and YFP channels (60 frames, 0.8 sec/frame) after 18-24h expression. The images at left show the first frame from each movie. The figures at right show enlarged views of the highlighted dendritic segments together with kymographs that illustrate organelle movements in the YFP and CFP channels. Prominent examples of moving organelles are

highlighted in red (YFP) and green (CFP) on a second copy of each kymograph. For the cell expressing two dendritic markers, most moving organelles, traveling in both anterograde and retrograde directions, could be visualized in both channels. Less frequently, moving organelles were labeled with only one of the two markers (such as the anterograde TfR-CFP vesicle in dendrite 2 in **D**). In the cell expressing axonal and dendritic proteins, most moving vesicles were labeled with only one marker, independent of the direction of their movement. Stationary organelles (horizontal lines in the kymographs) were not analyzed systematically, but the degree of overlap appeared similar to that of the moving vesicles. Organelle transport in cells expressing these pairs of markers is shown in Supplemental Movies 2 and 3. **E** In live cells, colocalization between marker pairs in moving vesicles was quantified by comparing vesicle traces in the CFP and YFP kymographs. For each pair, the average percentage of CFP-labeled vesicles that were also YFP-labeled was determined (left bar), and vice versa (right bar). Bars represent mean ± standard deviation of between 7 and 9 cells per pair from at least two independent experiments. Values for NgCAM vs LDLR were significantly different from TfR vs LDLR and from the control TfR vs TfR ($p<0.05$). n= # cells(# total transport events)

Figure 4. Before dendritic markers have arrived at the cell surface, and at a time when prominent Golgi fluorescence is observed, LDLR and NgCAM, but not TfR, is found in Transferrin-negative transport vesicles. Living neurons expressing GFP-LDLR or TfR-GFP were exposed to 25nm Alexa568 Transferrin beginning 1.5h after transfection and

continuing through the end of image acquisition. Cells expressed constructs for 3.5h at 37° C, then 1h at 19° C, then were imaged sequentially in GFP and Alexa568 channels (100 frames, 0.6 sec/frame) after warming cells to 35° C. A single frame from a two-color movie of GFP-LDLR (**A**) and Alexa568 Transferrin (**B**) is shown. Since images were acquired on a spinning disk confocal microscope, most of the signal from the Alexa568 Transferrin included in the imaging chamber was eliminated, but some background fluorescence in **B** is still evident. Scale bar: 20 μm Kymographs from the boxed regions are shown in **C**, illustrating organelle movements in the GFP (left) and Alexa568 (center) channels. Prominent examples of moving organelles are highlighted in green and red on a second copy of the Alexa568 Transferrin kymograph (right). Most moving vesicles were labeled with only Transferrin or LDLR, independent of the direction of their movement. Organelle transport in a cell expressing this pair of markers is shown in Supplemental Movie 4. **D** Quantification of the percentage of TfR-GFP, NgCAM-GFP or GFP-LDLR vesicles that was Transferrin-positive for between 6-15 cells from three independent experiments.

Figure 5. Axonal and dendritic membrane proteins are transported in separate biosynthetic vesicle populations, but point mutations that disrupt the dendritic targeting of LDLR cause it to be transported in NgCAM-containing vesicles. Cells expressed constructs for 3.5h at 37° C, then 1h at 19° C, then were imaged immediately after warming cells to 35° C on the spinning disk confocal. Living neurons expressing

NgCAM-CFP and YFP-LDLR (**A**), or CFP-LDLRmut and NgCAM-YFP (**B**) were imaged sequentially in CFP and YFP channels (60 frames, 0.8 sec/frame) after release from 19° C Golgi block. Kymographs that illustrate organelle movements in the CFP (left) and YFP (center) channels are shown for two different cells. Prominent examples of moving organelles are highlighted in green (CFP) and red (YFP) on a second copy of the YFP kymograph (right). Most moving vesicles in **A** were labeled with only NgCAM-CFP or YFP-LDLR, independent of the direction of their movement. Organelle transport in a cell expressing this pair of markers is shown in Supplemental Movie 5. **B** Unlike wild-type LDLR, mutant LDLR (CFP-LDLRmut) localized to a population of transport vesicles that contain NgCAM-YFP. Some NgCAM-YFP vesicles do not contain CFP-LDLR mut, and vice versa. Organelle transport in a cell expressing this pair of markers is shown in Supplemental Movie 6.

Figure 6. Quantification of colocalization between markers in moving biosynthetic organelles. The average percentage of vesicles containing both markers was quantified by comparing vesicle traces in the CFP and YFP kymographs. For each marker pair, the average percentage of CFP-labeled vesicles that were also YFP-labeled was determined (left bar), and vice versa (right bar). Bars represent mean ± standard deviation of between 4 and 9 cells per pair from at least two independent experiments. Values for NgCAM vs LDLR were significantly different from NgCAM vs LDLRmut and NgCAM vs NgCAM ($p<0.05$). n= # cells(# total transport events)

## Supplementary Data

### Supplementary Materials and Methods

DNA Constructs

NgCAM-CFP and NgCAM-YFP were constructed by excising NgCAM (acc#Z75013, a gift from P. Sonderreger, University of Zurich) from pNF314-NgCAM-eGFP (Burack et al., 2000) with HindIII, subcloning it into pJPA7 at the HindIII site, then inserting YFP or CFP downstream with AgeI/XbaI. A similar strategy was used to tag TfR-GFP (Burack et al., 2000) with CFP or YFP.

LDLR (a gift from I. Mellman, Yale University) was initially tagged with GFP at the C-terminus using the following strategy. The LDLR coding sequence was amplified by PCR from pCB6 using primers designed to add SalI and NotI sites to the 5' end, an Age1 site to the 3' end, and to change the LDLR stop codon to glycine. The PCR product was then inserted into pJPA7 with SalI and AgeI upstream of GFP, which was inserted in pJPA7 with AgeI and XbaI, creating a short linker between LDLR and GFP (GGAGGACCGGTCGCCACC). The N-terminally tagged CFP- or YFP-LDLR was constructed by inserting C/YFP between the endogenous LDLR signal sequence and the LDLR mature protein using the following strategy. C/YFP was amplified by PCR from peC/YFP-N1, adding the endogenous LDLR signal sequence at the 5' end (with

additional *ClaI* and *NheI* sites upstream) by three nested PCR reactions, and changing the C/YFP stop codon to threonine at the 3' end, as well as adding an *EcoRI* site. The sequence of the region 5' to the Y/CFP was

*ATCGAT*A*GCTAGC*ACC**ATG**GGGCCCTGGGGCTGGAAATTGCGCTGGACCGTT GCCTTGCTTCTTGCCGCTGCTGGAACTGCAGTTGGCGACAGAAGTACT-Y/CFP (start methionine removed on Y/CFP); the sequence of the linker between the FP and the LDLR mature protein sequence was GGAGGGGGA *GAATTC* (enzyme sites are underlined and italicized). The LDLR coding sequence (Acc# NM_000527) starting 25 amino acids from the ATG, plus a 235 nucleotide 3' UTR, was inserted downstream of YFP, creating N-terminally tagged LDLR with an intact LDLR signal sequence. The LDLR mutant construct contained three tyrosine-to-alanine substitutions in the cytoplasmic tail, Y18,35,37A. It was created by amplifying the LDLR C-term from the endocytosis-deficient LDLR Y18A (Gift from I. Mellman) using a 5' primer over an endogenous *BglII* site (5'CT*AGATCT*CCTC AGTGGCCGCCTCTAC3'), and a 3' primer over an endogenous *XhoI* site, engineered to convert tyrosines **35** and **37** to alanines, and to introduce a silent mutation in serine 36 to make a unique BsrB1 site (5'ATCTGT*CTCGAG*GG**agc**Gg**aagc**GCCGTCCTGGTTGT3'). This PCR product was then subcloned into the N-terminally tagged wild type LDLR construct using BglII and XhoI.

Analyzing Colocalization in Fixed Cells

Assessing the extent of overlap from deconvolved, two-color images images of fixed cells can be problematic because it is highly dependent on gain and color balance used in preparing the overlay. Moreover, counting the number of double labeled organelles in such images does not discriminate between organelles brightly labeled in both colors from those brightly labeled in one and dimly labeled in the other. As a measure of overlap, we used correlation analysis, which compares the intensity of CFP and YFP fluorescence at each pixel and generates a coefficient (r), a measure of the correlation of fluorescence intensity in the two channels (Costes et al., 2004; Lin et al., 2004). An r-value of 1 indicates a perfect correlation while an r-value near 0 indicates no correlation. To validate this approach, we analyzed the degree of overlap in cells coexpressing CFP- and YFP-tagged versions of the same marker. Supplementary Figure 1 shows a high-magnification view of a cell expressing TfR-CFP and TfR-YFP and the corresponding correlation plot. As expected, the two markers exhibited a high degree of overlap and a high correlation coefficient (Figure 2D ,$r = 0.72 \pm 0.13$, $n=10$). To assess the degree of overlap due to chance, we scrambled one of the two images. The randomized image of a portion of a dendrite expressing TfR-YFP in Supplementary Figure 1C was generated by dividing the image into five squares of equal dimension, then rotating and/or flipping each square independently and reassembling the squares to form the final randomized image. The resulting pair of images (scrambled and unscrambled) showed no overlap (Supplementary Figure 1C) and the correlation coefficient was reduced to 0.02 (Supplementary Figure 1D). In order to establish a reference for

interpretation of correlation coefficients that are less than one but still far from zero, we performed correlation analyses on copies of the same image, but with one of the images shifted slightly out of register. A one-pixel shift in the x and y position (corresponding to a shift of 0.11 μm in each direction) resulted in a reduction of the correlation coefficient from 1.0 to 0.75. A two-pixel shift reduced the correlation coefficient to 0.41 (Supplementary Figure 1E), which still indicates a highly significant degree of overlap (Rappoport and Simon, 2003).

Two-color Live Cell Imaging

Coexpression of protein pairs labeled by different GFP color variants made it possible to use live-cell imaging to ask if two proteins were in the same moving vesicles. When we visualized CFP- and YFP-labeled markers in live cells, we found that vesicles labeled by constructs that were tagged with YFP in the luminal domain were difficult to detect. YFP fluorescence is strongly dependent on pH, much more so than CFP (Llopis et al., 1998), so it seemed likely that the acidified pH of intracellular compartments (pH 5.5-6.5, (Mellman, 1992)) caused quenching of YFP. When we treated cells with the weak base $NH_4Cl$ (Boron et al., 1978), the fluorescence of YFP-labeled organelles was rapidly and markedly enhanced (Supplementary Figure 2 A-C) in a reversible fashion. We did not detect a significant change in fluorescence for constructs tagged in the cytoplasmic domain with YFP, or tagged in either domain with CFP. Since proper targeting of the dendritic proteins required that they be tagged in the luminal domain, we added $NH_4Cl$ to the imaging medium. We restricted our analysis to the first 5 minutes

after addition of $NH_4Cl$ because there is evidence that neutralization of endosomal pH for longer times slows the kinetics of the recycling pathway (Presley et al., 1997b). When NgCAM-YFP (tagged in its cytoplasmic domain) was coexpressed with a luminally tagged dendritic marker, it was possible to compare their trafficking both in the presence and absence of $NH_4Cl$. No differences were observed.

To determine if two markers are transported together, we imaged cells expressing CFP and YFP pairs, taking sequential 800 msec exposures in the two channels over a time period of 48 seconds, and analyzed vesicle movements in such movies using the kymograph function in Metamorph. When displayed as a kymograph, moving organelles are represented as diagonal lines whose slopes correspond to the velocity of movement; stationary structures appear as horizontal lines (Supplementary Figure 2 D,E). As a control, we made two-color movies of cells cotransfected with TfR-CFP and TfR-YFP (Supplementary Figure 2, F-I). Supplementary Figure 2F and H, which show the first YFP and CFP frames from a 48-second movie, illustrate the overall similarity in the two channels. Supplementary Figure 2G and I show kymographs from the dendrite segment outlined in 2F and H. The moving organelles that can be detected in the kymographs were labeled with both fluorophores. The movie from this dendrite is shown in the Data Supplement (Movie 1). Based on an analysis of 9 cells cotransfected with TfR-CFP and TFR-YFP, an average of 93±12% of moving TfR-YFP-labeled vesicles (diagonal kymograph lines) also contained TfR-CFP, while 89%±9% of TfR-CFP-labeled vesicles contained TfR-YFP (Figure 3E).

**Supplementary Data--Figure and Movie Legends**

Figure S1. Analyzing colocalization between CFP- and YFP-tagged membrane proteins in fixed hippocampal neurons. Images of fixed cells were processed by deconvolution to eliminate out-of-focus fluorescence. **A** High-magnification images of a dendrite from a cell expressing TfR-YFP (pseudocolored red) and TfR-CFP (pseudocolored green), illustrating each marker individually and in a two-color overlay. Most organelles were double-labeled. **B** After excluding background fluorescence, overlap was quantified by plotting the intensity of YFP (x-axis) and CFP (y-axis) at each pixel in the image and a correlation coefficient (r) was calculated using Metamorph software. The points fall along a straight line, indicating that the relative intensities are similar in the YFP- and CFP-channels. This is reflected by the high correlation coefficient (r=0.83). **C, D** As a measure of random overlap, the CFP image in A was scrambled. The corresponding images show minimal overlap. In the correlation plot, the points are clustered along the x- and y-axes and the correlation coefficient was reduced to 0.02. **E** To serve as a guide for interpreting the correlation coefficient, an image of TfR-CFP was plotted against itself, or against versions of the same image that had been x-y shifted 1 or 2 pixels. A 1-pixel shift, which had a barely detectable effect on the apparent overlap, reduced the correlation coefficient from 1.0 to 0.75. A 2-pixel shift (corresponding to the dimensions of a very small organelle) produced a 2-color image with partial overlap and reduced the correlation coefficient to 0.41. Scale bar: 2 μm

Figure S2. Two-color live cell imaging of transport intermediates containing CFP- and YFP-tagged proteins. Living neurons expressing dendritic proteins tagged with YFP or CFP were imaged continuously for up to 60 frames (0.8 sec/frame, 30 frames each color). **A** One frame from a movie of a cell expressing YFP-LDLR is shown. **B, C** High magnification images of the boxed dendrite in A shown before (**B**) and 4 minutes after addition of 50 mM NH4Cl (**C**), which greatly enhanced the fluorescence of intracellular vesicles containing the luminally tagged YFP-labeled constructs. **D** Individual frames from a movie illustrating organelle transport in a segment of dendrite (corresponding to the white line in A). **E** A kymograph illustrating organelle transport in the same segment. Kymographs show the maximal fluorescence intensity across the width of the neurite at each position along it (represented on the vertical axis) for each successive time point (shown along the horizontal axis). Diagonal lines represent moving vesicles, with a positive slope corresponding to movement away from the cell body; horizontal lines represent stationary structures. **F-I** As a control, we made two-color movies of cells cotransfected with TfR-YFP and TfR-CFP. A single movie frame for each color shows the overall similarity in the distribution of the YFP- and CFP-tagged proteins (**F, H**). Kymographs taken from the boxed region are shown in **G** and **I**. Moving vesicles (white lines on kymographs), including organelles undergoing anterograde or retrograde transport, were labeled with both markers. Stationary structures were also double labeled. A movie of organelle transport in the cell in **F** is provided in the Supplement (Movie 1). Scale bar: 5 μm

Figure S3. Transferrin uptake in cells expressing dendritic and axonal marker proteins. Cells expressing the indicated constructs were exposed to Alexa568 Transferrin (25 nM) for 30 minutes, then fixed, imaged and processed by deconvolution. **A, B** TfR-CFP and YFP-LDLR colocalized with Transferrin in many fluorescent structures in dendrites, although a few Transferrin-negative structures were also present (circles). **C** Organelles labeled by NgCAM-CFP seldom colocalized with Transferrin. In color overlays, Transferrin is shown in red and the coexpressed marker in green. All images show high-magnification views of dendrites. Scale bar: 2 μm.

Figure S4. Timing of initial arrival of constructs at the cell surface. Neurons were transfected with GFP-tagged versions of NgCAM (**A,B**), TfR (**C,D**), or LDLR (**E,F**). In order specifically label protein that had arrived at the cell surface, cells were exposed to Cy3-conjugated primary antibodies directed against extracellular epitopes specific for each construct. Antibody exposure began 1.5h after transfection and continued throughout the experiment. At 3.75h after transfection, cells were mounted in a live-cell imaging chamber containing Cy3-conjugated primary antibody and monitored for GFP and Cy3 fluorescence on the spinning disk confocal. By 4h after transfection (**A,C,E**), several cells showed bright GFP fluorescence in the Golgi region. A few of these also had low levels of antibody staining (**C,E**) By 5-6 hours, more cells showed GFP fluorescence and antibody staining was generally brighter (**B,D,F**).

**Supplementary Movies**

Two-color imaging of transport vesicles in living neurons

Movies were acquired from cells expressing pairs of CFP- and YFP-tagged marker proteins. In order to orient the viewer, the first few movies (1-3) are displayed sandwiched in between the corresponding kymographs taken from CFP (left) and YFP (right) channels. In addition, examples of anterogradely and retrogradely moving vesicles are pointed out in these movies by arrowheads, and scale bars (2 μm) are shown. Sequential 800 msec images (alternating between CFP and YFP fluorescence) were acquired for 48 seconds (60 frames total, 30 frames each color). The neurites in each movie were oriented with the distal end pointing upwards. The contrast was inverted so that fluorescent pixels appear dark. Movies are played back at 16x real speed. All supplemental movies were made and displayed using these parameters, except for Movie 4, in which sequential 600 msec exposures were acquired for 60 seconds (100 frames total, 50 frames each color); Movie 4 is played back 16x real time, like all other movies. Movies 1-3 were acquired on a wide-field epifluorescent microscope after 18-24h expression, Movies 4-6 were acquired with a spinning disk confocal microscope at about 4.5h after expression using the Golgi-block protocol from Figures 4-6.

**Movie 1** was taken from the boxed region of the cell coexpressing TfR-CFP and TfR-YFP in Supplementary Figure Figure 2(**F-I**). In both CFP and YFP channels of this movie, two prominent vesicles start from about the same position, but travel in opposite directions.

**Movie 2** was taken from a cell coexpressing NgCAM-CFP and YFP-LDLR. A section from a branched dendrite is shown, together with the kymograph from the diagonal branch. None of the vesicles in this dendrite was labeled by both markers.

**Movie 3** was taken from a cell coexpressing TfR-CFP and YFP-LDLR (dendrite 1 of the cell in Figure 3C and D). Most vesicles contained both markers. Three vesicles that show labeling with both proteins are highlighted by black arrowheads.

**Movie 4** was taken from a cell expressing GFP-LDLR for 3.5h at 37° C, then switched to 19° C for 1h, and finally warmed to 35° C 10 minutes before the start of the movie. Cells were exposed to Alexa568 Transferrin starting 1.5h after transfection and continuing through the movie. This two-color movie of GFP-LDLR and Alexa568 Transferrin shows no transport vesicles containing both markers.

**Movie 5** was taken from a cell coexpressing NgCAM and LDLR. No vesicles were labeled with both markers in this movie.

**Movie 6** was taken from a cell coexpressing NgCAM and LDLRmut. Many vesicles containing both markers can be observed.

Figure 1

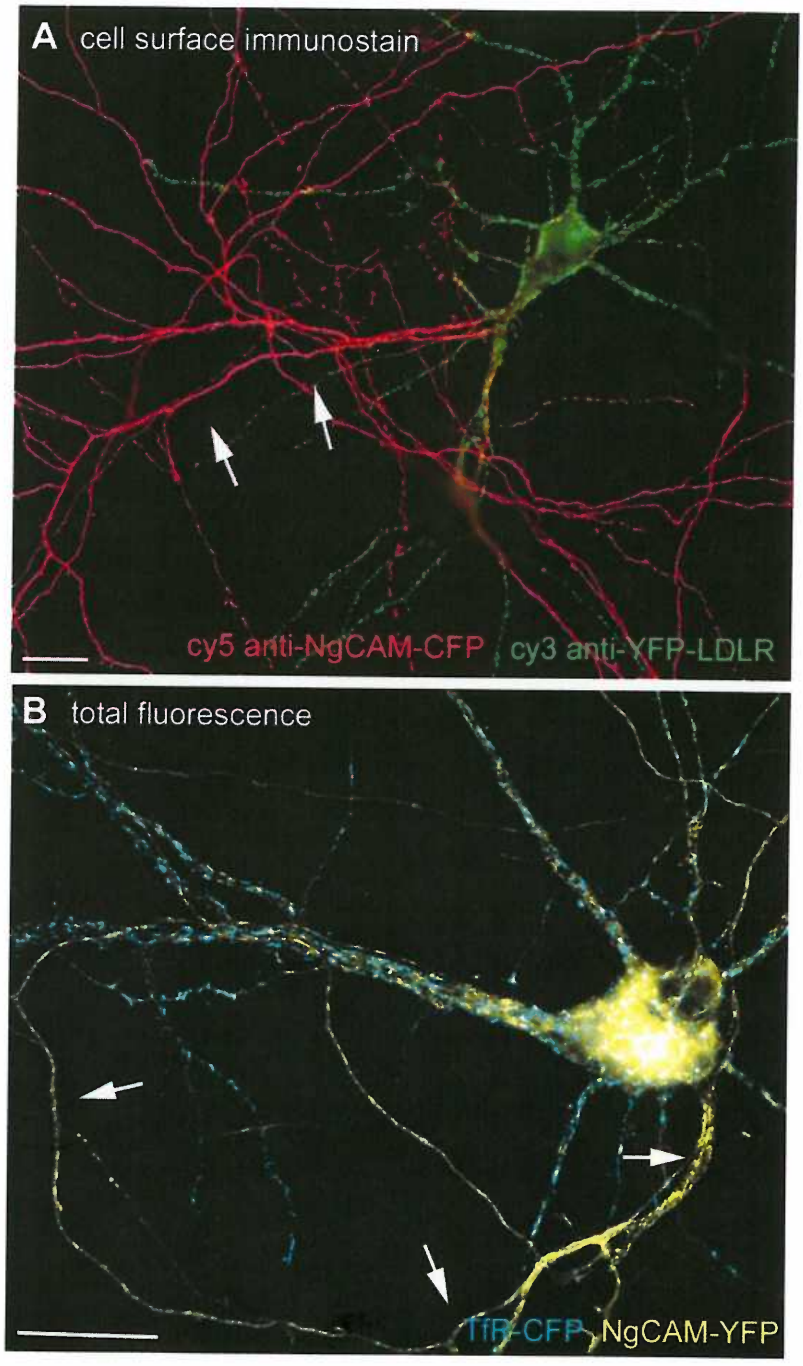
A cell surface immunostain
cy5 anti-NgCAM-CFP
cy3 anti-YFP-LDLR
B total fluorescence
TfR-CFP
NgCAM-YFP

Figure 2

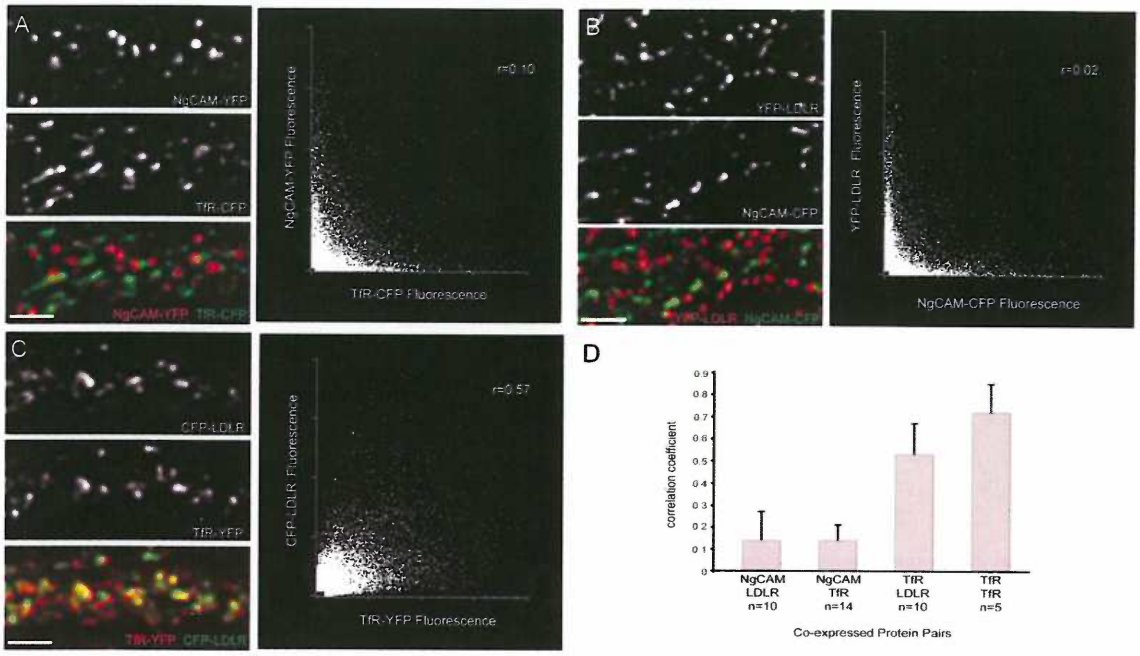
A
NgCAM-YFP
TfR-CFP
NgCAM-YFP TfR-CFP
r=0.10
NgCAM-YFP Fluorescence
TfR-CFP Fluorescence
B
YFP-LDLR
NgCAM-CFP
YFP-LDLR NgCAM-CFP
r=0.02
YFP-LDLR Fluorescence
NgCAM-CFP Fluorescence
C
CFP-LDLR
TfR-YFP
TfR-YFP CFP-LDLR
r=0.57
CFP-LDLR Fluorescence
TfR-YFP Fluorescence
D
correlation coefficient
0.9
0.8
0.7
0.6
0.5
0.4
0.3
0.2
0.1
0
NgCAM LDLR n=10
NgCAM TfR n=14
TfR LDLR n=10
TfR TfR n=5
Co-expressed Protein Pairs

Figure 3

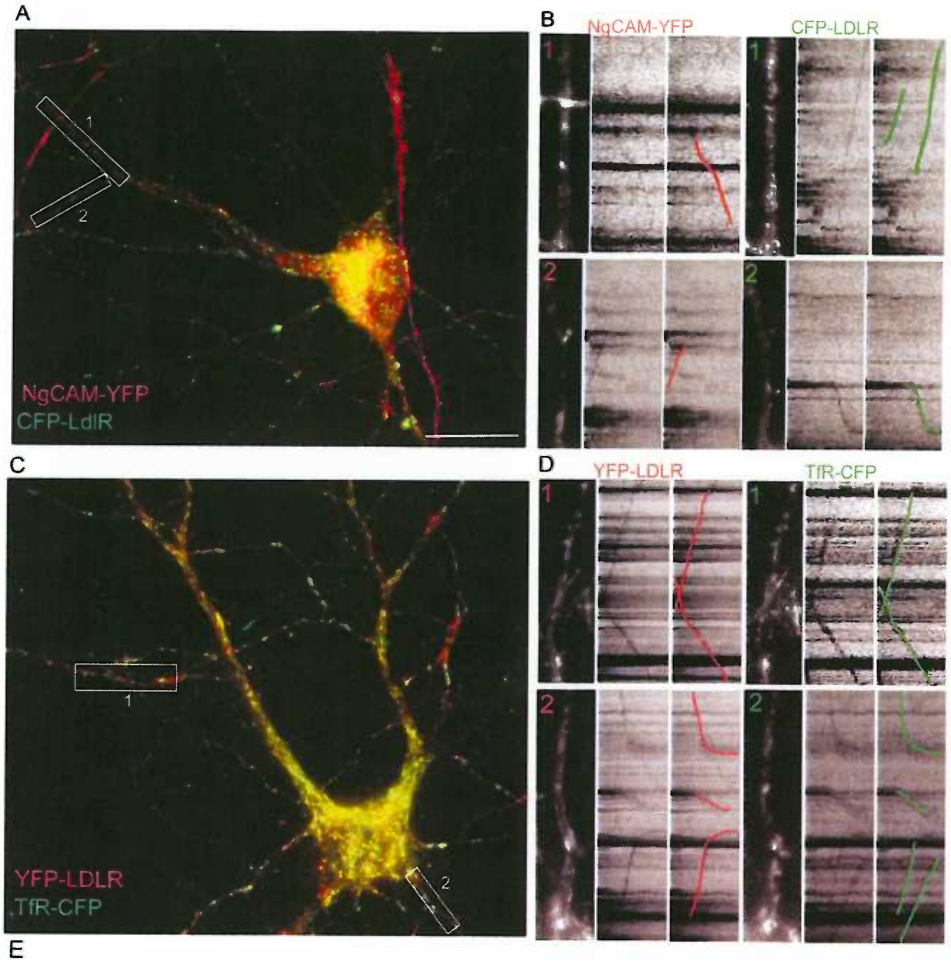
A
B
NgCAM-YFP
CFP-LDLR
NgCAM-YFP
CFP-LdlR
C
D
YFP-LDLR
TfR-CFP
YFP-LDLR
TfR-CFP
E
Colocalization in Moving Vesicles
% vesicles with both markers
100
80
60
40
20
0
NgCAM-CFP
YFP-LDLR
n=7(278)
TfR-CFP
YFP-LDLR
n=8(182)
TfR-CFP
TfR-YFP
n=9(109)
Co-expressed Protein Pairs

Figure 4

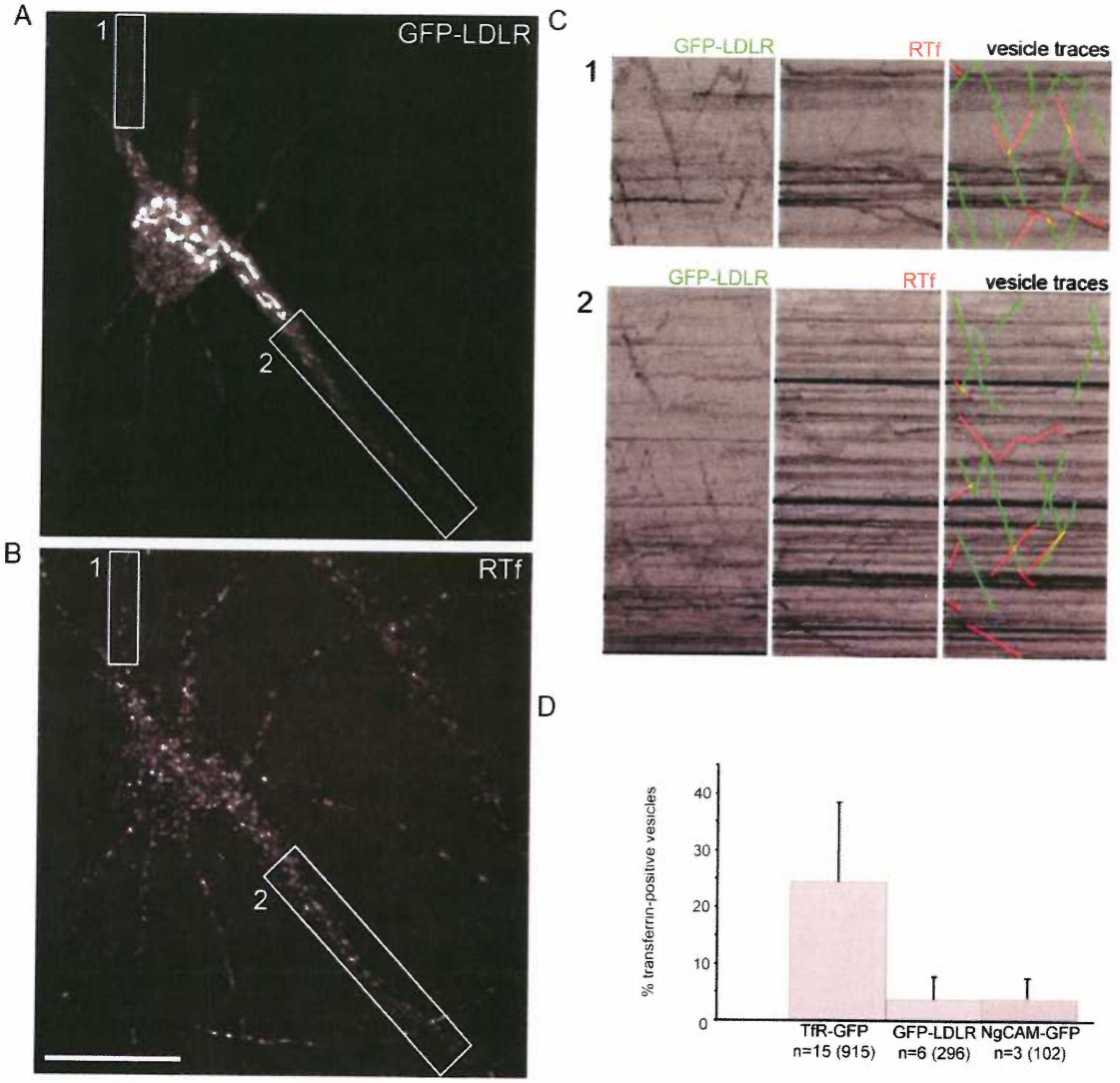
A
1
GFP-LDLR
2
B
1
RTf
2
C
GFP-LDLR
RTf
vesicle traces
1
GFP-LDLR
RTf
vesicle traces
2
D
% transferrin-positive vesicles
40
30
20
10
0
TfR-GFP
n=15 (915)
GFP-LDLR
n=6 (296)
NgCAM-GFP
n=3 (102)

Figure 5

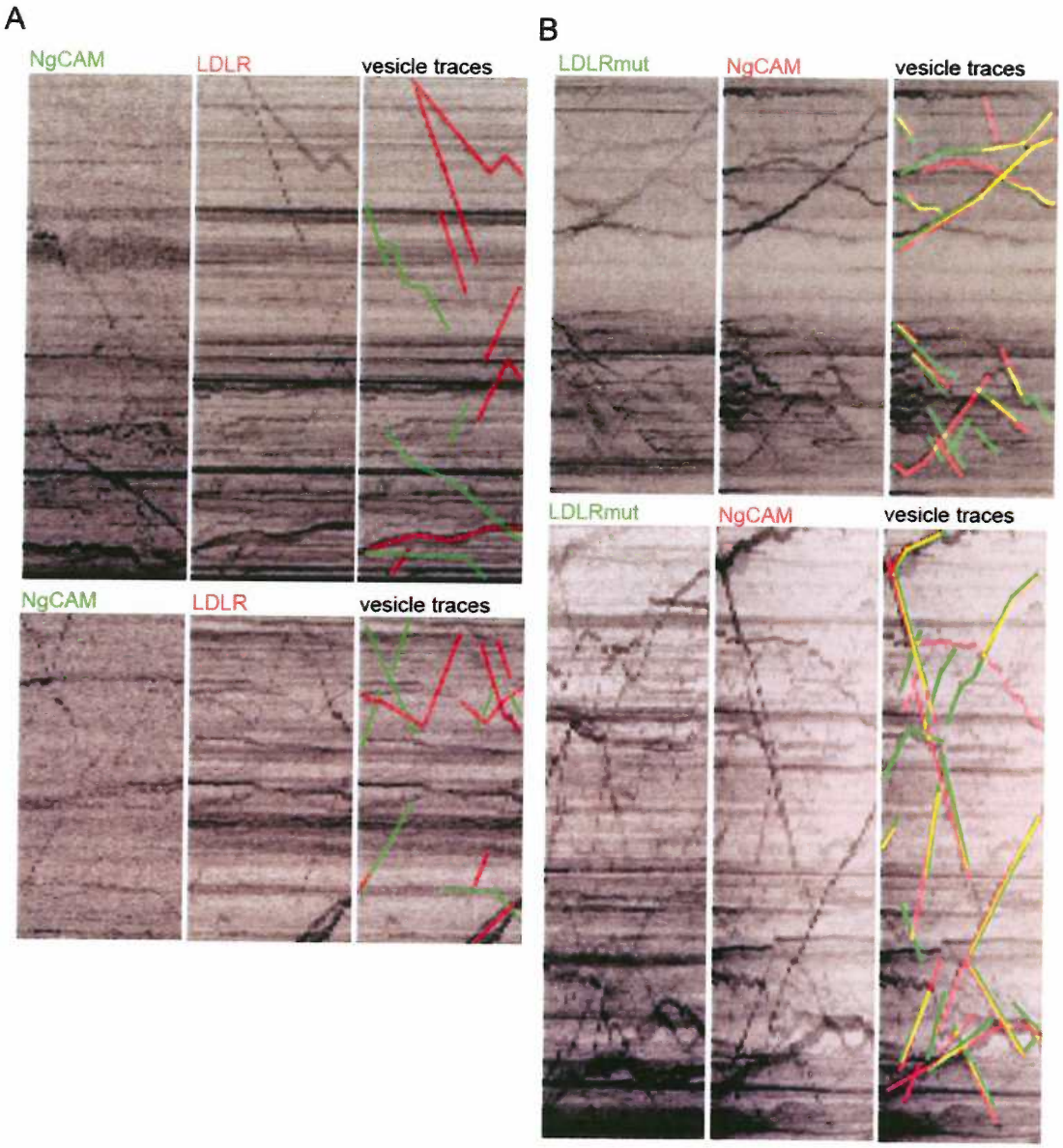
A
NgCAM
LDLR
vesicle traces
NgCAM
LDLR
vesicle traces
B
LDLRmut
NgCAM
vesicle traces
LDLRmut
NgCAM
vesicle traces

Figure 6

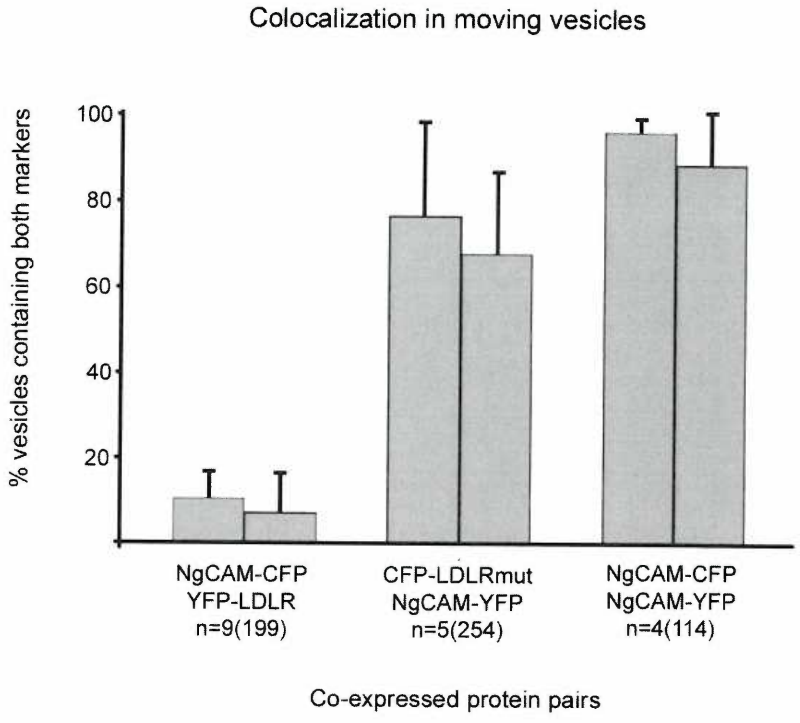
Colocalization in moving vesicles
% vesicles containing both markers
100
80
60
40
20
NgCAM-CFP
YFP-LDLR
n=9(199)
CFP-LDLRmut
NgCAM-YFP
n=5(254)
NgCAM-CFP
NgCAM-YFP
n=4(114)
Co-expressed protein pairs

Supplementary Figure 1

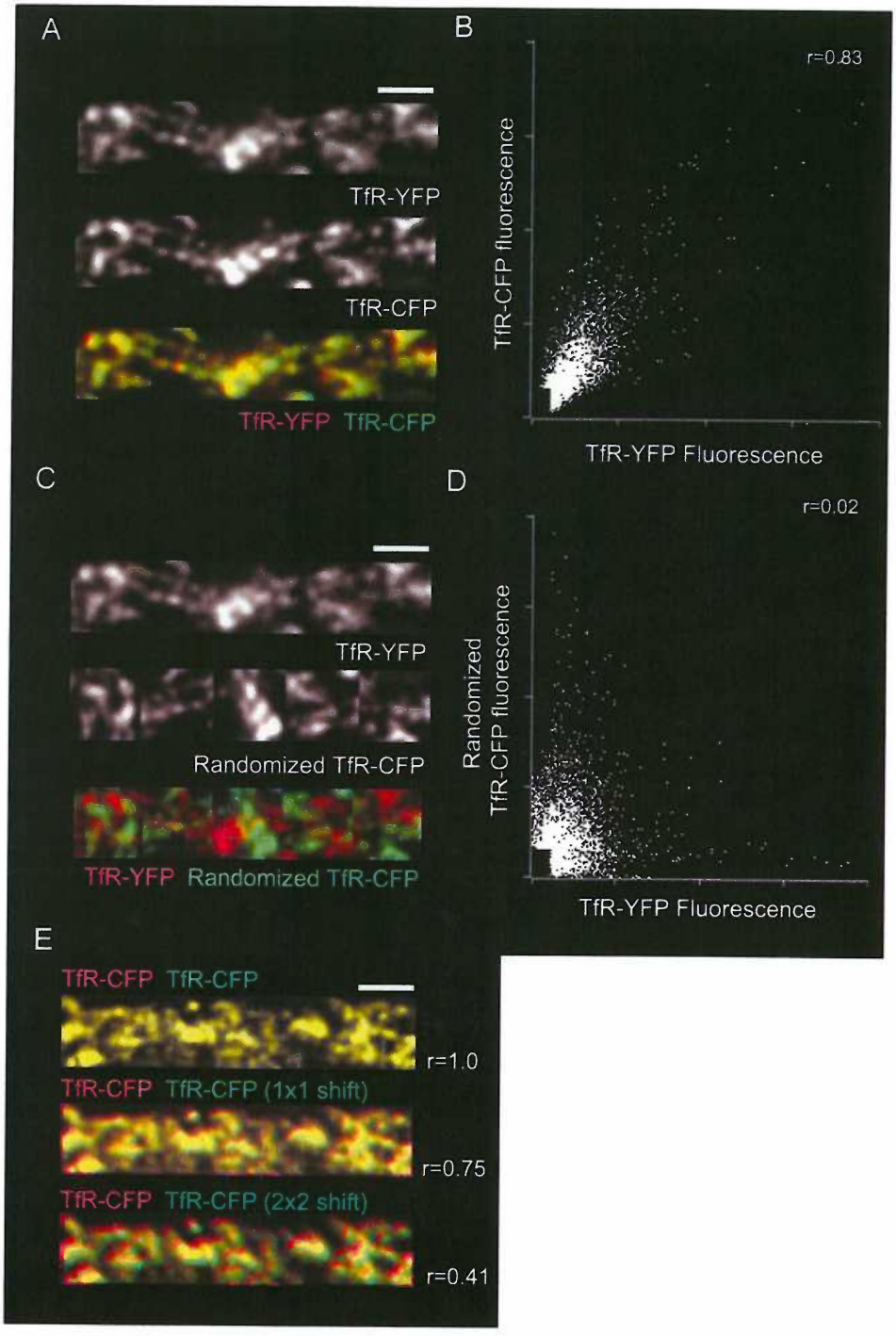

Supplementary Figure 2

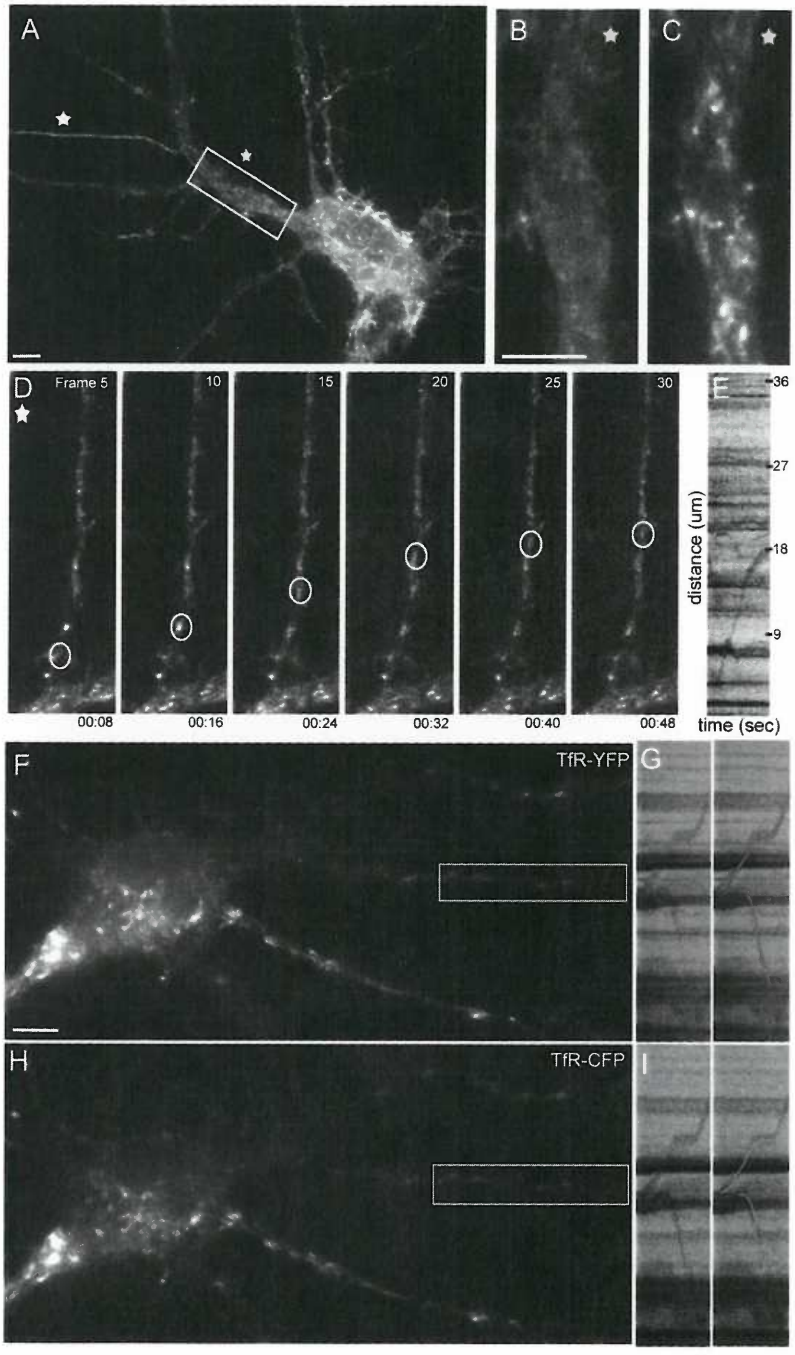

Supplementary Figure 3

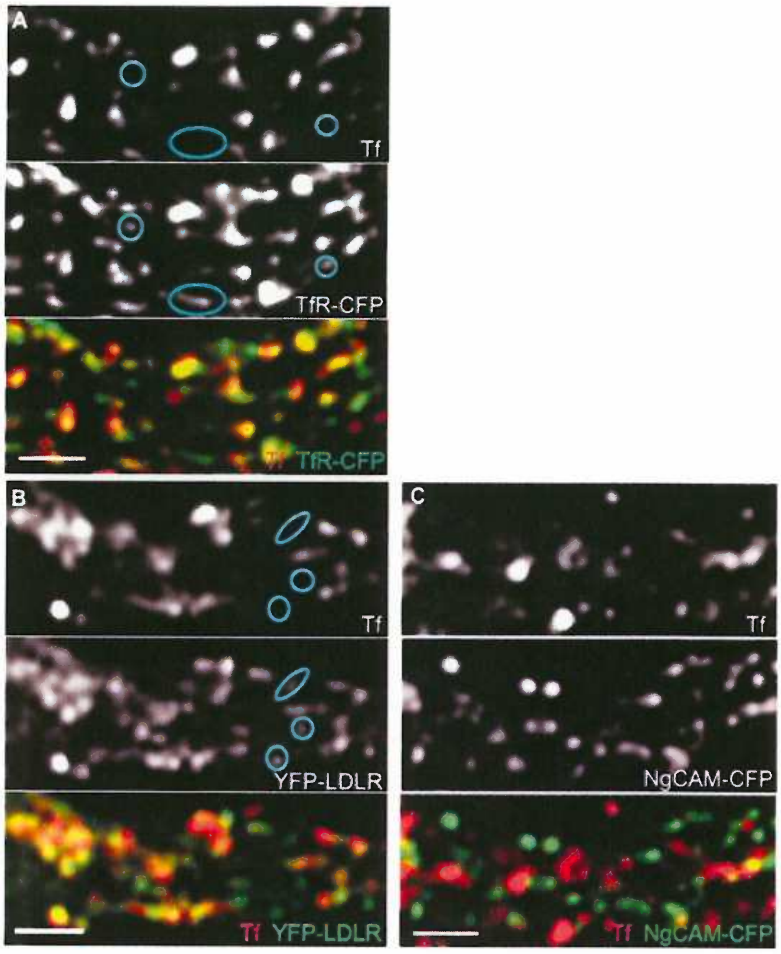

Supplementary Figure 4

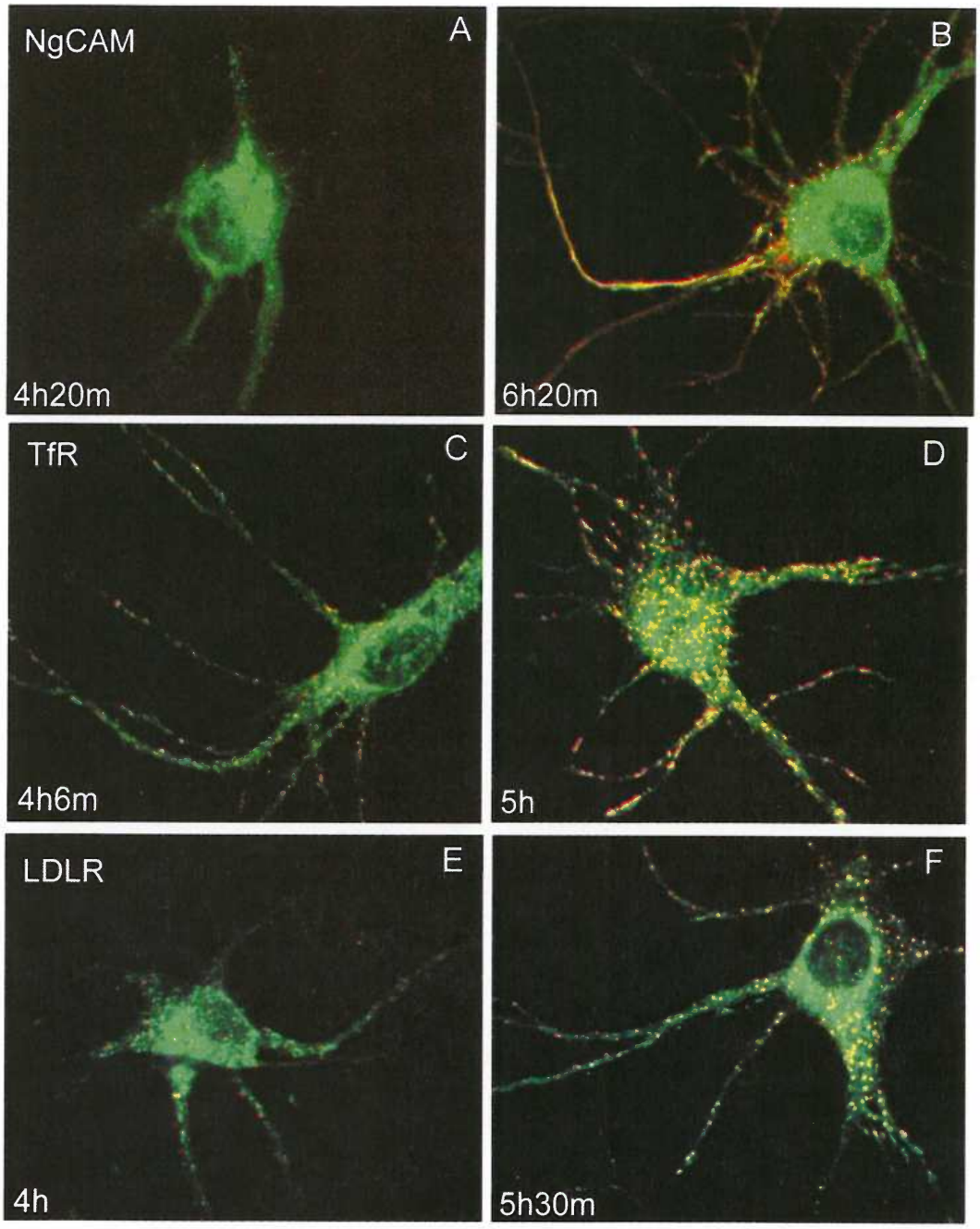

**Chapter 3**

# A Novel Sorting Motif in the Glutamate Transporter Excitatory Amino Acid Transporter 3 Directs Its Targeting in Madin-Darby Canine Kidney Cells and Hippocampal Neurons

Chialin Cheng[1], Greta Glover[2], Gary Banker[2], and Susan G. Amara[1]
[1] Howard Hughes Medical Institute and Vollum Institute and [2] Center for Research on Occupational and Environmental Toxicology, Oregon Health and Science University, Portland, Oregon 97239

key words: dendritic sorting signal; apical sorting signal; glutamate transporter; polarized trafficking; EAAT3; excitatory amino acid carrier

Published in: The Journal of Neuroscience, December 15, 2002, 22(24):10643-10652

In this chapter, I performed all experiments in hippocampal neurons, Chialin Cheng performed all experiments in MDCK epithelial cells, Barabara Smoody prepared hippocampal cultures.

**Abstract**

The glutamate transporter excitatory amino acid transporter 3 (EAAT3) is polarized to the apical surface in epithelial cells and localized to the dendritic compartment in hippocampal neurons, where it is clustered adjacent to postsynaptic sites. In this study, we analyzed the sequences in EAAT3 that are responsible for its polarized localization in Madin-Darby canine kidney (MDCK) cells and neurons. Confocal microscopy and cell surface biotinylation assays demonstrated that deletion of the EAAT3 C terminus or replacement of the C terminus of EAAT3 with the analogous region in EAAT1 eliminated apical localization in MDCK cells. The C terminus of EAAT3 was sufficient to redirect the basolateral-preferring EAAT1 and the nonpolarized EAAT2 to the apical surface. Using alanine substitution mutants, we identified a short peptide motif in the cytoplasmic C-terminal region of EAAT3 that directs its apical localization in MDCK cells. Mutation of this sequence also impairs dendritic targeting of EAAT3 in hippocampal neurons but does not interfere with the clustering of EAAT3 on dendritic spines and filopodia. These data provide the first evidence that an identical cytoplasmic motif can direct apical targeting in epithelia and somatodendritic targeting in neurons. Moreover, our results demonstrate that the two fundamental features of the localization of EAAT3 in neurons, its restriction to the somatodendritic domain and its clustering near postsynaptic sites, are mediated by distinct molecular mechanisms.

## Introduction

The actions of glutamate, the major excitatory neurotransmitter in the mammalian CNS, are terminated by sodium-dependent glutamate transporters located on the plasma membrane of neurons and glia. Glutamate transporters constitute a distinct gene family of which five human glutamate transporters [excitatory amino acid transporters 1-5 (EAAT1-5)] have been identified (Arriza et al., 1997; Arriza et al., 1994; Fairman et al., 1995). The rodent homologues of EAAT1 (glutamate/aspartate transporter) and EAAT2 (glutamate transporter-1) are primarily expressed in glia (Lehre et al., 1995; Rothstein et al., 1994), whereas EAAT3 (EAAC1) and EAAT4 are expressed predominantly in neurons(Dehnes et al., 1998; Furuta et al., 1997). EAAT3 is widely expressed in the CNS as well as in epithelial cells in the kidney and gut. Surprisingly, the carrier is not found on the axons or presynaptic terminals, which release glutamate. Instead, EAAT3 and EAAT4 are targeted to the somatodendritic domain and concentrated near postsynaptic sites (Coco et al., 1997; Conti et al., 1998; Dehnes et al., 1998; Furuta et al., 1997; He et al., 2001) where they are thought to regulate synaptic signaling by limiting the diffusion of glutamate to extrasynaptic receptors (Brasnjo and Otis, 2001).

The Madin-Darby canine kidney (MDCK) cell line has been used extensively as a simple system to study the sorting of polarized membrane proteins (Kryl et al., 1999; Martinez-Maza et al., 2001; McCarthy et al., 2001; Poyatos et al., 2000; Scannevin et al., 1996). In MDCK cells, apical and basolateral proteins are segregated from each other as they exit the trans-Golgi network and then subsequently delivered to the appropriate

surface. In the case of basolateral proteins, sorting depends on short motifs present in the cytoplasmic tails of the proteins. Apical sorting is less well understood. Some proposed apical sorting mechanisms include glycosylphosphatidylinositol linkage, raft association, and glycosylation (Winckler and Mellman, 1999). More recently, evidence has emerged that cytoplasmic regions of proteins may also contain information important for apical sorting. For instance, a 39-amino acid sequence in the cytoplasmic C terminus of rhodopsin directs its apical localization in MDCK cells (Chuang and Sung, 1998). Similarly, a 32-amino acid sequence at the C terminus of GABA transporter 3 (GAT-3) confers apical localization (Muth et al., 1998). This region contains a motif that may bind to postsynaptic density-95/*Drosophila* disc large protein/zona occludens protein 1 domains (Muth et al., 1998), but it is not known whether this mediates its targeting. Discrete, well defined sorting motifs have yet to be defined in these, or other, apically targeted proteins.

Many proteins that are dendritically localized in neurons are concentrated on the basolateral surface of MDCK cells, and in some cases, the same motifs mediate sorting in both cell types. The endogenous localization of EAAT3 represents an exception to this idea: EAAT3 is present at the apical membrane in kidney cells and on the soma and dendrites of neurons (Coco et al., 1997; Shayakul et al., 1997). If the sorting of EAAT3 depends on its association with lipid rafts or its glycosylation, as observed for some apical proteins, this would be the first instance in which such signals mediated dendritic targeting in neurons. It would be equally unusual to find a cytoplasmic, dendritic targeting motif that mediated apical sorting in MDCK cells. Alternatively, it may be that

different motifs mediate sorting in the two cell types. To elucidate the motifs involved in the sorting of EAAT3 and to resolve this paradox, we have investigated the sorting of EAAT3 in MDCK cells and in hippocampal neurons. By expressing a series of mutated proteins, we have identified a novel 11-amino acid motif in the cytoplasmic tail of EAAT3 that mediates its apical sorting in MDCK cells and its somatodendritic localization in hippocampal neurons.

## Materials and Methods

### Cell Culture

MDCK cells (American Type Culture Collection, Manassas, VA) were maintained in DMEM (Invitrogen, Carlsbad, CA) supplemented with 10% fetal bovine serum, 89 U/ml penicillin, and 89 µg/ml streptomycin. Media for stable MDCK cell lines were further supplemented with 500 µg/ml geneticin (G418) (Invitrogen). The cells were plated at high density onto 12 or 24 mm Transwell-COL filters (Costar, Cambridge, MA) and grown to confluency before use. Primary hippocampal cultures were prepared from embryonic day 18 rats as described previously (Banker and Goslin, 1998). Neurons were plated at 300,000 cells per 6 cm dish.

### Mutagenesis

Various PCR-based mutagenesis protocols were used to create the mutant constructs. All the mutant constructs were sequenced to confirm that no unintended mutations were introduced. All constructs were subcloned into the pEGFPC vector

(Clontech, Palo Alto, CA). To construct the EAAT1/EAAT3 C-terminal chimeras (E1CT3 and E3CT1), silent mutations at $E^{501}L^{502}$ and $L^{470}$ of EAAT1 and EAAT3 cDNAs, respectively, were introduced by using the three-primer PCR mutagenesis technique (Seal and Amara, 1998) to create the SacI restriction site. The C termini of EAAT1 and EAAT3 were exchanged at the SacI restriction site to produce the resultant E1CT3 and E3CT1 constructs. EAAT3 C-terminal deletion constructs were made with the last amino acid of the mutant being the following: $E^{469}$, $P^{484}$, $S^{497}$, and $V^{510}$ for E3470-524, E3485-524, E3498-524, and E3511-524, respectively. The constructs containing C-terminal regions of EAAT3 fused to EAAT2 were created by attaching EAAT3 C-terminal cDNA fragments to full-length EAAT2 cDNA separated by a linker (containing the sequence GCC GGA TCT GCC). The amino acid residues of EAAT3 contained in the EAAT3 C-terminal fragments are denoted in parentheses. For instance, E2-3(469-524) contains the amino acids $E^{469}$-$F^{524}$ of EAAT3 fused to full-length EAAT2. The QuikChange site-directed mutagenesis kit from Stratagene (La Jolla, CA) was used to create the triple or double alanine substitution mutants. The template was green fluorescent protein (GFP)-E2-3(498-524), and primers were created with the least nucleotide changes to the alanine codon.

Stable transfection into MDCK cells

MDCK cells (at 50-80% confluency) in each well of a six-well plate were transfected with a mixture containing 2 μg of DNA and 40 μg of LipofectAMINE (Invitrogen) in serum-free DMEM. After 5 hr, 10% fetal bovine serum, 89 U/ml

penicillin, and 89 μg/ml streptomycin were added to the mixture. Twenty-four hours after the start of transfection, the DNA-LipofectAMINE-DMEM mixture was replaced with fresh DMEM containing serum, penicillin, streptomycin, and 500 μg/ml G418 (G418 media). Forty-eight to 72 hr after the start of transfection, three wells containing the greatest number of fluorescent cells were replated at low density and placed in G418 media for 2-3 weeks to select for stably transfected cell lines. G418-resistant cell lines were screened for detectable GFP fluorescence, and cell lines with higher GFP fluorescence levels were chosen for use in this study. For each construct, results were verified with at least two independently derived stable cell lines.

Transient transfection into MDCK cells

For each construct to be transfected, 1.2 μg of DNA was combined with 2.4 μg of LipofectAMINE 2000 (Invitrogen) in serum-free DMEM and incubated at room temperature for 30 min. The mixture was then combined with MDCK cells in media and plated at high density onto a 12 mm Transwell-COL filter. The bottom of the transwell filter was filled with media. Twenty-four hours after the start of transfection, the wells of transfected cells were replaced with fresh media. The cells were allowed to grow to confluency for a further 48-72 hr before use.

Transient transfection of dissociated hippocampal neuronal cultures.

Constructs were introduced into cultures at 8-10 d *in vitro* using Effectene-mediated transfection (Qiagen, Valencia, CA). Briefly, for each construct, 1 μg of DNA

was mixed with 8 µl of enhancer and then 10 µl of Effectene according to the manufacturer's instructions. After addition of the DNA-Effectene complexes to the media, the cells were incubated for 2 or 9 d at 37°C. The cells were then fixed in 4% paraformaldehyde and 4% sucrose and permeabilized in 0.25% Triton X-100, and coverslips were mounted on slides using elvanol. GFP fluorescence was used to measure cell surface distribution. Expression of the constructs for a minimum of 2 d allowed for accumulation at the cell surface and minimized the contribution of intracellular fluorescence. Under these conditions, the GFP signal appears enriched at the surface when examined at high magnification. Moreover, expression of the EAAT constructs had reached a steady state at these times.

Immunohistochemistry and confocal microscopic imaging

All steps were performed at room temperature. The cells were initially rinsed twice with PBS (containing 100 µM $CaCl_2$ and 1 mM $MgCl_2$) before they were fixed with 4% paraformaldehyde (with 50 mM HEPES in PBS, pH 7.4) for 20 min. Then the cells were rinsed twice with PBS and incubated with a blocking and permeabilization solution containing 5% horse serum, 1% BSA, and 0.2% Triton X-100 in PBS for 30 min. Subsequently, staining for E-cadherin was performed with the monoclonal antibody anti-uvomorulin clone DECMA-1 (Sigma, St. Louis, MO). The cells were incubated in the primary antibody for 2-3 hr. The cells were washed three times for 3 min with PBS and probed with rhodamine red-conjugated secondary antibody (Jackson ImmunoResearch, West Grove, PA). The cells were washed three times for 3 min with PBS before the filter

containing the cells was excised from its support and mounted onto a slide with ProLong antifade reagent (Molecular Probes, Eugene, OR). Images were constructed by measuring the fluorescence signal using confocal microscopy (MRC 1024 system; Bio-Rad, Hercules, CA) with excitation lines of 488 and 568 nm for the GFP and rhodamine signals, respectively. The *z*-series was collected by initially focusing on the middle section of the cells (position 0) and scanning 8 μm above to 8 μm below this plane at 0.1 μm intervals.

Cell surface biotinylation assay

Cell surface expression of the EAAT constructs was assayed with modifications of the method described previously (Daniels and Amara, 1998). All steps before the Western blot analysis were performed at 4°C unless otherwise specified. Briefly, the cells were washed once quickly with room temperature PBS and then three times for 10 min with cold PBS. The cells were then incubated with 2 mg/ml sulfosuccinimidyl 2-(biotinamido)ethyl-1,3-dithiopropionate (sulfo-NHS-SS-biotin) (Pierce, Rockford, IL) in biotinylation buffer (in mM: 2 $CaCl_2$, 150 NaCl, and 10 triethanolamine, pH 7.5) for 40 min placed either on the top or bottom of the transwell filter to assay for apical or basolateral expression of the transporters, respectively. The side not incubated with sulfo-NHS-SS biotin was incubated with biotinylation buffer only. The reaction was quenched by incubation with 100 mM glycine in PBS for 20 min. The cells were washed with PBS and then lysed with lysis buffer [1% Triton X-100, 150 mM NaCl, 5 mM EDTA, and 50 mM Tris, pH 7.5, containing a protease inhibitor mixture (1×; Roche Molecular

Biochemicals, Indianapolis, IN)], and the cell lysate was collected after centrifugation at 14,000 × *g* for 10 min. The cell lysate was incubated with Ultralink immobilized NeutrAvidin beads (Pierce) for 2-3 hr. The beads were separated from the supernatant by centrifugation at 5000 × *g* for 15 min. The beads contained cell surface proteins, whereas the supernatant contained cytosolic proteins. The beads were washed three times with lysis buffer, twice with high-salt wash buffer (0.1% Triton X-100, 500 mM NaCl, 5 mM EDTA, and 50 mM Tris, pH 7.5), and once with no-salt wash buffer (50 mM Tris, pH 7.5). Subsequently, the proteins on the beads were released by incubation with SDS loading buffer containing 200 mM DTT. The proteins were separated on 8% polyacrylamide gels and then transferred onto Immobilon-P blots (Millipore, Bedford, MA). The blots were probed for the expression of EAATs with either polyclonal antibodies to the C terminus of the EAATs or a monoclonal antibody to GFP (JL-8; Clontech) and visualized with horseradish peroxidase-conjugated secondary antibody and chemiluminescent reagent (PerkinElmer, Beverly, MA). Blots were exposed to film to obtain nonsaturated exposures, which could be used for densitometric quantitation of chemiluminescent signals. Films were scanned using a Duoscan F40 (Agfa, Ridgefield Park, NJ), and band intensities in each lane (same area size in each lane) were background-subtracted and quantitated by using the software program TINA (Fuji Medical Systems, Stamford, CT). Statistical significance was determined with the Newman-Keuls multiple-comparisons test for independent groups using WINKS evaluation software (Texasoft, Cedar Hill, TX).

Imaging and quantitation of GFP fluorescence in hippocampal neurons

Neurons were chosen for analysis only if they were sufficiently separated from other transfected cells to ensure that all labeled processes arose from the cell pictured. Images were acquired on a Leica (Nussloch, Germany) DMIRBE microscope linked to a Princeton Instruments Micromax chilled CCD camera controlled by Metamorph imaging software (Universal Imaging, Downingtown, PA). For cells at 11 d *in vitro*, low-magnification images were acquired using a 16×, 0.5 numerical aperture (NA) Plan Fluotar objective, and high-magnification images for quantification were acquired using a 63×, 1.32 NA Plan Apo objective. Cells at 19 d *in vitro* were imaged on the same microscope at 63× by acquiring a through-focal series of images at 0.2 μm intervals (~30 planes). Stacks of these images were subject to constrained-iterative deconvolution (15 iterations) using Deltavision SoftWoRx 2.5 software (Applied Precision, Issaquah, WA) based on the point spread function determined for our microscope. High-magnification images of 19 d *in vitro* cells are displayed as single planes of the resulting deconvolved stacks.

Images for quantification were corrected for background fluorescence and uneven field illumination. The average fluorescence intensity in axons and dendrites was obtained by drawing a series of ~10 one-pixel-wide lines down the center of processes on corrected high-magnification digital images. For each cell, the fluorescence for each line in the axons and dendrites was averaged to obtain the final values for axon and dendrite intensity. These averages were used to calculate the axon/dendrite ratio. Theoretically, one would expect a uniformly distributed protein to have an axon/dendrite ratio of 1. In

practice, the axon/dendrite ratio for nonpolarized proteins averages between 0.5 and 1. This is probably because of a greater contribution of out-of-focus fluorescence in the thicker dendrites compared with the relatively thin axons. Statistical significance of differences between groups was determined by performing the Newman-Keuls multiple-comparisons test for independent groups using WINKS evaluation software.

## Results

### Localization of wild-type EAATs in MDCK cells

We stably expressed EAAT1-5 tagged on the N terminus with GFP in polarized MDCK cells and examined their localization using confocal microscopy and cell surface biotinylation. EAAT3 was extremely polarized to the apical surface, whereas EAAT1 and EAAT2 were expressed at both the apical and basolateral surfaces (Figs. 1, 2B) with EAAT1 more basolateral-preferring than EAAT2 ($22 \pm 8\%$ apical versus $54 \pm 1\%$ apical; Table 1). It is important to note that our stably transfected, GFP-tagged EAAT3 retained the normal apical localization of endogenous EAAT3 in kidney epithelial cells (Shayakul et al., 1997). EAAT4 and EAAT5 were expressed at lower levels than the other EAATs, but they appeared to be present at both cell surfaces (data not shown). Therefore, EAAT3 is the only glutamate transporter that is completely polarized in MDCK cells.

The C-terminal motif directs apical localization of EAAT3 in MDCK cells

To identify the region of EAAT3 important for its apical localization, we made chimeras between EAAT1 and EAAT3, exchanging the three large less conserved regions: the N terminus, the large second extracellular loop (which contains consensus N-linked glycosylation sites), and the C terminus (Fig. 2A). Replacing the C terminus of EAAT3 with the C terminus of EAAT1 (E3CT1) abolished apical targeting (Figs. 2B, 3; Table 1). Conversely, replacing the C terminus of EAAT1 with the analogous C-terminal region of EAAT3 (E1CT3) conferred specific apical localization, changing from 22 ± 8% apical localization of wild-type EAAT1 to 97 ± 1% apical localization of E1CT3 (Table 1). Replacing the large second extracellular loop or the N-terminal region of EAAT3 with the corresponding regions of EAAT1 did not affect the polarization of EAAT3 (although the chimera including the N-terminal region of EAAT1 showed little cell surface expression). Replacing these domains of EAAT1 with the corresponding regions of EAAT3 did not cause EAAT1 to become apically localized. These substitutions indicated that the cytoplasmic C terminus of EAAT3 contains information important for its apical localization.

To further test the role of the EAAT3 C terminus, we constructed addition and deletion mutants. We first tested whether this small region of EAAT3 could redirect a nonpolarized protein to the apical domain. The addition of the C terminus of EAAT3 to full-length EAAT2 [E2-3(469-524)] changed its localization from nonpolarized to apically polarized as judged by cell surface biotinylation assays (Fig. 3A, Table 1) and

confocal microscopy (Fig. 3B). The C terminus of EAAT3 similarly redirected the taurine transporter to the apical surface (data not shown). Conversely, deleting the C terminus of EAAT3 (E3470-524) resulted in a nonpolarized localization (54 ± 3% apical); this mutant could be detected at both the basolateral and apical surfaces (Figs. 2B, 3). Together, the results from stably transfected chimeric, addition, and deletion mutants in MDCK cells demonstrate that the C terminus of EAAT3 is necessary for its apical sorting and sufficient to confer apical localization on a nonpolarized protein.

Next, we sought to narrow down the region within the C terminus of EAAT3 that is important for its apical localization. First, we made successively smaller truncations of the C terminus of EAAT3. All the truncated EAAT3 mutants have reduced apical localization (Fig. 2B, Table 1). Subsequent analyses (see next paragraph) showed that all of the truncations eliminated all or part of the sequence required for apical sorting. We also used a complementary approach of adding successively smaller regions of the EAAT3 C terminus to the end of full-length EAAT2. This strategy revealed the importance of the region between the last 27 and 14 amino acids of EAAT3. The mutant E2-3(498-524) showed an apical localization, whereas E2-3(511-524) had a significantly less polarized distribution (Figs. 2B, 4; Table 1). Similar results were found when the same regions of the C terminus of EAAT3 were fused to the full-length taurine transporter (data not shown). These results show that amino acids between $D^{498}$ and $D^{511}$ of the C terminus of EAAT3 contain an apical localization signal.

We used two additional, complementary methods to pinpoint residues within the 14 amino acids of the EAAT3 C terminus responsible for apical targeting. For these experiments, constructs were expressed transiently, and localization was assessed by confocal microscopy. First, we examined constructs of EAAT2 fused to short segments from the C terminus of EAAT3 (Fig. 5A; see supplemental data on-line at www.jneurosci.org). Constructs containing residues $D^{498}$-$V^{510}$ were apically polarized, whereas constructs containing residues upstream of $V^{504}$ were not. This indicates that residues $N^{505}$-$V^{510}$ (NGGFAV) are crucial for apical localization. Second, we made sequential triple or double alanine substitutions in the EAAT3 region of the mutant consisting of EAAT2 attached to amino acids $D^{498}$-$F^{524}$ of EAAT3 [E2-3(498-524)] (Fig. 5). The substitution with three alanine residues between amino acids $V^{504}$ and $A^{509}$ disrupted apical localization; substitution of amino acids $K^{501}$-$Y^{503}$ had a smaller effect (40% of transfected cells exhibited a polarized distribution). Alanine substitutions N-terminal to amino acid $K^{501}$ or C-terminal to amino acid $A^{509}$ did not disrupt apical localization. Next, we examined double alanine substitutions between amino acids $V^{504}$ and $D^{511}$. Substitution of the residues $V^{504}N^{505}$ and $F^{508}A^{509}$ resulted in loss of apical polarity. Substitution of residues $V^{510}D^{511}$ slightly disrupted the polarized distribution (70% of the transfected cells still showed apical localization). Replacing residues $G^{506}G^{507}$ with alanine did not alter apical localization of the mutant protein, but this may be because alanine and glycine are similar in structure. Substituting bulkier amino acid residues at positions 506 and 507 may have an impact on the polarity of EAAT3. The substitution of $A^{509}$ with serine (the rat homolog of EAAT3 has a serine at this position)

did not alter the apical localization of the mutant construct (data not shown). Thus, the residues $V^{504}N^{505}$ and $F^{508}A^{509}$ within the motif are critical in apical sorting, whereas the neighboring residues may influence the specific localization motif. The apical localization sequence motif is KSYVNGGFAVD (amino acids $K^{501}$-$D^{511}$).

The C-terminal sorting motif targets EAAT3 to the somatodendritic region in neurons

Next, we tested whether the apical targeting motif in EAAT3 also directs the localization of EAAT3 in neurons. We transfected both wild-type and mutated EAATs tagged with GFP or yellow fluorescent protein (YFP) into polarized neurons in primary hippocampal cultures. We quantified the average fluorescence in axons and dendrites for each cell and used the ratio of axon to dendrite fluorescence as a measure of polarity. The wild-type EAAT3-YFP was extremely polarized to dendrites (Figs. 6A, 7B), with an average axon/dendrite ratio of $0.06 \pm 0.02$ (Table 2), a value comparable with that of other dendritically polarized proteins such as transferrin and low density lipoprotein receptors (G. Banker, unpublished observations). In older neurons (19 d *in vitro*), which are highly innervated, EAAT3 was present in clusters on the dendritic surface and on spines and filopodia (Fig. 7C). Some of these clusters lie adjacent to synaptophysin-positive presynaptic specializations (data not shown), consistent with the postsynaptic localization of EAAT3 that has been reported previously. Thus, in all respects, transfected GFP- or YFP-tagged EAAT3 showed the same polarized distribution in neurons as for endogenous EAAT3 (Coco et al., 1997). When live cells were imaged, transport of EAAT3 carriers was readily observed within the dendrites, but no carriers were visible in

the axon (data not shown). Thus in neurons, the polarization of EAAT3 in the dendritic membrane reflects its selective delivery to dendrites, not its selective retention in the dendritic membrane.

In contrast, two EAAT3 C-terminal truncation mutants lacking the apical-targeting motif (E3470-524 and E3485-524) were significantly less polarized (average axon/dendrite ratios, 0.28 ± 0.03 and 0.29 ± 0.05, respectively). Moreover, the substitution of residues 504-509 within the sorting motif of EAAT3 with alanines [E3(504-509AAAAAA)] disrupted somatodendritic polarity to the same extent as deleting the entire cytoplasmic tail (average axon/dendrite ratio, 0.26 ± 0.02). In all cases, mutant EAAT3s extended throughout the entire axonal arbor, a result not observed with the wild-type protein. However, disruption of the sorting motif in EAAT3 did not result in a complete loss of polarity (compare with EAAT2, whose axon/dendrite ratio was 0.68). Therefore, other regions of EAAT3 may also contain dendritic targeting information. Although such mutations disrupted the polarization of EAAT3, they did not prevent its clustering on dendritic spines (Fig. 7F). These results suggest that the apical sorting signal is not required for the synaptic clustering of EAAT3. Rather, these results show that the apical sorting motif in EAAT3 is responsible for its dendritic targeting in neurons.

We next investigated whether adding the EAAT3 sorting motif to a uniformly distributed protein was sufficient to cause its redistribution to the dendrites. When EAAT2 was expressed in hippocampal neurons, it was approximately equally distributed in axons and dendrites, exhibiting an average axon/dendrite ratio of 0.68 ± 0.09 (Figs. 6D,

7D; Table 2), a value comparable with that found for nonpolarized proteins such as NgCAM-related cell adhesion molecule and CD8 (B. Sampo and G. Banker, unpublished observations). To test whether the EAAT3 sorting motif could redirect EAAT2 to the dendrite, we fused the last 27 amino acids of EAAT3 (containing the sorting motif) to full-length EAAT2 [E2-3(498-524)]. E2-3(498-524) was significantly more dendritic than wild-type EAAT2 (axon/dendrite ratio, 0.31 ± 0.04) but was less polarized than wild-type EAAT3. A similar mutant, which differed only in that alanines were substituted for residues 504-506 within the sorting motif [E2-3(498-524:504-506AAA)], was as nonpolarized as wild-type EAAT2 (axon/dendrite ratio, 0.82 ± 0.10). This indicates that the EAAT3 sorting motif has some ability to redirect a uniform protein in neurons but is not sufficient to completely redirect EAAT2, as it is in MDCK cells. It may be that EAAT2 itself contains its own sorting information that influences its localization in neurons and thus competes with the EAAT3 motif.

Together, our results clearly show that EAAT3 contains a sorting motif in its cytoplasmic tail. This motif, KSYVNGGFAVD, directs the apical localization of EAAT3 in MDCK cells and is required for its dendritic localization in hippocampal neurons.

**Discussion**

In this study, we identified a novel sorting motif in the cytoplasmic C-terminal region of EAAT3 (KSYVNGGFAVD) that directs its specific localization to the apical

domain of MDCK cells and the somatodendritic region of hippocampal neurons. This is the first well defined motif known to be required for apical sorting in MDCK cells and dendritic sorting in hippocampal neurons and capable of redirecting the localization of nonpolarized proteins to these domains. A database search did not reveal any other known membrane proteins that contain the motif VNGGFA, but other epithelial sorting motifs shared by different proteins have proved difficult to identify solely on the basis of the amino acid sequence.

The EAAT3 sorting motif is one of several different motifs found in the cytoplasmic tails of neuronal proteins that target them to dendrites (Jareb and Banker, 1998; Poyatos et al., 2000; Ruberti and Dotti, 2000). It is, however, one of the first instances of a defined cytoplasmic motif that mediates apical sorting in MDCK cells. Traditionally, it has been thought that basolateral and dendritic sorting shared many common features, as did apical and axonal sorting (Dotti and Simons, 1990). Over the past few years, it has become clear that apical proteins are not always segregated to the axonal domain in neurons. For example, other amino acid transporters, such as GAT-3 and glycine transporter 2, are sorted to the apical domain in MDCK cells but are uniformly distributed in neurons (Ahn et al., 1996; Poyatos et al., 2000). Our results, however, represent the first instance in which a well- defined dendritic targeting motif mediates apical targeting in epithelia.

The EAAT3 sorting motif likely directs dendritic and apical targeting by interacting with other proteins involved in targeting. Proteins that bind to the EAAT3

sorting motif have not yet been identified. Recently, the protein glutamate transporter EAAC1-associated protein (GTRAP)3-18 has been shown to interact with the C terminus of the rat homolog of EAAT3 (Lin et al., 2001). However, increasing the expression of GTRAP3-18 in cells decreases the affinity of the transporter for its substrate but does not alter the cell surface expression of the transporter. Thus, it is not likely that GTRAP3-18 is involved in the sorting of EAAT3 to the appropriate cell surface.

The mechanism by which the EAAT3 sorting motif may direct apical and dendritic targeting could involve any of the steps in membrane protein targeting. It is thought that sorting motifs, particularly those that reside in the cytoplasmic domain, are recognized by cytoplasmic adaptor proteins (APs). These adaptor proteins concentrate the membrane proteins within discrete domains and link them with coat proteins. The coat proteins then induce vesicle budding, hence leading to the sorting of distinct membrane proteins into unique transport carriers (Gu et al., 2001). For example, specific subunits of two adaptor complexes, AP-1 and AP-4, have been shown to be necessary for the basolateral sorting of some proteins containing C-terminal sorting signals (Folsch et al., 1999; Simmen et al., 2002). It is possible that neurons and epithelia express a common adaptor that recognizes the EAAT3 motif and sorts EAAT3 protein into a specific population of carrier vesicles but that the fate of these carriers differs in neurons and epithelia. Because there are profound differences in the organization of microtubules in neurons and epithelia, it is possible that differences in the microtubule-based transport of EAAT3 carriers contribute to their apparently divergent localization in neurons and epithelia. In MDCK cells, microtubules are oriented with their minus ends directed

toward the apical surface and their plus ends directed toward the basolateral domain (Bacallao et al., 1989). In neurons, microtubules in the axons are oriented with the plus end directed away from the cell body, whereas microtubules in the dendrites have a mixed orientation (Baas et al., 1988). Thus a minus end-directed motor might be expected to move carrier vesicles to the apical domain in MDCK cells and to the dendritic domain in neurons, as proposed by Goldstein and Yang (2000).

There is already evidence for the involvement of the minus end motor dynein in the apical sorting of rhodopsin, an example of an apical protein whose sorting is directed by a cytoplasmic motif (Chuang and Sung, 1998; Tai et al., 2001). The 39-amino acid tail of rhodopsin interacts with the dynein light chain TcTex-1 but not another light chain dynein, RP3 (Tai et al., 1999). RP3 and TcTex-1 can compete for binding to the dynein complex, and the overexpression of RP3 in MDCK cells leads to a decrease in the expression of TcTex-1 as well as the nonpolarized localization of rhodopsin (Tai et al., 2001). Thus, the apical targeting of rhodopsin in MDCK cells is dependent on TcTex-1-mediated dynein function. It would be of interest to determine whether the sorting motif in EAAT3 interacts with components of dynein or other minus end-directed motor proteins, such as kinesin family member C2 (Goldstein and Yang, 2000; Yang et al., 2001).

The clustering of EAAT3-GFP on dendritic spines and filopodia also deserves comment. In the brain, EAAT3 has a "perisynaptic" location, lying just beyond the active zone where postsynaptic glutamate receptors are most highly concentrated. This location

suggests that neuronal glutamate transporters are poised to regulate the activity of extrasynaptic glutamate receptors by controlling the diffusion of glutamate away from the synapse, as has been demonstrated recently at parallel fiber synapses in the cerebellum (Brasnjo and Otis, 2001). These results indicate that the correct localization of glutamate transporters is critical to their role in regulating neurotransmission. The EAAT3 clusters we observed, which might be difficult to detect by immunostaining of intact tissue, bear a striking resemblance to postsynaptic receptor clusters seen on cultured hippocampal neurons (Allison et al., 2000; Naisbitt et al., 2000). The clustering of EAAT3 is not affected by deletion or mutation of the dendritic targeting signal, suggesting that it is mediated by a different molecular mechanism. It would be of interest to know whether interaction with membrane scaffolding proteins contributes to the localization of postsynaptic transporters such as EAAT3.

**Footnotes**

Received June 27, 2002; revised Sept. 23, 2002; accepted Sept. 30, 2002.

This work was supported by Howard Hughes Medical Institute and National Institutes of Health Grants NS 33273 (S.G.A.), NS17112 (G.B.), and MH 66179 (G.B.). We thank Dr. D. M. Fass for critical review of this manuscript and B. Smoody for preparing the neuronal cell cultures.

Correspondence should be addressed to Dr. Susan G. Amara, Howard Hughes Medical Institute and Vollum Institute, Oregon Health and Science University, L-474, 3181 Southwest Sam Jackson Park Road, Portland, OR 97239. E-mail: amaras@ohsu.edu.

**Figure Legends**

Figure 1. Localization of wild-type EAAT1-3 in MDCK cells. MDCK cells were stably transfected with EAAT1-3 that was tagged with GFP at the N terminus and grown on transwell filters. **A**, Representative Western blots from a cell surface biotinylation assay. This assay assessed the stable expression level of each EAAT at each cell surface by the application of biotin at the apical or basolateral surfaces. There is no signal when biotin was not included in the assay. The control blots show that $Na^+/K^+$-ATPase is detected at the basolateral but not the apical cell surface fraction, and actin is only detected in the intracellular fraction. **B**, Representative confocal images of EAAT1-3 in a vertical section (z-series) illustrating the localization of GFP-EAAT (green) and a basolateral marker, E-cadherin (red). The top panel of each construct is a composite image illustrating both GFP and basolateral marker signals, and the bottom panel contains only the GFP signal. In the vertical section, a fluorescence signal at the apical surface appears as a horizontal line at the top of the cell, whereas a signal at the basolateral surface appears as vertical lines at the sides of the cell. Occasionally, there is fluorescence attributable to the underlying filter, which appears as a horizontal line at the bases of all the cells. This fluorescence signal is not scored as basolateral localization. All EAATs are expressed at both surfaces, except EAAT3, which is restricted to the apical surface. Each blot and image is representative of at least two additional experiments. Scale bar, 20 μm.

Figure 2. Schematic representation and localization of the EAAT3 mutants. **A**, Topology of EAAT1 (Seal et al., 2000) and regions that are exchanged with EAAT3. The C terminus (orange), the large second extracellular loop (purple), and the N-terminal region (blue) are shown. Numbers denote transmembrane domains. OUT, Extracellular; IN, intracellular. **B**, Schematic diagram of the EAAT1/3 C-terminal chimeras, EAAT3 deletions, and EAAT3 C terminus attached to the end of full-length EAAT2. Regions containing sequences from EAAT1, EAAT2, and EAAT3 are denoted by yellow, red, and green, respectively. The localization of the stably transfected mutants was determined by both confocal microscopic imaging and a cell surface biotinylation assay. The presence or absence of a signal at a domain is denoted by + or -, respectively.

Figure 3. The cytoplasmic C terminus of EAAT3 is important in its apical localization. Representative Western blot analysis (**A**) and confocal vertical (z-series) images (**B**) of MDCK cells stably transfected with EAAT1-3 C-terminal chimeras or truncation mutant constructs are shown. The presence of the C terminus of EAAT3 in the mutant proteins confers stable expression predominantly at the apical surface, whereas its absence results in a more nonpolarized localization. Results are representative of at least two additional experiments. Scale bar, 20 μm.

Figure 4. A 14-amino acid sequence in the C terminus of EAAT3 contains the signal for apical localization. Representative Western blots (**A**) and confocal images (**B**) of MDCK cells stably transfected with constructs containing full-length EAAT2 fused to various

regions of the EAAT3 C terminus are shown. The mutant proteins containing at least the most distal 27-amino acid sequence of the EAAT3 C terminus attached to EAAT2 [E2-3(498-524)] shows an apical localization, whereas the mutant with a smaller distal region (14-amino acid sequence) of the C terminus of EAAT3 [E2-3(511-524)] has a more nonpolarized localization. These results suggest that the region in EAAT3 between 27 and 14 amino acids from the C-terminal end contains the sorting motif. Results are representative of at least two additional experiments. Scale bar, 20 μm.

Figure 5. Delineation of the residues in the sorting motif for apical localization of EAAT3. **A**, Representative confocal images of MDCK cells transiently transfected with constructs that contained full-length EAAT2 fused to either short regions of the EAAT3 C terminus or the most distal 27-amino acid sequence of EAAT3 [E2-3(498-524)] with triple or double alanine substitution mutations. Both E2-3(498-510) and E2-3(485-497) contained a 12-amino acid sequence from the C terminus of EAAT3, but only E2-3(498-510) was apically localized. **B**, Sequences of the constructs containing sequential triple or double alanine substitution of E2-3(498-524) and localization of the mutants. Regions of EAAT2 and 3 are represented in red and green, respectively, and the residues that are substituted with alanines are denoted in black. Substitution of residues with alanine of the following sequence disrupts the apical localization of the parent construct: KSYVNGGFAVD (the critical residues are gray). Results are representative of at least three additional experiments in duplicate. Scale bar, 20 μm.

Figure 6. Distribution of wild-type and mutant EAATs in polarized hippocampal neurons. Hippocampal cultures were transiently transfected with GFP- or YFP-tagged EAATs, and expression of the constructs was assessed in 11-d-old hippocampal neurons. The EAAT3-YFP signal (**A**) is completely restricted to dendrites, whereas cotransfected soluble cyan fluorescent protein (CFP; **B**) fills the entire cell, including its axon. Mutant E3(504-509AAAAAA) with a six-alanine replacement in the apical sorting domain is present in both axons and dendrites (**C**), as is EAAT2 (**D**). Arrows indicate axons; arrowheads indicate dendrites. Scale bar, 100 μm.

Figure 7. Higher-magnification images of wild-type and mutant EAATs in polarized hippocampal neurons. EAAT3-YFP is enriched on the surface of dendrites but absent from axons (**B**). Coexpressed soluble cyan fluorescent protein (CFP) fills the entire volume of the axon and dendrites (**A**). The mutant EAAT3 [E3(504-509AAAAAA)] and EAAT2 are present in both dendrites and axons (**D**, **E**). In older neurons (transfected at 10 d *in vitro* and imaged 9 d later), both wild-type and mutant EAAT3 are frequently present in clusters on spines and filopodia in the dendrites, and mutant EAAT3 is present in axons. Dendrites (arrowheads) are thicker, taper as they extend away from the cell body, and have filopodia and developing spines present all along them. Axons (arrows) are thinner, maintain a relatively uniform diameter, and lack spines. Scale bars: **A**, **B**, **D**, **E**, 10 μm; **C**, **E**, **F**, 2 μm.

Figure 1

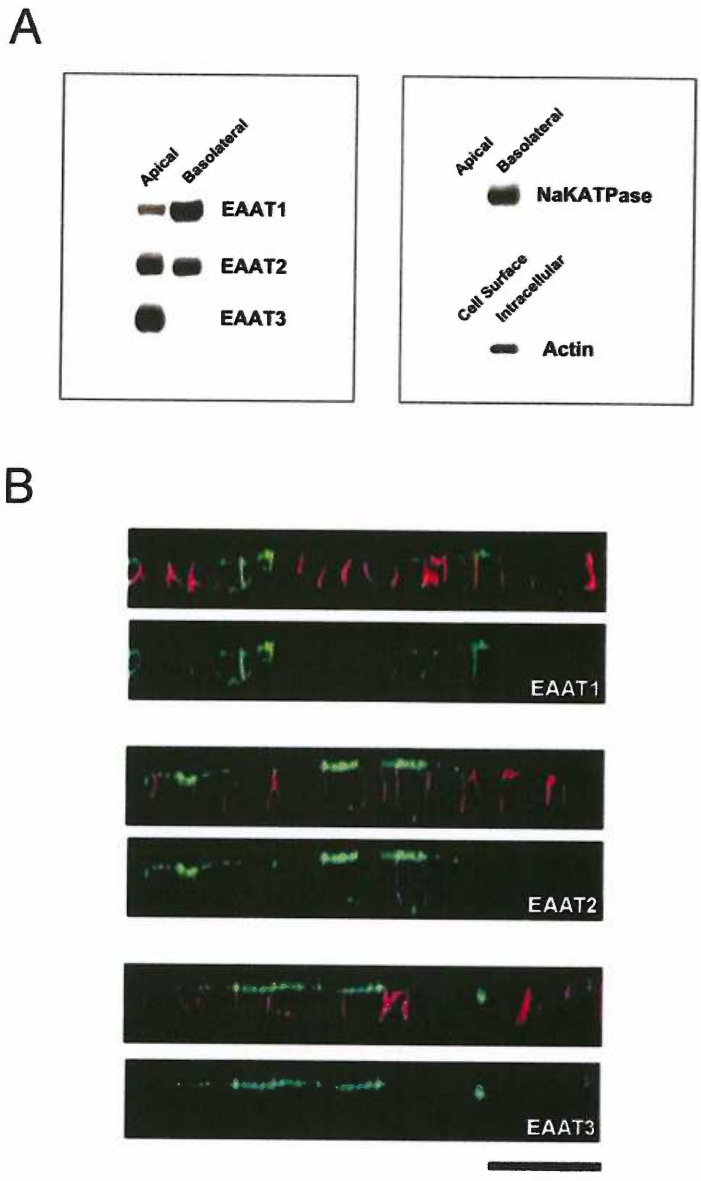
A
Apical
Basolateral
EAAT1
EAAT2
EAAT3
Apical
Basolateral
NaKATPase
Cell Surface
Intracellular
Actin
B
EAAT1
EAAT2
EAAT3

Figure 2

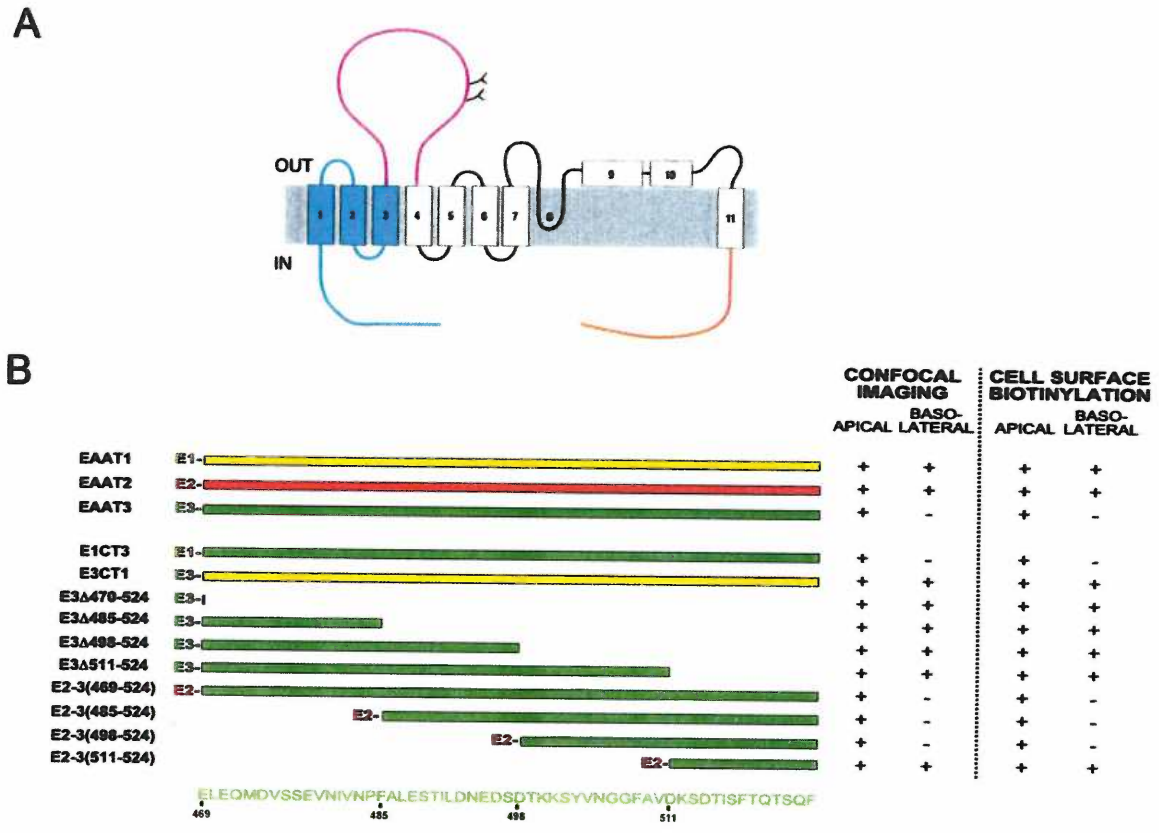
A
OUT
IN
1
2
3
4
5
6
7
8
9
10
11
B
CONFOCAL IMAGING
CELL SURFACE BIOTINYLATION
APICAL
BASO-LATERAL
EAAT1
EAAT2
EAAT3
E1CT3
E3CT1
E3Δ470-524
E3Δ485-524
E3Δ498-524
E3Δ511-524
E2-3(469-524)
E2-3(485-524)
E2-3(498-524)
E2-3(511-524)
ELEQMDVSSEVNIVNPFALESTILDNEDSDTKKSYVNGGFAVDKSDTISFTQTSQF
469
485
498
511

Figure 3

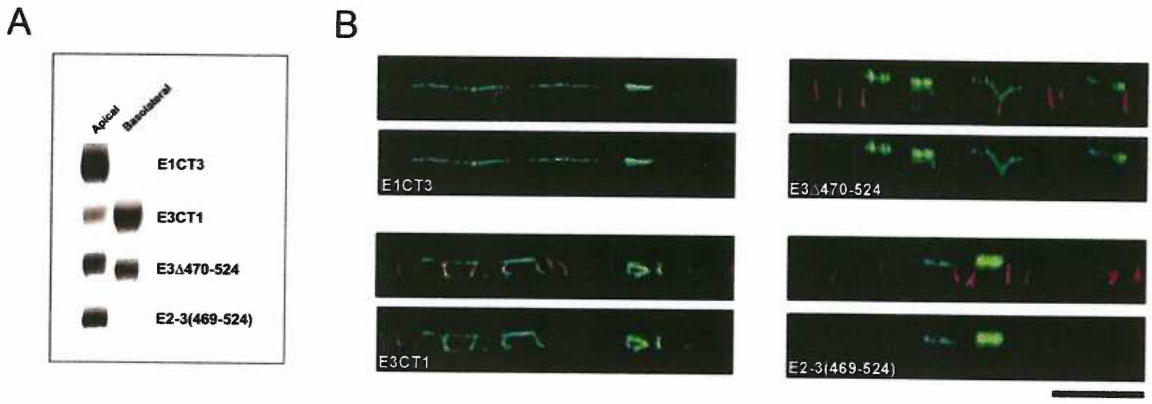
A
Apical
Basolateral
E1CT3
E3CT1
E3Δ470-524
E2-3(469-524)
B
E1CT3
E3Δ470-524
E3CT1
E2-3(469-524)

Figure 4

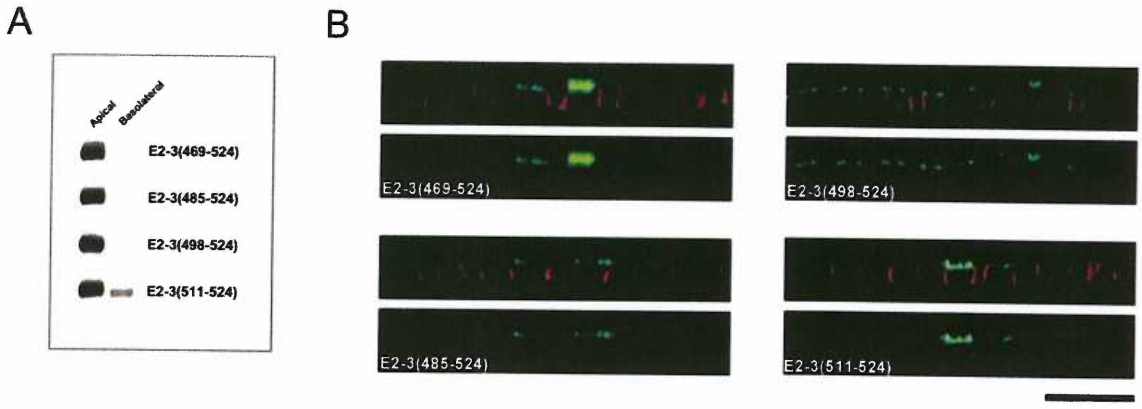
A
Apical
Basolateral
E2-3(469-524)
E2-3(485-524)
E2-3(498-524)
E2-3(511-524)
B
E2-3(469-524)
E2-3(498-524)
E2-3(485-524)
E2-3(511-524)

Figure 5

A

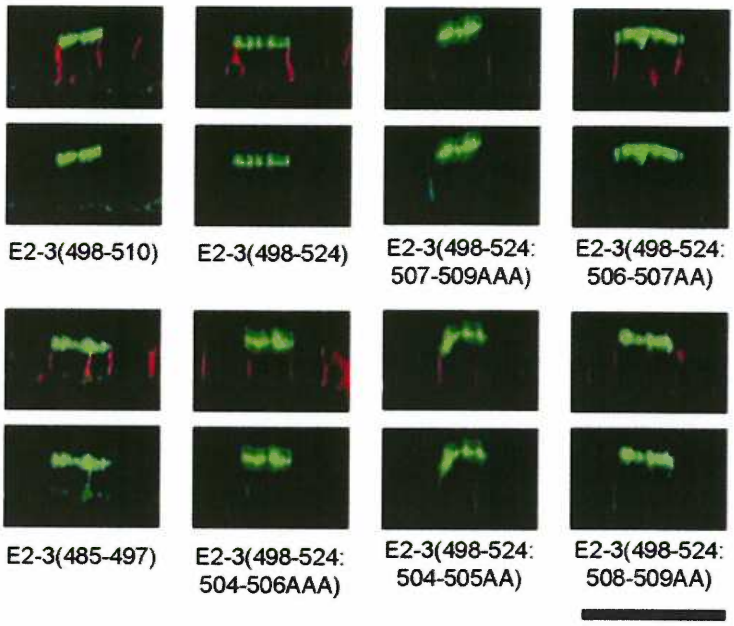


B

| E2-3(498-524) Containing: | | CONFOCAL IMAGING APICAL | BASO-LATERAL |
|---|---|---|---|
| 498-500AAA | EAAT2-EKAGSADTKKSYVNGGFAVDKSDTISFTQTSQF | + | - |
| 501-503AAA | EAAT2-EKAGSADTKAAAVNGGFAVDKSDTISFTQTSQF | + | +/- |
| 504-506AAA | EAAT2-EKAGSADTKKSYAAAGFAVDKSDTISFTQTSQF | + | + |
| 507-509AAA | EAAT2-EKAGSADTKKSYVNGAAAVDKSDTISFTQTSQF | + | + |
| 510-512AAA | EAAT2-EKAGSADTKKSYVNGGFAAAASDTISFTQTSQF | + | - |
| 513-515AAA | EAAT2-EKAGSADTKKSYVNGGFAVDKAAAISFTQTSQF | + | - |
| 516-518AAA | EAAT2-EKAGSADTKKSYVNGGFAVDKSDTAAATQTSQF | + | - |
| 519-521AAA | EAAT2-EKAGSADTKKSYVNGGFAVDKSDTISFAAASQF | + | - |
| 522-524AAA | EAAT2-EKAGSADTKKSYVNGGFAVDKSDTISFTQTAAA | + | - |
| 504-505AA | EAAT2-EKAGSADTKKSYAAGGFAVDKSDTISFTQTSQF | + | + |
| 506-507AA | EAAT2-EKAGSADTKKSYVNAAFAVDKSDTISFTQTSQF | + | - |
| 508-509AA | EAAT2-EKAGSADTKKSYVNGGAAVDKSDTISFTQTSQF | + | + |
| 510-511AA | EAAT2-EKAGSADTKKSYVNGGFAAAKSDTISFTQTSQF | + | -/+ |

Figure 6

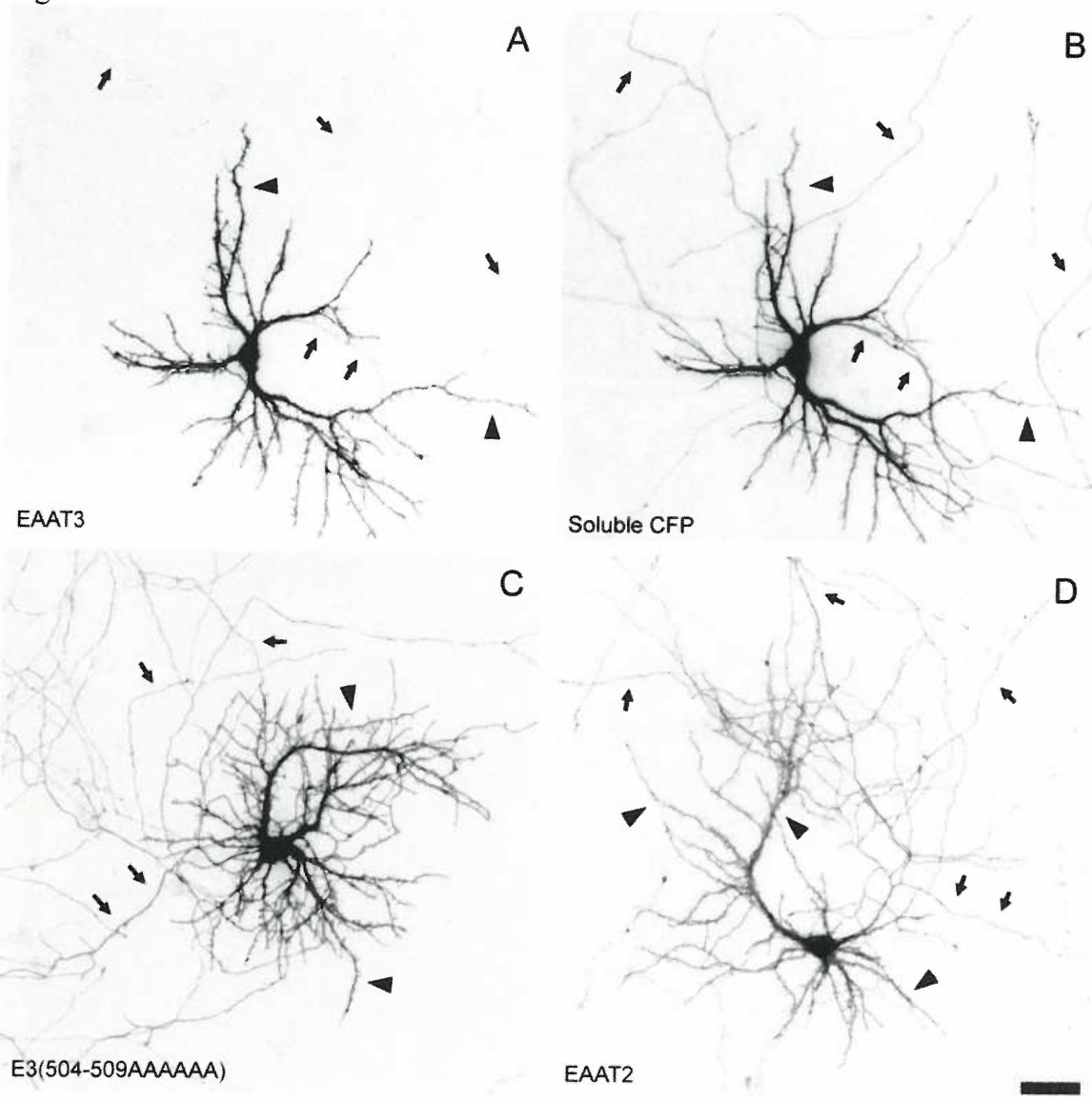

Figure 7

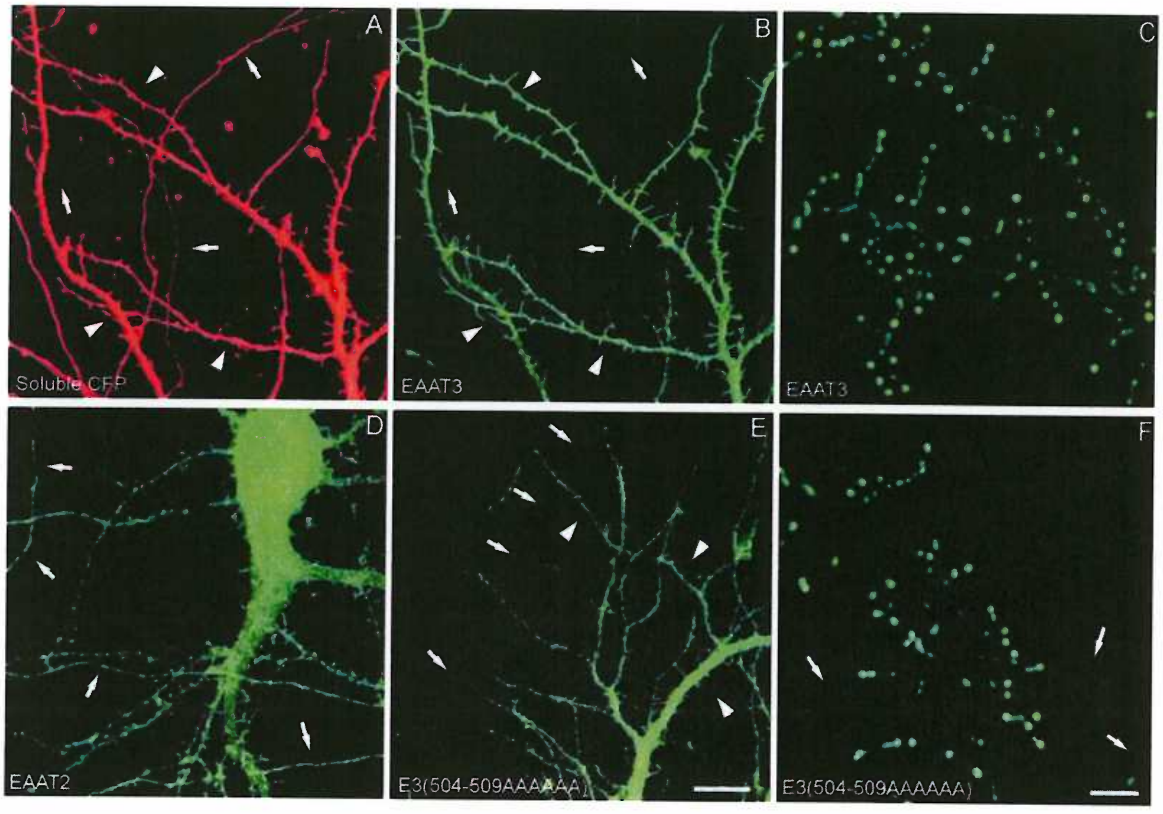
A
Soluble CFP
B
EAAT3
C
EAAT3
D
EAAT2
E
E3(504-509AAAAAA)
F
E3(504-509AAAAAA)

Table 1

**Table 1. Quantitative analysis of the cell surface expression of stably transfected EAAT constructs in MDCK cells**

| Construct | Apical (%) |
|---|---|
| EAAT1 | 22 ± 8 |
| EAAT3 | 97 ± 3 |
| E1CT3 | 97 ± 1* |
| E3CT1 | 24 ± 5** |
| E3Δ470–524 | 54 ± 3** |
| E3Δ485–524 | 67 ± 5** |
| E3Δ498–524 | 72 ± 5** |
| E3Δ511–524 | 74 ± 7** |
| EAAT2 | 54 ± 1 |
| E2-3(469–524) | 93 ± 3*** |
| E2-3(485–524) | 93 ± 3*** |
| E2-3(498–524) | 96 ± 2*** |
| E2-3(511–524) | 68 ± 2 |

Values are mean ± SEM.

*Significantly different from EAAT1; **significantly different from EAAT3; ***significantly different from EAAT2 ($p < 0.05$).

Table 2

**Table 2. Quantitative analysis of the polarity of EAAT constructs in hippocampal neurons**

| Construct | Cells ($n$) | Presence in axons | Presence in dendrites | Axon/dendrite ratio[a] |
|---|---|---|---|---|
| EAAT3 | 10 | − | ++ | 0.06 ± 0.02 |
| E3Δ470–524 | 11 | + | ++ | 0.28 ± 0.03* |
| E3Δ498–524 | 11 | + | ++ | 0.29 ± 0.05* |
| E3(504–509AAAAAA) | 14 | + | ++ | 0.26 ± 0.02* |
| EAAT2 | 10 | ++ | ++ | 0.68 ± 0.09 |
| E2-3(498–524) | 12 | + | ++ | 0.31 ± 0.04** |
| E2-3(498–524:504–506AAA) | 11 | ++ | ++ | 0.82 ± 0.10 |

Expression of the EAAT constructs was analyzed at 11 d *in vitro*.

[a]Values are mean ± SEM.

*Significantly different from EAAT3; **significantly different from EAAT2 ($p < 0.05$).

Supplementary Table 1

| EAAT2 Fused to: | | CONFOCAL IMAGING | |
|---|---|---|---|
| | | APICAL | BASO-LATERAL |
| 3(469-524) | EAAT2-EKAGSAELEQMDVSSEVNIVNPFALESTILDNEDSDTKKSYVNGGFAVDKSDTISFTQTSQF | + | - |
| 3(498-518) | EAAT2-EKAGSADTKKSYVNGGFAVDKSDTISF | + | - |
| 3(498-510) | EAAT2-EKAGSADTKKSYVNGGFAV | + | - |
| 3(498-504) | EAAT2-EKAGSADTKKSYV | + | + |
| 3(485-504) | EAAT2-EKAGSAFALESTILDNEDSDTKKSYV | + | + |
| 3(485-497) | EAAT2-EKAGSAFALESTILDNEDS | + | + |
| 3(469-497) | EAAT2-EKAGSAELEQMDVSSEVNIVNPFALESTILDNEDS | + | + |
| 3(469-494) | EAAT2-EKAGSAELEQMDVSSEVNIVNPFALESTILD | + | + |

**Chapter 4**

# Motifs that Mediate Dendritic Targeting in Hippocampal Neurons: A Comparison With Basolateral Targeting Signals

**Silverman, M. A[1,2*], Peck., R[1*], Glover, G[1]., He, C. [3], Carlin, C. [3], and Banker, G.[1] ****

[1]Center for Research on Occupational and Environmental Toxicology, Oregon Health & Science University, Portland, Oregon
[2]Biological Sciences Department, California State Polytechnic University, Pomona, California
[3] Department of Physiology and Biophysics, School of Medicine, Case Western Reserve University, Cleveland, Ohio

*Equal Authorship

**Corresponding author: Gary Banker, Center for Research on Occupational and Environmental Toxicology, L606, Oregon Health & Science University, 3181 SW Sam Jackson Park Rd, Portland, Oregon, 97239, e-mail: bankerg@ohsu.edu

Published in Molecular Biology of the Cell, June, 2005, 29:173-180

In this chapter, R. Peck (supervised by M. Silverman) performed all experiments except Supplementary Figure 1, which was performed by me. I contributed to this study by initiating experiments with FcRγII-B2 during my rotation, writing the final version of the paper with G. Banker's help, and responding to the reviewers' concerns.

**Abstract**

One model for dendritic protein sorting in neurons is based on parallels with basolateral targeting in Madin-Darby Canine Kidney (MDCK) epithelial cells. The goal of this study was to further evaluate this model by analyzing the neuronal targeting of several proteins that contain well-defined basolateral sorting motifs. When we expressed FcRγII-B2 and CD44, two basolateral markers whose sorting depends on di-hydrophobic motifs, they were unpolarized in hippocampal neurons. We also assessed the localization of the Epidermal Growth Factor Receptor (EGFR), a basolateral protein whose sorting signal contains a proline-rich motif and two di-hydrophobic motifs. EGFR was restricted to the dendrites in neurons, and relied on the same sorting signal for proper targeting. These results show that the dendritic sorting machinery in neurons does not recognize dihydrophobic-based basolateral sorting signals. In contrast, the sorting signal present in EGFR directs both basolateral and dendritic targeting and defines a novel dendritic targeting motif.

## Introduction

Neurons are polarized into two functionally and biochemically distinct domains: somatodendritic and axonal. Proper neuronal function depends on the accurate sorting and targeting of membrane proteins, such as neurotransmitter receptors and cell adhesion molecules, to these domains (Craig and Banker, 1994). Like neurons, epithelial cells maintain two different domains within their plasma membrane: basolateral and apical. Based on a comparison of the targeting of viral proteins in Madin-Darby Canine Kidney (MDCK) epithelial cells and hippocampal neurons, Dotti and colleagues hypothesized that neurons and MDCK cells use common mechanisms for sorting membrane proteins (Bradke and Dotti, 1998; Craig and Banker, 1994; Dotti and Simons, 1990). In their model, the basolateral domain is equivalent to the somatodendritic domain, the apical domain to the axon. In support of this hypothesis, several basolateral proteins are targeted to dendrites when expressed in neurons. In contrast, the epithelial/neuronal parallel does not hold for apical/axonal sorting; apical proteins investigated thus far are not restricted to the axon in cultured hippocampal neurons (Jareb and Banker, 1998). Although further studies have led to revisions of the original hypothesis, comparison of polarity in MDCK cells and neurons continues to provide a useful framework for the study of polarized protein trafficking (Horton and Ehlers, 2003b; Muth and Caplan, 2003; Ponnambalam and Baldwin, 2003; Winckler and Mellman, 1999).

Further support for the parallel between dendritic and basolateral targeting derives from more detailed studies of the mechanism involved. For several proteins it has been shown that the same stretch of cytoplasmic amino acid residues mediates targeting to both somatodendritic and basolateral domains (Mostov et al., 2000). For example, in both cell types the targeting of the Low density lipoprotein receptor (LDLR) requires a tyrosine-based sorting signal (Matter et al., 1994); targeting of the transferrin receptor (TfR) also depends on overlapping sorting signals (Odorizzi and Trowbridge, 1997; West et al., 1997). In epithelia, basolateral sorting depends on the interaction between these cytoplasmic sorting signals and specific adaptor subunits that govern cargo selection into transport vesicles. For TfR and LDLR, proper targeting relies on the presence of μ1B, a subunit of the AP-1 adaptor complex (Gan et al., 2002). This adaptor subunit is expressed in MDCK cells, but not in neurons, indicating that a different adaptor protein must mediate targeting of these proteins in neurons (Ohno et al., 1999). In addition to μ1B, the adaptor complex AP-4 is also known to function in basolateral sorting (Simmen et al., 2002). It is possible that this or other as yet unidentified adaptor molecules mediate dendritic sorting.

The targeting of another class of basolateral proteins, which includes the macrophage Fc receptor γII-B2 (FcRγII-B2) and the Epidermal Growth Factor Receptor (EGFR), does not depend on μ1B (Ang et al., 2003; Mullin and McGinn, 1987). We were interested in knowing if the basolateral targeting signals in these proteins are also recognized by the dendritic sorting machinery. FcRγII-B2 relies on a di-hydrophobic

amino acid motif for basolateral sorting. Point mutations of the Leu-Leu sequence in the cytoplasmic tail of FcRγII-B2 abolish basolateral targeting in MDCK cells as assayed by confocal microscopy and cell-surface biotinylation (Sheikh and Isacke, 1996). Another basolateral protein that utilizes a di-hydrophobic motif for its targeting is the hyaluronate receptor CD44, which relies on a Leu-Val sequence in its cytoplasmic tail (Sheikh and Isacke, 1996). The EGFR uses a different, though partially related, basolateral sorting signal consisting of a dominant, proline-based motif and two weaker di-hydrophobic motifs (He et al., 2002). In the current study, we determined whether the basolateral targeting motifs present in these proteins act as dendritic sorting signals in cultured hippocampal neurons. When cDNAs encoding FcRγII-B2 and CD44 were expressed, they were unpolarized on the neuronal plasma membrane. In contrast, EGFR was restricted to the somatodendritic surface. Furthermore, the same mutations that disrupt EGFR sorting in epithelial cells caused its mistargeting in neurons. These results expand upon previous studies of the parallel between dendritic and basolateral sorting, showing that only a subset of basolateral sorting signals are recognized as dendritic sorting signals in neurons.

## Materials and Methods

### Antibodies and Expression Vectors

We thank the following people for generously providing these reagents: Dr. I. Stamenkovic, Harvard Medical School, human CD44 cDNA; Dr. I. Mellman, Yale

University, mouse FcRII-B2 cDNA; Dr. John Adelman, Vollum Institute, pJPA expression vector; Dr. C. Enns, Oregon Health and Science University, pCB6-human TfR. Golgi-CFP and eGFP were from Clontech (Palo Alto, CA). The cDNAs encoding eGFP, human CD44, and mouse FcRγII-B2 were subcloned into the pJPA expression vector. The following human EGFR cDNAs are previously described by Hobert et al., 1997 and He et al. 2002; pCB6+EGFRWT, pCB6+EGFR C'652STOP, pCB6+EGFR C'674, pCB6+EGFR C'675STOP-LL, LV-4xA, pCB6+EGFR C'675STOP-PxxP-2xA, pCB6+EGFR C'675STOP-LL, LV, PxxP-6xA. Monoclonal antibodies specific for human CD44 (1:100) and human EGFR (1:200) were from Santa Cruz Biotechnology (Santa Cruz, CA), mouse FcRγII-B2 (1:100) antibodies were from Pharmingen (San Diego, CA), and antibodies against human TfR (1:100) (B3/25) were from Roche (Basel, Switzerland). Working dilutions for immunocytochemistry are given in parentheses.

Hippocampal Cell Culture and Expression of Transgenes

Primary cultures of dissociated neurons from E18 embryonic rat hippocampi were prepared essentially as described (Banker and Goslin, 1998). Cells 6-8 days *in vitro* were transfected with the transmembrane marker protein of interest along with soluble enhanced green fluorescent protein (eGFP) using Effectene (Qiagen, Valencia, CA) or Lipofectamine2000 (Invitrogen, Carlsbad, CA). Cells were allowed to express for 4 - 48 hours at 37° C under a controlled atmosphere containing 5% $CO_2$. To detect expressed proteins on the cell surface, living neurons were incubated in primary antibody diluted to the appropriate concentration in culture medium for 7-10 minutes at 37°C. Coverslips

were then rinsed in phosphate buffered saline (PBS) and fixed in 4% paraformaldehyde/4% sucrose in PBS. Cells were incubated in 0.50% fish skin gelatin (Sigma-Aldrich, St. Louis, MO) in PBS for 1 hr at 37°C to block nonspecific antibody-binding sites. Coverslips were then incubated either in biotinylated secondary antibody for 1 hr at 37°C followed by Cy3-conjugated streptavidin or directly in cy3 conjugated secondary antibody for 1 hr at 37°C (Jackson Immunoresearch Laboratories, West Grove, PA). For immunostaining of total protein (surface and intracellular), cells were fixed as above, permeablized with Triton-X-100 (.25%), then immunostained.

Microscopy and Quantitative Measurements of Polarity

Images of immunofluorescently labeled cells were acquired using a Princeton Instruments Micromax cooled CCD camera (Photometrics, Tuscon, AZ) controlled by Metamorph Software (Universal Imaging, Downingtown, PA). Low magnification images were taken with a 16X 0.5 N.A. Plan Fluotar objective (Leica Microsystems AG, Wetzlar, Germany). Exposure time was adjusted so that the maximum pixel value did not reach saturation. Only cells whose labeled processes did not overlap with other labeled cells were selected for quantification.

All image processing was done with Metamorph software (Universal Imaging, Downingtown, PA). Two different corrections were performed on the raw image prior to analysis of polarity. First, a shading correction was applied (based on an image of a uniformly fluorescent slide) to compensate for the uneven illumination. Next, an average

background fluorescence value was determined from several regions containing unlabeled neurites, then subtracted from the whole image. In order to quantify the fluorescence in axons and dendrites, several, 1-pixel wide, 100 μm lines were drawn on randomly selected portions of the axon and the dendrites (6-10 lines each) using the soluble GFP signal as a guide, then these regions were transferred to the live-cell immunostain image and the average fluorescence for each region was calculated. The average intensities from axons and dendrites of each cell were transferred to an Excel (Microsoft, Redmond, WA) spreadsheet. The dendrite:axon ratios for each construct were calculated from minimally 8 cells from at least two different cultures. Statistical significance was assessed using the Newman-Keuls multiple comparisons test for independent groups.

**Results**

CD44 and the FcRγII-B2 Receptor Are Unpolarized When Expressed in Hippocampal Neurons

CD44 and FcRγII-B2 are targeted to the basolateral domain in MDCK cells based on well-defined dihydrophobic motifs in their cytoplasmic tails (Hunziker and Fumey, 1994; Sheikh and Isacke, 1996). We sought to determine whether these proteins were dendritic when expressed in cultured hippocampal neurons.

To determine the cell surface distribution of CD44 and FcRγII-B2, we expressed each marker in hippocampal neurons for 18-24 h, then immunostained living cells using species-specific antibodies directed against extracellular epitopes. We coexpressed soluble eGFP along with each membrane protein in order to label the entire axonal and dendritic arbor of the cell. Comparison with the distribution of this soluble marker showed that FcRγII-B2 (Figure 1 D-F) and CD44 (Figure 1 G-I) were uniformly distributed on the plasma membrane throughout both axons and dendrites. A comparable distribution was observed after expression for 5.5h h, the earliest time when the proteins could be detected on the cell surface (shown for FcRγII-B2 in Supplementary Figure 1 A,B). Intracellular labeling (revealed by fixation and permeablization before immunostaining) was associated with the Golgi complex as well as many tubulovesicular profiles, which were found throughout the neurites (Supplementary Figure 1C-E). The latter likely correspond to the carriers that deliver these proteins to the cell surface, as revealed in previous, live-cell imaging studies (Burack et al., 2000; Kreitzer et al., 2003; Lippincott-Schwartz et al., 2000). The unpolarized surface distribution of CD44 and FcRγII-B2 was distinctly different from the localization of TfR, a basolateral protein that is polarized to the somatodendritic domain (Figure 1 A-C). To quantify the polarity of these proteins, we measured the average fluorescence intensity in dendrites and axons, using the method described by Sampo et al. (2003). The ratio of fluorescence in dendrites compared to axon (the D:A ratio) was 1.9:1 for CD44 and 1.6:1 for the FcRγII-B2 (Table 1). These values are comparable to those of unpolarized proteins assessed using this approach (Cheng et al., 2002; Sampo et al., 2003). When we quantified the

polarity of TfR, whose dendritic targeting has been studied extensively (Burack et al., 2000; West et al., 1997), we found that its D:A ratio was 7.7:1 (Table 1), significantly different from the D:A ratio of FcRγII-B2 and CD44. Other dendritically polarized proteins show D:A ratios similar to that of TfR (Cheng et al., 2002; Rivera et al., 2003).

The EGF Receptor Is Targeted to the Somatodendritic Domain

To determine the cell surface distribution of the EGFR in neurons, we expressed human EGFR for 18-24h and performed live-cell immunostaining using a species-specific monoclonal antibody directed against an extracellular epitope. Cell surface fluorescence was polarized to the somatodendritic domain (Figure 2 A, B). Quantification of cell-surface fluorescence revealed that EGFR was polarized to the dendrites, with a D:A ratio of 6.7:1 (Table 1). The dendritic polarity of EGFR was somewhat reduced when expression was high, suggesting that the cellular machinery responsible for its sorting may be saturable. In cells expressing lower levels of EGFR, the D:A ratio was slightly higher, about 8:1. We did not observe a relationship between overexpression and polarity with any of the other constructs examined.

In MDCK cells, a 22-amino acid region (Lys652-Ala674) of the cytoplasmic juxtamembrane domain targets EGFR to the basolateral membrane (Hobert et al., 1997). Truncation of the entire cytoplasmic tail results in its mislocalization to the apical domain, while truncation just beyond the critical juxtamembrane region has no affect on its polarity (Figure 3; (He et al., 2002). We observed parallel results when these

constructs were expressed in hippocampal neurons. When the cytoplasmic domain of EGFR was truncated at the end of the 22-amino acid sorting region (P675STOP), the protein was still accurately sorted to the dendrites. Truncation of the entire cytoplasmic tail (K652STOP) resulted in a significant loss of polarity. The D:A ratio was reduced from 7.2 to 3.2, a value slightly greater than was observed for unpolarized proteins. These data show that the same 22-amino acid domain that governs the basolateral targeting of EGFR also contains information necessary for its dendritic targeting.

Within the 22 amino acid juxtamembrane domain, He et al. (2002) identified several residues important for basolateral localization, including two di-hydrophobic motifs and a novel, proline-dependent motif (Figure 3). Mutating both prolines markedly reduced its basolateral polarization, whereas mutating both dihydrophobic motifs had only a slight effect. Mutating all six residues simultaneously reduced its polarity even further.

Expression of these truncation/substitution constructs in neurons gave parallel results. Mutation of both dihydrophobic motifs (P675STOP-LL, LV-4xA) resulted in a small, but not significant reduction in the dendritic polarity of EGFR (D:A ratio, 5.8:1, Figure 4 A, B). Mutation of both proline residues (P675STOP-PxxP-2xA) resulted in a greater reduction in polarity (D:A ratio, 4.8:1). Mutation of both dihydrophobic motifs and both proline residues (P675STOP-LL, LV, PxxP-6xA) decreased its polarity to the same extent as truncating the entire cytoplasmic domain (D:A ratio, 3.5:1; Figure 4 C, D).

## Discussion

In order to test whether multiple basolateral sorting signals are recognized by neurons, we expressed several markers with well-defined basolateral targeting signals in cultured hippocampal neurons and assayed their polarity on the cell surface. Our results show that the dihydrophobic motifs present in FcRγII-B2 and CD44 do not mediate dendritic targeting. In contrast, we found that EGFR is polarized to the somatodendritic domain in neurons, and relies on the same signal that mediates its basolateral targeting in epithelial cells.

### The Role of Di-leucine Targeting Motifs

Two types of dihydrophobic trafficking signals have been particularly well characterized. Motifs conforming to (DE)xxxL(LI) bind to subunits of AP-1, AP-2 and AP-3, mediating endocytosis and lysosomal targeting, while DxxLL binds to the VHS domain of another class of sorting adaptors, the GGAs (Bonifacino and Traub, 2003). Basolateral di-leucine motifs typically do not conform to either of these sequences. CD44 contains both an upstream and a downstream acidic residue, but neither are important for basolateral targeting (Sheikh and Isacke, 1996). FcRγII-B2 and E-Cadherin both contain an acidic residue downstream of the di-leucine motif, but again this residue is not involved in targeting (Hunziker and Mellman, 1989; Miranda et al., 2001). We found that the di-hydrophobic motifs in FcRγII-B2 and CD44 do not mediate dendritic targeting in neurons. Another dendritic protein, the EGFR-like protein DNER, also

contains a di-hydrophobic motif in its cytoplasmic tail, but this signal is not required for its dendritic targeting (Eiraku et al., 2002).

There are also examples where di-hydrophobic motifs play a role in neuronal membrane trafficking. Garrido et al. (2001) have investigated the role of leucine residues in the axonal targeting of a construct consisting of the C-terminal of the $Na^{2+}$ channel linked to a reporter protein. They show that the axonal localization of this construct depends on its selective endocytosis from the dendritic membrane, which in turn requires a dileucine motif in the cytoplasmic tail. Rivera et al. (2003) demonstrated that the dendritic targeting of the potassium channel Kv4.2 is disrupted by mutations of its cytoplasmic dileucine motif as well as of surrounding amino acid residues. In neurons, as in other cells types, it is likely that dihydrophobic motifs play multiple roles in protein trafficking, which depend in part on position and on the context of surrounding amino acid residues (Gu et al., 2001; Rohrer et al., 1996).

A Novel Dendritic Targeting Signal in EGFR

EGFR contains a short region in its cytoplasmic domain that is important for its basolateral targeting in epithelia. Within this region lie specific amino acid motifs that are necessary for proper targeting: a dominant proline-based motif and two less important di-hydrophobic motifs. We found that these motifs are also important for proper dendritic targeting. No other proline-rich dendritic targeting motifs have been described, though at least one other basolateral protein contains a similar motif within its basolateral

sorting signal (Odorizzi and Trowbridge, 1997). The sorting machinery that binds to this novel targeting signal is not known; however, this PxxP motif conforms to a type I SH3-binding domain, which mediates protein-protein interactions important for signal transduction, synaptic vesicle endocytosis, and lysosomal sorting (Blott et al., 2001; Kay et al., 2000; McPherson, 1999).

When we expressed a near complete c-terminal truncation of EGFR (K652STOP), the protein was still slightly more dendritic than unpolarized proteins. It is possible, though unlikely, that the few amino acids remaining in the cytoplasmic domain contribute to dendritic targeting. Alternatively, the expressed constructs may have formed dimers with endogenously expressed copies of EGFR (Tucker et al., 1993). If this were the case, wild-type copies of EGFR, with intact dendritic targeting signals, could pull mutant copies into the proper dendritic sorting pathway, leading to partial dendritic polarity of overexpressed mutants. We have observed a similar phenomenon in the studies of the dendritic targeting of the (LDLR). When LDLR was coexpressed with a sorting signal mutant of LDLR, the wild-type protein was not completely excluded from the axon, and the mutant protein was slightly polarized to dendrites (unpub. obs.).

## Conclusion

It is well documented that both dendritic and basolateral proteins rely on short amino acid sequences within their cytoplasmic tails for polarized sorting. Do the same motifs that mediate basolateral sorting also mediate dendritic sorting? In some cases,

they clearly do not. As shown in this study, the basolateral proteins FcRγII-B2 and CD44 are unpolarized in neurons. In addition, basolateral proteins which utilize a different class of sorting motifs, such as TrKB, are also unpolarized when expressed in neurons (Kryl et al., 1999). A particularly striking case of disparate targeting is illustrated by the sorting of the excitatory amino acid transporter EAAT3. This protein, which is expressed endogenously in both hippocampal neurons and epithelial cells, relies on the same short stretch of amino acids for targeting to the dendrites in neurons, but to the apical domain in epithelia (Cheng et al., 2002).

Other proteins, such as TfR and LDLR, do use similar motifs for dendritic and basolateral targeting. Even for these proteins, however, there are subtle differences. For TfR, residues important for basolateral targeting are slightly distal to those important for dendritic polarity (Odorizzi and Trowbridge, 1997; West et al., 1997). In LDLR, a naturally occurring point mutation that causes mistargeting in epithelia (Koivisto et al., 2001) does not disrupt dendritic targeting (unpub. obs.). Adding a C-terminal GFP tag does not disrupt basolateral targeting of LDLR in MDCK cells (Kreitzer et al., 2003), but a nearly identical construct is unpolarized when expressed in neurons (unpub. obs). Subtle differences were also observed in the case of EGFR. For example, alanine substitution of the di-hydrophobic motifs appears to have a greater effect on dendritic sorting than on basolateral sorting.

What could account for the differences between dendritic and basolateral targeting? In the case of proteins that are dendritic in neurons but not basolateral in epithelia, or vice versa, an obvious possibility is that the adaptors that recognize their sorting motifs are expressed in only one of the two cell types. Alternatively, the same adaptors may be expressed in both cell types, but downstream events may direct the proteins to different domains. Subtle differences between basolateral and dendritic sorting signals could be explained by differences in the regulation of adaptors. For example, phosphorylation could modify the interaction between sorting motifs and adaptors (Dietrich et al., 1994; von Essen et al., 2002). In addition, adaptor-modulating proteins may also be differentially expressed (Hinners et al., 2003; Rapoport et al., 1997; Shang et al., 2004). A clearer picture of the molecular details of polarized targeting in neurons will depend on further characterization of such sorting signal binding partners.

**Acknowledgments**

This research was supported by NIH grants NS17112 and MH66179 (to GB) and NS48047 (to MS). We thank B. Smoody for the preparation of neuronal cultures, J. Luisi Harp for assistance with fluorescence quantification, and M. Lasarev for assistance with the statistical analysis. S. Kaech, S. Das, and B. Sampo provided for insightful comments on the manuscript.

**Figure Legends**

Figure 1. The basolateral proteins CD44 and FcRγII-B2 are unpolarized when expressed in rat hippocampal neurons. Cell surface immunostaining of human TfR (A) was highly polarized to the dendrites. The axon and dendrites were identified by coexpression of soluble GFP, which fills the entire cell (B). In contrast, cell surface immunostaining of CD44 (D) and FcRγII-B2 (G) extended throughout both the dendrites and axons (compare with soluble GFP images--E, H). Phase images are shown with an arrowhead marking the cell body of the transfected cell (C, F, I). Cells from 7-9 day old cultures were doubly transfected with soluble GFP and the indicated protein, then allowed to express the constructs for 18-24 hours. Arrows show axons, while arrowheads denote dendrites. Scale bar, 50μm.

Figure 2. Cell surface immunostaining of full-length EGFR and truncated EGFR. Wild-type EGFR was polarized to the dendritic cell surface (A). Faint staining extended into the very proximal portion of the axon. Soluble GFP labeled the entire cell, including the axon and dendrites (B). Truncation of the entire cytoplasmic domain of EGFR (EGFR K652-STOP) resulted in a marked reduction in polarity (C, D). Hippocampal neurons from 7-9 day old cultures were cotransfected with EGFR and soluble GFP, then allowed to express the constructs for 18-24 hours. Arrows show axons, while arrowheads denote dendrites. Scale bar, 50 μm.

Figure 3. Quantification of the polarity of EGFR constructs expressed in hippocampal neurons in culture. **A** Schematic drawings showing the domain structure wild-type EGFR as well as the cytoplasmic truncations, K652-STOP and P675-STOP. The area in gray shows the region necessary for basolateral localization of EGFR in MDCK cells. **B** Point mutations introduced into the P675-STOP truncation (at the positions underlined). Quantification of the polarity (dendrite:axon ratio) is shown to the right of each construct.. Values are means ± standard deviations. * Significantly different from wild-type EGFR, $p < 0.05$.

Figure 4. Cell surface distribution of EGFR sorting signal mutants. Mutation of both dihydrophobic motifs in the cytoplasmic juxtamembrane domain of the truncated EGFR (EGFR P675-LL, LV-4xA) had little effect on the protein's dendritic distribution (A, B). Mutation of the proline-rich motif together with both dihydrophobic motifs (EGFR P675-LL, LV, PxxP-6xA) led to a significant reduction in polarity (C, D). Cells from 7-9 day old cultures were cotransfected with mutated EGFR and soluble GFP, then analyzed after expression for 18-24 hours. Arrows denote axons, arrowheads show dendrites. Scale bar, 50μm.

Supplementary Figure 1. Surface and intracellular distribution of FcRγII-B2 early after transfection. Comparison with soluble GFP (A), which labels all neurites, indicated that FcRγII-B2 was unpolarized as soon as the protein was detectable on the surface, 5.5h after transfection (B). At this time, intracellular FcRγII-B2 (revealed by fixation and

permeablization of cells before incubation with primary antibody--C) was present in tubulovesicular structures in all neurites (labeled by cotransfected soluble YFP--D), and concentrated in the Golgi complex, labeled by transfected CFP-beta1,4-galactosyltransferase (E). A similar pattern of intracellular staining was observed 24 h after transfection (data not shown).

**Figure 1.**

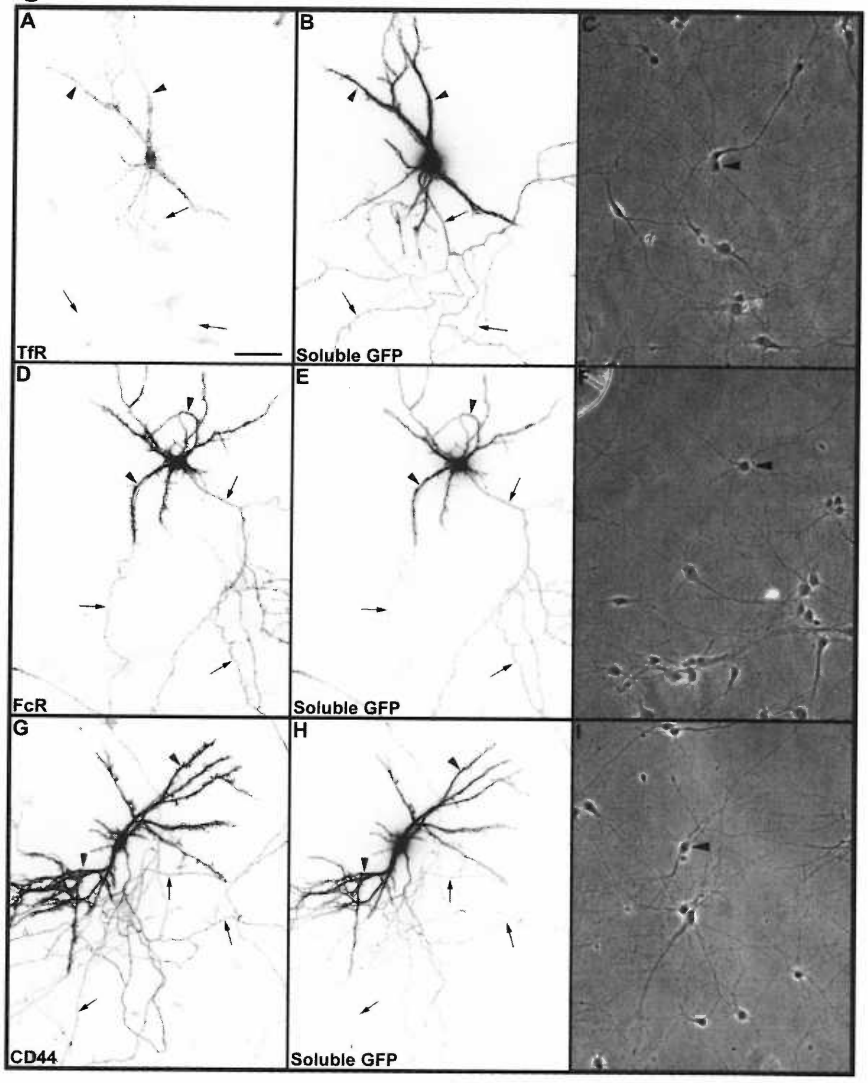

**Figure 2.**

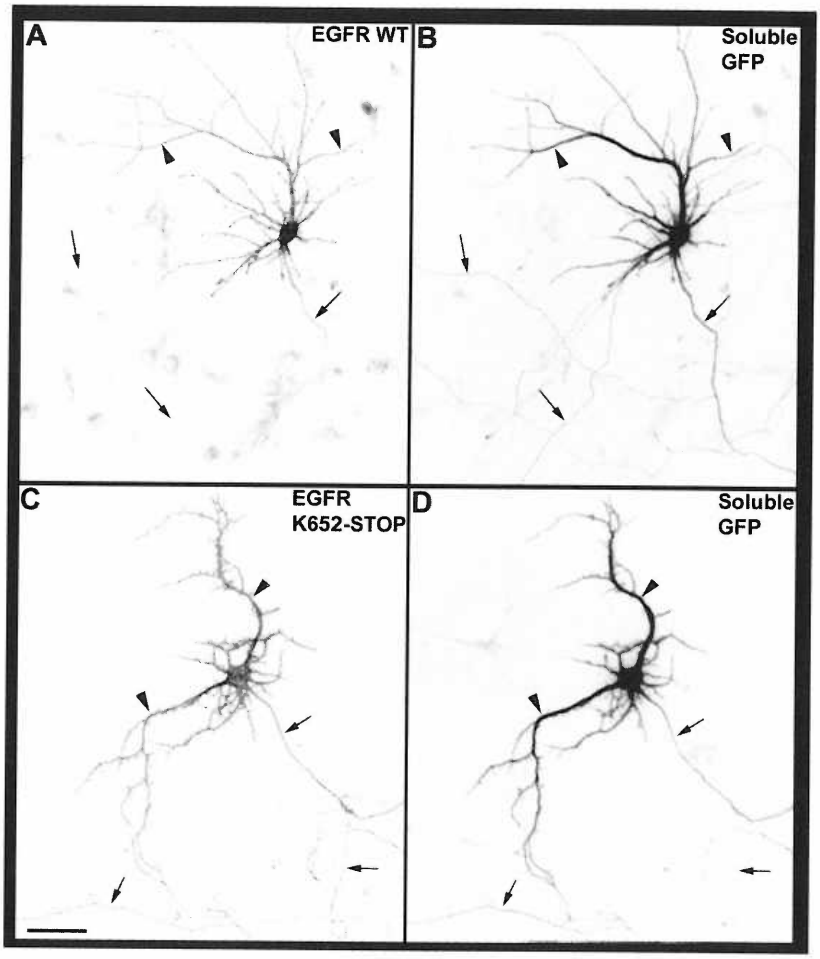

**Figure 3.**

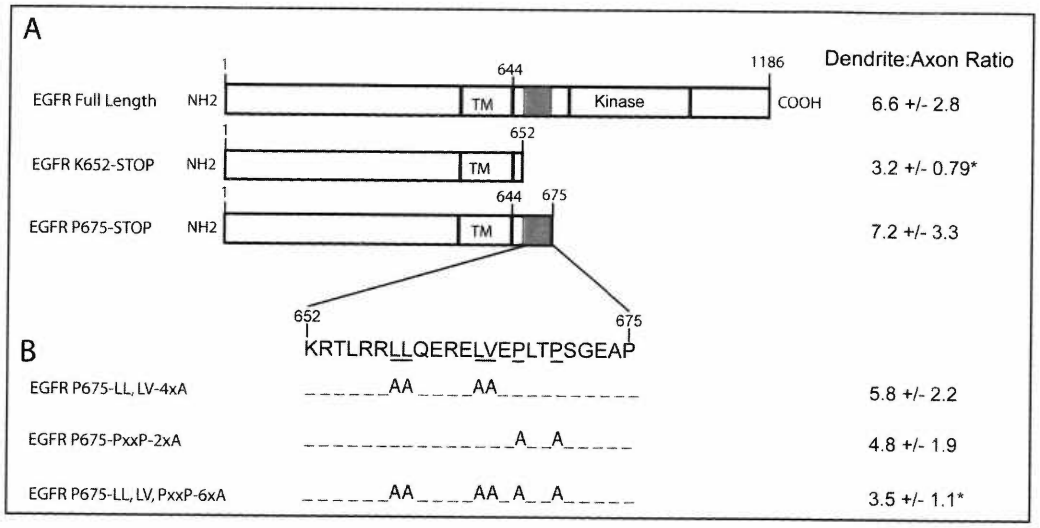
A
Dendrite:Axon Ratio
EGFR Full Length
NH2
1
644
1186
TM
Kinase
COOH
6.6 +/- 2.8
EGFR K652-STOP
652
3.2 +/- 0.79*
EGFR P675-STOP
675
7.2 +/- 3.3
652
675
B
KRTLRRLLQERELVEPLTPSGEAP
EGFR P675-LL, LV-4xA
AA AA
5.8 +/- 2.2
EGFR P675-PxxP-2xA
A A
4.8 +/- 1.9
EGFR P675-LL, LV, PxxP-6xA
AA AA A A
3.5 +/- 1.1*

**Figure 4.**

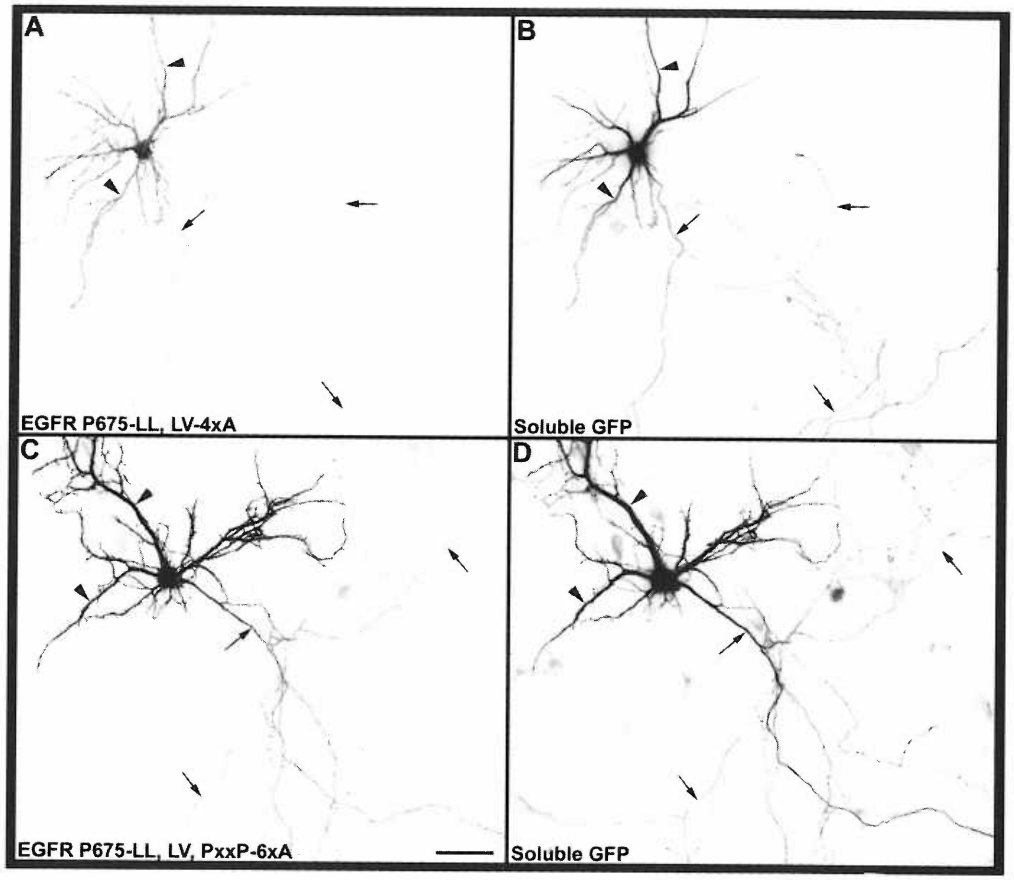
A
EGFR P675-LL, LV-4xA
B
Soluble GFP
C
EGFR P675-LL, LV, PxxP-6xA
D
Soluble GFP

Table 1

Quantification of polarity of basolateral proteins expressed in hippocampal neurons

| Protein | *n* | Polarity (dendrite:axon ratio) |
|---|---|---|
| TfR | 8 | 7.7 ± 2.1 |
| CD44 | 11 | 1.9 ± 0.56* |
| FcRγII-B2 | 15 | 1.6 ± 0.55* |
| EGFR | 33 | 6.6 ± 2.8 |

Values are means ± SD.

Ideally, quantification of an unpolarized protein's distribution should yield a 1:1 ratio of fluorescence in the dendrites versus axon; however, the dendrites are five to ten times thicker than the axon, so it is likely that a greater contribution of out of focus fluorescence in the dendrites results in a dendrite:axon ratio slightly greater than one.

* Significantly different than TfR ( $p < 0.05$).

**Supplementary Figure 1.**

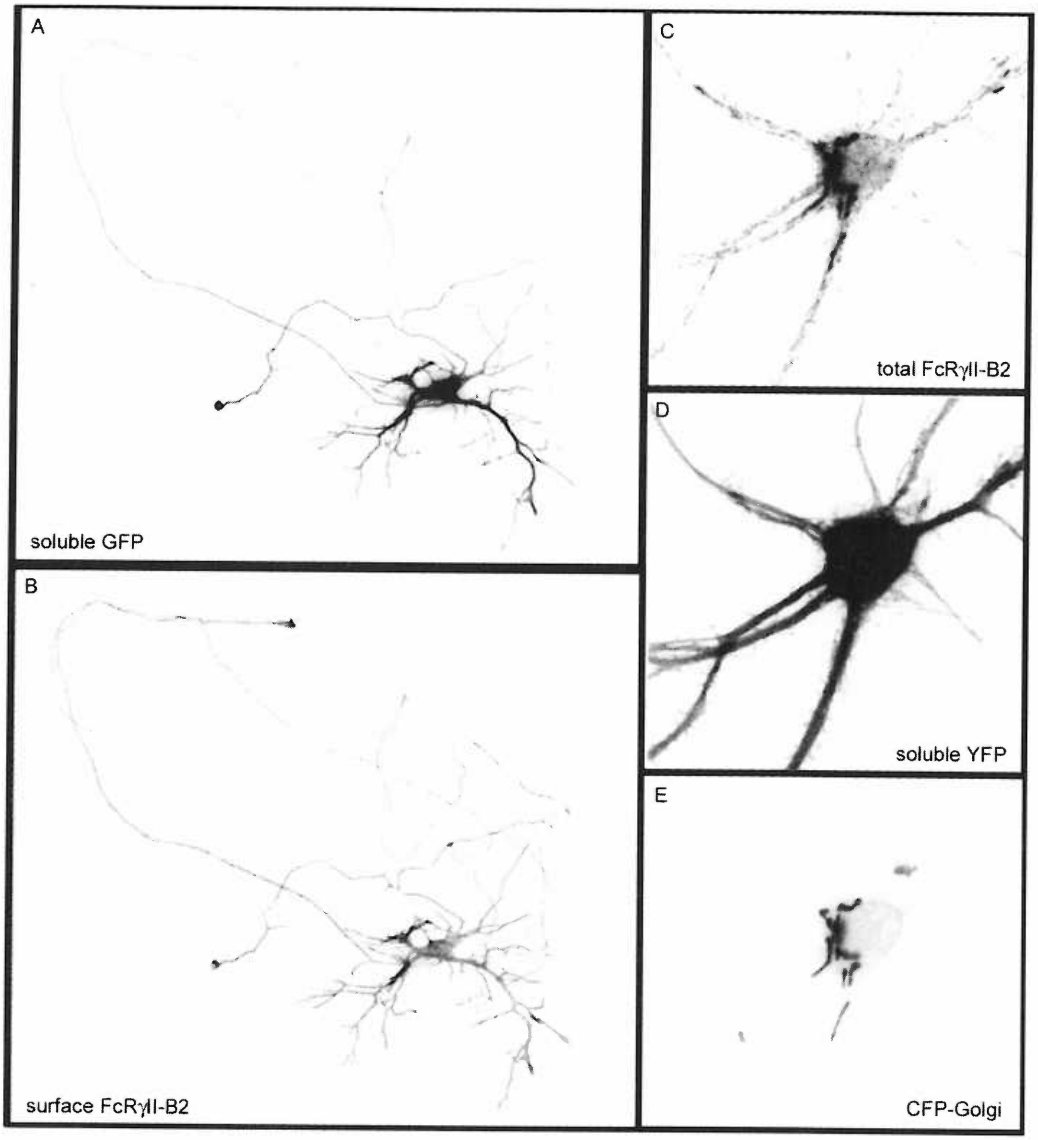

# Chapter 5 Discussion and Future Directions

Sorting Axonal and Dendritic Proteins in the Biosynthetic Pathway

In Chapter 2, trafficking of the axonal marker NgCAM was compared to trafficking of the dendritic marker LDLR. NgCAM and LDLR labeled different vesicle populations under conditions in which vesicles in the biosynthetic pathway were preferentially labeled. This indicates that a sorting event must separate these two proteins at least as early in the biosynthetic pathway as the Golgi complex (although this separation could first occur even earlier in the ER, see below). These findings support a model that has dominated the field of polarized protein sorting for years. Proteins going to different plasma membrane domains are thought to be sorted into different vesicle populations as they leave the Golgi, and are then delivered to the correct domain. This model has rested solely on indirect experiments, and some of the very same labs that proposed the model in the first place are still seeking direct proof of their hypothesis (Keller et al., 2001; Kreitzer et al., 2003). The experiments in Chapter 2 provide this direct proof by using an assay that allows visualization of two vesicle populations in a polarized cell, something that has been lacking in the field previously.

Repeating these experiments using additional axonal and dendritic markers is a necessary next step to determine whether sorting axonal and dendritic markers into separate vesicles is a general rule for most proteins. Unlike NgCAM, other axonal markers, such as VAMP2, become transiently incorporated into the dendritic plasma membrane (Sampo et al., 2003). Could VAMP2 travel to the dendrites in the same

carrier as LDLR? Likewise, many dendritic proteins are completely excluded from the axon (G. Glover, S. Das unpub. obs.), but do they all travel from the Golgi to the dendritic plasma membrane in the same vesicle population? Or are there separate dendritic vesicles that carry synaptically localized proteins such as glutamate receptors, or proteins such as Kv2.1 that are restricted to clusters on the proximal dendrites? By making different vesicle populations, trafficking of proteins could be regulated independently. For instance, a signal to move AMPA receptors from an intracellular compartment to the cell surface would be independent from a signal that increases surface expression of a growth factor receptor. Likewise, if multiple proteins use the same pathway, a signal to increase the trafficking of one protein could have many other side effects— a drug designed to downregulate surface expression of a neurotransmitter transporter could also cause a decrease in iron uptake by removing the Transferrin receptor from the plasma membrane. Two-color live cell imaging of vesicles in polarized neurons can help understand how the sorting and trafficking of various proteins are connected.

A Possible Role for the ER in Polarized Sorting

Recent studies of ER exit have concluded that a sorting signal is necessary for efficient exit from the ER (Gorelick and Shugrue, 2001; Nishimura and Balch, 1997), contrary to the classical belief that ER exit occurred by bulk flow (Wieland et al., 1987). ER exit of VSVG can be inhibited by a soluble peptide version of the VSVG cytoplasmic tail, but not by a soluble version of the EGFR cytoplasmic tail, which contains a different

type of ER export signal (Soza et al., 2004). The COPII subunit sec24p has multiple binding sites for different ER exit signals, indicating that many types of proteins could be sorted into the same vesicle (Miller et al., 2003). It is possible that multiple vesicle types are produced at the ER. But this raises the question of the purpose of this sorting step, if all cargo moves from the ER to the Golgi. The recent proposal that different types of cargo leave the *trans* Golgi from different cisternae, rather than from subdomains of the same cisterna, supports the existence of a pre-sorting step that would ensure that different cargoes are targeted to the correct *trans* Golgi exit cisterna (Ladinsky et al., 1999; Ladinsky et al., 2002). However, this sorting step could just as easily occur during inter-cisternal transport within the Golgi complex, eliminating a potential role for the ER in protein sorting.

The protocols used in Chapter 2 to label vesicles in the biosynthetic pathway did not attempt to eliminate vesicles traveling from the ER to the Golgi. None of the markers studied in Chapter 2 exhibited reticular ER fluorescence, even very early after transfection. The first strong fluorescence was observed in the Golgi complex at about 3.5h after transfection for all markers. The CFP and YFP tags require oxygenation steps after their folding to acquire fluorescence; this occurs with a $t_{1/2}$ of about 30 minutes (Tsien, 1998) . Therefore, proteins that have a simple structure and do not require assembly with other subunits may fold very quickly and be efficiently exported from the ER soon after folding but before they are fluorescent. For GFP-tagged proteins with more complex structures such as AMPAR, NMDAR, mGluR, and EAATs, reticular

fluorescence is easily observed at 3.5h after transfection, and often remains visible for hours (unpub. obs.).

While we did not observe any fluorescence corresponding to the characteristic reticular pattern associated with the ER, newly synthesized proteins exiting the ER become concentrated 4 to 10-fold in ER-derived vesicles (Mironov et al., 2003; Presley et al., 1997a). Even if no reticular fluorescence above background is observed, it is still possible that the ER-derived vesicles will be visible for TfR, LDLR and NgCAM. For typical movies, vesicle fluorescence can be 30-100 arbitrary intensity units (AIU) above background, which is low enough that a 4 to 10-fold concentration increase could easily mean the difference between undetectable fluorescence in the ER and detectable fluorescence in an ER-to-Golgi vesicle. Therefore, while we attempted to make movies at a time when all markers had arrived in the Golgi but had not yet been delivered to the surface, the possibility remains that some fraction of vesicles in the movies from Chapter 2 are actually ER-to-Golgi vesicles instead of Golgi-derived vesicles.

If this were the case, the only way our results could be affected would be if one marker were enriched in mostly ER-derived vesicles, while the second marker was present in mostly Golgi-derived vesicles. In this case, we could observe two vesicle populations and come to the false conclusion that we had observed proteins that were sorted into different vesicles at the Golgi. It is very unlikely that any of our markers behaved this way, since all markers followed a very similar time course of expression, arriving in the Golgi at about the same time, and on the cell surface at about the same time. Even so, blocking protein synthesis by addition of cycloheximide during the 19° C

block could eliminate contamination from ER-derived vesicles. In a recent study in epithelial cells, cycloheximide was added two hours before imaging Golgi-derived vesicles containing LDLR (Kreitzer et al., 2003). Using a similar protocol in neurons could eliminate any questions about ER-derived vesicles.

This control would not address the question of whether the ER is also a sorting station. Determining the role of the ER in polarized sorting would be possible if protein exit from the ER could be synchronized (such as can be done with the temperature-sensitive mutant VSVGts045), and two-color imaging techniques were used to visualize vesicles as they emerge from the ER. Alternatively, a third color could be used to label ER exit sites (by an FP-tagged sec24p, for example (Horton and Ehlers, 2003a)), then cargo exit from these sites could be monitored in the remaining two colors, and absolute synchronicity of ER exit would not be required.

## A Mechanism for Dendritic Sorting

Dendritic sorting signals were examined in two ways in this dissertation. First, in Chapters 3 and 4, the targeting of proteins with several different sorting signals was studied by exogenous expression and mutational analysis. As a result of these studies, two new dendritic sorting signals were identified. In the cytoplasmic domain of EGFR, a combination of proline residues and di-leucine motifs was shown to be necessary for dendritic polarity on the cell surface. In the cytoplasmic domain of EAAT3, a novel motif consisting of the amino acid sequence VNGGFA was shown to be necessary for

dendritic polarity and was also able to partially redirect an unpolarized protein, EAAT2. Neither of these targeting signals fall into previously established categories such as tyrosine-based or di-leucine-based motifs. Their mechanism of action is presumed to be in cargo selection into specialized dendritic vesicles, since GFP-tagged versions of EGFR and EAAT3 were never found in the axon (G. Glover unpub. obs). This indicates that EGFR and EAAT3, like other dendritic proteins, were sorted into a vesicle that can only be transported in dendrites, rather than being transported everywhere in the cell but then fusing only with the dendritic plasma membrane. If the latter situation were true, then some GFP signal should be observed in vesicles in axons even if no axonal plasma membrane staining can be observed.

These results provide indirect evidence that dendritic sorting signals are important for cargo selection into nascent vesicles. Chapter 2 reported a second method of studying dendritic sorting signals. Two-color live cell imaging was used to image vesicles containing wild type or mutant versions of the dendritic marker LDLR. From these experiments, it has become clear that the dendritic sorting signal in LDLR is critical for its incorporation into the proper vesicle population in the biosynthetic pathway. Mutant LDLR was packaged in a vesicle containing the axonal protein NgCAM, but wild type LDLR was packaged into a separate vesicle population that did not contain NgCAM.

The studies in this dissertation support the following model of dendritic targeting. In the biosynthetic pathway (most likely as dendritic proteins exit the Golgi), dendritic sorting signals direct protein-protein interactions with cytosolic factors, leading to the formation of transport vesicles that have specific characteristics. First, these vesicles

almost never contain axonal proteins. Second, these vesicles are able to bind motor proteins and be transported only in dendrites, while they are unable to enter the axon. The vesicles that carry dendritic markers in the endosomal pathway also possess both of these characteristics.

If this model proves to be generally correct, several major outstanding questions about dendritic targeting remain. First, what are the interacting partners of dendritic sorting signals that are necessary to recruit them into this specialized type of transport vesicle? Are members of the adaptor family important for dendritic targeting? The sorting signal of LDLR binds to two different adaptors, AP-1B and AP-4, which are each necessary for its basolateral targeting in epithelial cells (Gan et al., 2002; Simmen et al., 2002). Since AP-1B is not expressed in neurons, AP-4 is left as the most likely candidate for its dendritic targeting. Using an RNAi approach to knock down AP-4 expression in neurons could determine what role AP-4 plays in dendritic targeting of LDLR and other dendritic proteins. If AP-4 is important for dendritic sorting, we expect that LDLR and possibly other dendritic proteins will be unpolarized in cells in which AP-4 has been knocked down. This type of experiment is appealing since the expected result is clear and quantifiable—the presence of some proportion of a dendritic protein on the axonal surface can be easily observed. Similar experiments could be performed for other candidate dendritic sorting molecules, either using RNAi or by expressing dominant negatives. The small GTPases rab8 and cdc42 might be candidates to consider for this approach since they have both been shown to function in basolateral sorting, and dominant negative versions of each are available (Ang et al., 2003; Musch et al., 2001).

Future experiments will also be necessary to determine how many different populations of dendritic vesicles are present in neurons. For instance, EGFR, LDLR and EAAT3 have unrelated sorting signals. In epithelial cells, LDLR sorting to the basolateral domain can be disrupted by knocking down expression of the adaptors AP-1B or AP-4, but EGFR's basolateral sorting is not affected by AP-1B knock-down, and EAAT3 is targeted to the apical domain (Gan et al., 2002; Mullin and McGinn, 1987; Simmen et al., 2002). Each of these markers could be sorted into a different dendritic vesicle population in neurons, or perhaps multiple adaptors or adaptor-like molecules could mediate incorporation of cargo into the same vesicle. Comparing multiple dendritic markers to one another in two-color movies of vesicle transport could distinguish between these possibilities.

In Chapter 2, an attempt at such a comparison was made between the dendritic markers LDLR and TfR. Technical issues arose when trying to enrich TfR and LDLR in the biosynthetic pathway at the same time. Soon after release of the low temperature Golgi block, TfR started to colocalize with its ligand, Tf, in endosomes. Was this because TfR is endocytosed from the dendritic surface into endosomes very rapidly? Or does TfR go through these endosomes on its way to the surface? An attempt to use fluorescently labeled antibody to differentiate between these two possibilities was hampered by artifacts. The antibody appeared to fall off of its target and also seemed to aggregate in endosomes. A different, antibody-free method to fluorescently label the surface population of a protein has recently been developed (Howarth et al., 2005). In the future, this method (based on biotin-streptavidin binding) could be used to follow the

arrival of TfR and other markers in endosomes and to determine whether some dendritic proteins pass though endosomes before reaching the dendritic surface.

Perhaps the most striking feature of dendritic vesicles is their inability to enter the axon. This feature is common to dendritic vesicles of both the biosynthetic and endosomal varieties. The molecular basis for this phenomenon is completely unknown. It is likely that molecules on dendritic vesicles interact with motors in such a way that transport along axonal microtubules is impossible. Perhaps motors recognize biochemical differences between dendritic and axonal microtubules (Craig and Banker, 1994), or perhaps dendritic motors are "turned off" by a regulatory factor as dendritic vesicles enter the axon initial segment (Reilein et al., 2001). No cargo-motor interactions that provide clues to the mechanism underlying dendritic vesicle transport have been identified. A recent study described an interaction *in vitro* between the scaffolding protein complex Mint 1 and the neuron-specific minus-end directed motor KIF17 (Setou et al., 2000). This interaction was thought to be essential for the synaptic delivery of the NMDA receptor subunit NR2B (Guillaud et al., 2003). However, in the Mint 1 knockout mice, long term potentiation was induced normally, implicating that NMDA receptors were properly localized (Ho et al., 2003). Thus, it seems that there is only a minor or redundant role of KIF17 in dendritic transport. The question of how dendritic vesicles are restricted to the dendrites remains completely open for study.

## A Mechanism for Axonal Sorting

The axonal marker NgCAM was rarely found in a vesicle with a dendritic marker. Therefore, axonal proteins, like dendritic proteins, may also participate in specific interactions that mediate their incorporation into an "axonal" vesicle. Unlike dendritic markers, however, NgCAM vesicles are not transported directly into the axon. Instead, they are able to enter and exit the dendrites, but these vesicles must not fuse with the dendritic membrane (Burack et al., 2000; Sampo et al., 2003). For both axonal and dendritic vesicles, an unknown molecule or molecules must associate with the vesicles in order for the cargo within to become polarized. In the case of dendritic vesicles containing LDLR or TFR, preferential transport seems to be critical for dendritic protein polarity. In contrast, while transport is slightly biased into the axon for NgCAM (Burack et al., 2000), fusion or retention in the axonal plasma membrane is likely critical for axonal polarity. The molecular machinery necessary for axonal polarity of NgCAM is also a mystery.

## NgCAM and the Unpolarized Marker LDLRmut

One peculiar feature of NgCAM vesicles stands out. When NgCAM was coexpressed with a mutant form of LDLR, which is unpolarized, a high percentage of carriers contained both markers (this result has been confirmed independently by S. Kaech). This means that LDLRmut is nearly exclusively packaged into these vesicles. How can this be if NgCAM is only able to fuse with the axonal plasma membrane and

LDLRmut is found on the surface of the entire cell? Since we were unable to compare LDLRmut to the dendritic markers TfR and wild type LDLR due to technical issues, we cannot rule out the possibility that some fraction of LDLRmut is present in a vesicle that undergoes fusion with the dendritic plasma membrane. More than 2/3 of vesicles containing LDLRmut were NgCAM-labeled (and therefore not the kind that would contain wild type LDLR). That leaves about 1/3 of the vesicles that could be competent for fusion in the dendrites. This could be enough to account for the unpolarized distribution of LDLRmut if the axon is twice as large in surface area than the dendrites. This is a reasonable assumption at the period in development when these experiments were performed. In this case, twice as many vesicles could carry LDLRmut to the axon than to the dendrites, but the protein would still be unpolarized on the cell surface.

While it is tempting to consider the above scenario, the percentage of overlap between two markers in these experiments should not be interpreted as an absolute quantification. Signal-to-noise ratios were typically very low in these movies, so the percentage of overlap should be used as more of a guide than an absolute; quantification of overlap was intended to serve more as a basis of comparison between marker pairs than as stand-alone data. In addition, because of low signal, we do not address the relative concentration of two different markers in a vesicle. This parameter could be very important to consider when quantifying the contents of a vesicle in relation to the polarity on the cell surface. For instance, if there were twice as much NgCAM in a vesicle than LDLRmut, then the ratio of fluorescence of NgCAM on the axonal vs. dendritic surface would be higher than for LDLRmut upon fusion of this vesicle. Additionally, if we are

unable to detect the fluorescence signal from a vesicle with just a few copies of GFP associated with it, we could potentially miss many vesicles that contain few copies of one protein, but more of another. When attempting to image single GFP molecules in solution on the spinning disk confocal, I was unable to detect single GFPs. Meanwhile, a single GFP could be easily observed using total internal reflection microscopy when all other imaging parameters were equal (data not shown). To get a rough estimate of how many copies of GFP are in a typical vesicle, I used total internal reflection microscopy to image a cell expressing TfR-GFP with the exact same settings as I used for imaging single GFP molecules in solution. According to this experiment, a typical TfR-GFP vesicle contains between 50-200 GFPs, depending on its apparent size (data not shown). For fluorophores that are not as bright as GFP (such as CFP), I may not be able to detect small vesicles on the spinning disk. This is another potential caveat to quantification of two-color vesicle transport movies; there is a real potential that small or dim vesicles can be undetectable. Brighter and more stable fluorophores could be used to minimize this problem. An improved version of CFP that is brighter and more photostable, Cerulean, is now available, and a red fluorescent protein from coral has recently been modified to several potentially useful forms (Rizzo et al., 2004; Shaner et al., 2004). It would be wise to explore these options for future experiments.

The unpolarized surface localization of LDLRmut and the axonal surface localization of NgCAM were determined 18-24h after transfection (Jareb and Banker 1998; Sampo et al. 2003). Staining for surface protein at an earlier timepoint could show a different result. When cells expressing unpolarized proteins like FcRγII-B2 or CD44

are stained for surface protein at early times after transfection (i.e. 4-6h), they are found on both the surface of the axon and dendrites (Chapter 4 supp. mat.). However, a slight enrichment in the distal axon is visible in many cells, consistent with the model that addition of new membrane occurs preferentially at the distal tip of the axon (Craig et al., 1995). Perhaps the unpolarized LDLRmut is slightly polarized to the axon at early times. This would also help explain why LDLRmut is found in most NgCAM vesicles.

The protocol for quantifying surface polarity at steady state (18-24h after transfection) that was used in Chapters 3 and 4 cannot be directly transferred to the earliest timepoint when protein arrives on the surface. First, at early times, very little protein accumulates on the surface, and so the signal from the surface stain is closer to background than at steady state. Quantifying fluorescence is more reliable when background subtraction does not eliminate the majority of the fluorescence signal. In addition, the surface fluorescence at early times is not as uniformly distributed along the surface as it is at later times, especially in the axon. Instead, fluorescence is concentrated at the distal tip of the axon. This makes it difficult to get an accurate average fluorescence reading for the axon and therefore also makes it difficult to directly compare polarity at early and later times after transfection. A better measure for cell surface polarity at the earliest time possible must be developed. At early times, the surface polarity reflects the acute effect of biosynthetic vesicle trafficking. It is therefore an essential measure to consider for accurate interpretation of results from two-color vesicle trafficking studies. The methodological issues described in the context of the behavior

of LDLRmut are general problems that could impact the interpretation of results obtained in other experiments as well.

Conclusion

The studies in this dissertation have used modern microscopy methods to answer questions about conventional models for the establishment of protein polarity. Many of the results from these studies were somewhat predictable based on existing dogma. For example, axonal and dendritic proteins *are* sorted into separate vesicles, and sorting signals *do* mediate this sorting. A few surprises were also in store. An unpolarized marker, LDLRmut, was largely in the same vesicle population as an axonal marker, NgCAM. A Glutamate transporter was sorted to the apical domain of epithelia and the dendritic domain of neurons, and both localizations were dependant on the same novel cytoplasmic peptide motif. FcRγIIB2 and CD44, proteins with well-known basolateral sorting signals, were not differentially distributed in neurons. Both the predictable results and the surprises necessitate further study. To determine whether the results of Chapter 2 can be generalized for all proteins, two-color movies of vesicle transport should be performed with a variety of markers. Describing these vesicle populations is important, but the long-term goal is to understand all of the molecular interactions that are responsible for translating a peptide sorting signal into a specific vesicle population. This includes identifying the proteins and lipids that participate in recruiting cargo into forming vesicles, as well as identifying vesicle-specific motors and fusion machinery that mediate trafficking steps downstream of sorting.

## Bibliography


Ahn, J., Mundigl, O., Muth, T. R., Rudnick, G., and Caplan, M. J. (1996). Polarized expression of GABA transporters in Madin-Darby canine kidney cells and cultured hippocampal neurons. J Biol Chem *271*, 6917-6924.

Alberts, B., Bray, D., Lewis, J., Raff, M., Roberts, K., and Watson, J. D. (1994). Cell Junctions, Cell Adhesion, and the Extracellular Matrix. In Molecular Biology of the Cell Third Edition (New York and London, Garland Publishing, Inc.), pp. 949-1010.

Allison, D. W., Chervin, A. S., Gelfand, V. I., and Craig, A. M. (2000). Postsynaptic scaffolds of excitatory and inhibitory synapses in hippocampal neurons: maintenance of core components independent of actin filaments and microtubules. J Neurosci *20*, 4545-4554.

Anderson, E., Maday, S., Sfakianos, J., Hull, M., Winckler, B., Sheff, D., Folsch, H., and Mellman, I. (2005). Transcytosis of NgCAM in epithelial cells reflects differential signal recognition on the endocytic and secretory pathways. J Cell Biol *170*, 595-605.

Ang, A. L., Folsch, H., Koivisto, U. M., Pypaert, M., and Mellman, I. (2003). The Rab8 GTPase selectively regulates AP-1B-dependent basolateral transport in polarized Madin-Darby canine kidney cells. J Cell Biol *163*, 339-350.

Ang, A. L., Taguchi, T., Francis, S., Folsch, H., Murrells, L. J., Pypaert, M., Warren, G., and Mellman, I. (2004). Recycling endosomes can serve as intermediates during transport from the Golgi to the plasma membrane of MDCK cells. J Cell Biol *167*, 531-543.

Antonucci, D. E., Lim, S. T., Vassanelli, S., and Trimmer, J. S. (2001). Dynamic localization and clustering of dendritic Kv2.1 voltage-dependent potassium channels in developing hippocampal neurons. Neuroscience *108*, 69-81.

Aridor, M., Fish, K. N., Bannykh, S., Weissman, J., Roberts, T. H., Lippincott-Schwartz, J., and Balch, W. E. (2001). The Sar1 GTPase coordinates biosynthetic cargo selection with endoplasmic reticulum export site assembly. J Cell Biol *152*, 213-229.

Aridor, M., Guzik, A. K., Bielli, A., and Fish, K. N. (2004). Endoplasmic reticulum export site formation and function in dendrites. J Neurosci *24*, 3770-3776.

Arriza, J. L., Eliasof, S., Kavanaugh, M. P., and Amara, S. G. (1997). Excitatory amino acid transporter 5, a retinal glutamate transporter coupled to a chloride conductance. Proc Natl Acad Sci U S A *94*, 4155-4160.

Arriza, J. L., Fairman, W. A., Wadiche, J. I., Murdoch, G. H., Kavanaugh, M. P., and Amara, S. G. (1994). Functional comparisons of three glutamate transporter subtypes cloned from human motor cortex. J Neurosci *14*, 5559-5569.

Baas, P. W., Black, M. M., and Banker, G. A. (1989). Changes in microtubule polarity orientation during the development of hippocampal neurons in culture. J Cell Biol *109*, 3085-3094.

Baas, P. W., Deitch, J. S., Black, M. M., and Banker, G. A. (1988). Polarity orientation of microtubules in hippocampal neurons: uniformity in the axon and nonuniformity in the dendrite. Proc Natl Acad Sci U S A *85*, 8335-8339.
Bacallao, R., Antony, C., Dotti, C., Karsenti, E., Stelzer, E. H., and Simons, K. (1989). The subcellular organization of Madin-Darby canine kidney cells during the formation of a polarized epithelium. J Cell Biol *109*, 2817-2832.
Banker, G., and Goslin, K. (1998). Rat Hippocampal Neurons in Low-Density Culture. In Culturing Nerve Cells, G. Banker, and K. Goslin, eds. (Cambridge, MIT Press), pp. 339-370.
Barman, S., and Nayak, D. P. (2000). Analysis of the transmembrane domain of influenza virus neuraminidase, a type II transmembrane glycoprotein, for apical sorting and raft association. J Virol *74*, 6538-6545.
Bartlett, W. P., and Banker, G. A. (1984a). An electron microscopic study of the development of axons and dendrites by hippocampal neurons in culture. I. Cells which develop without intercellular contacts. J Neurosci *4*, 1944-1953.
Bartlett, W. P., and Banker, G. A. (1984b). An electron microscopic study of the development of axons and dendrites by hippocampal neurons in culture. II. Synaptic relationships. J Neurosci *4*, 1954-1965.
Bastaki, M., Braiterman, L. T., Johns, D. C., Chen, Y. H., and Hubbard, A. L. (2002). Absence of direct delivery for single transmembrane apical proteins or their "Secretory" forms in polarized hepatic cells. Mol Biol Cell *13*, 225-237.
Benson, D. L., Yoshihara, Y., and Mori, K. (1998). Polarized distribution and cell type-specific localization of telencephalin, an intercellular adhesion molecule. J Neurosci Res *52*, 43-53.
Ben-Tekaya, H., Miura, K., Pepperkok, R., and Hauri, H. P. (2005). Live imaging of bidirectional traffic from the ERGIC. J Cell Sci *118*, 357-367.
Bergmann, J. E., Tokuyasu, K. T., and Singer, S. J. (1981). Passage of an integral membrane protein, the vesicular stomatitis virus glycoprotein, through the Golgi apparatus en route to the plasma membrane. Proceedings of the National Asademy of Sciences *78*, 1746-1750.
Bishop, N. E. (2003). Dynamics of endosomal sorting. Int Rev Cytol *232*, 1-57.
Blott, E. J., Bossi, G., Clark, R., Zvelebil, M., and Griffiths, G. M. (2001). Fas ligand is targeted to secretory lysosomes via a proline-rich domain in its cytoplasmic tail. J Cell Sci *114*, 2405-2416.
Blumstein, J., Faundez, V., Nakatsu, F., Saito, T., Ohno, H., and Kelly, R. B. (2001). The neuronal form of adaptor protein-3 is required for synaptic vesicle formation from endosomes. J Neurosci *21*, 8034-8042.
Boehm, M., and Bonifacino, J. S. (2002). Genetic analyses of adaptin function from yeast to mammals. Gene *286*, 175-186.
Boll, W., Rapoport, I., Brunner, C., Modis, Y., Prehn, S., and Kirchhausen, T. (2002). The mu2 subunit of the clathrin adaptor AP-2 binds to FDNPVY and YppO sorting signals at distinct sites. Traffic *3*, 590-600.
Boman, A. L. (2001). GGA proteins: new players in the sorting game. J Cell Sci *114*, 3413-3418.

Bonifacino, J. S., and Traub, L. M. (2003). Signals for Sorting of Transmembrane Proteins to Endosomes and Lysosomes. Annu Rev Biochem *6*, 6.
Boron, W. F., Roos, A., and De Weer, P. (1978). NH4Cl and other weak bases in the activation of sea urchin eggs. Nature *274*, 190.
Bradke, F., and Dotti, C. G. (1998). Membrane traffic in polarized neurons. Biochim Biophys Acta *1404*, 245-258.
Brasnjo, G., and Otis, T. S. (2001). Neuronal glutamate transporters control activation of postsynaptic metabotropic glutamate receptors and influence cerebellar long-term depression. Neuron *31*, 607-616.
Brown, M. D., Banker, G. A., Hussaini, I. M., Gonias, S. L., and VandenBerg, S. R. (1997). Low density lipoprotein receptor-related protein is expressed early and becomes restricted to a somatodendritic domain during neuronal differentiation in culture. Brain Res *747*, 313-317.
Brown, P. S., Wang, E., Aroeti, B., Chapin, S. J., Mostov, K. E., and Dunn, K. W. (2000). Definition of distinct compartments in polarized Madin-Darby Canine Kidney (MDCK) cells for membrane-volume sorting, polarized sorting and apical recycling. Traffic *1*, 124-140.
Burack, M. A., Siverman, M. S., and Banker, G. (2000). The Role of Selective Transport in Neuronal Protein Sorting. Neuron *26*, 465-472.
Burgess, T. L., and Kelly, R. B. (1987). Constitutive and Regulated Secretion of Proteins. Annual Review of Cell Biology *3*, 243-293.
Caplan, M. J., Anderson, H. C., Palade, G. E., and Jamieson, J. D. (1986). Intracellular sorting and polarized cell surface delivery of (Na+,K+)ATPase, an endogenous component of MDCK cell basolateral plasma membranes. Cell *46*, 623-631.
Carlton, J., Bujny, M., Peter, B. J., Oorschot, V. M., Rutherford, A., Mellor, H., Klumperman, J., McMahon, H. T., and Cullen, P. J. (2004). Sorting nexin-1 mediates tubular endosome-to-TGN transport through coincidence sensing of high- curvature membranes and 3-phosphoinositides. Curr Biol *14*, 1791-1800.
Carlton, J., Bujny, M., Rutherford, A., and Cullen, P. (2005). Sorting nexins--unifying trends and new perspectives. Traffic *6*, 75-82.
Casanova, J. E., Apodaca, G., and Mostov, K. E. (1991). An autonomous signal for basolateral sorting in the cytoplasmic domain of the polymeric immunoglobulin receptor. Cell *66*, 65-75.
Chant, J. (1999). Cell polarity in yeast. Annu Rev Cell Dev Biol *15*, 365-391.
Chardin, P., and McCormick, F. (1999). Brefeldin A: The Advantage of Being Uncompetitive. Cell *97*, 153-155.
Chavrier, P., and Goud, B. (1999). The Role of ARF and Rab GTPases in Membrane Transport. Current Opinion in Cell Biology *11*, 466-475.
Cheng, C., Glover, G., Banker, G., and Amara, S. G. (2002). A novel sorting motif in the glutamate transporter excitatory amino acid transporter 3 directs its targeting in Madin-Darby canine kidney cells and hippocampal neurons. J Neurosci *22*, 10643-10652.
Chevet, E., Cameron, P. H., Pelletier, M. F., Thomas, D. Y., and Bergeron, J. J. (2001). The endoplasmic reticulum: integration of protein folding, quality control, signaling and degradation. Curr Opin Struct Biol *11*, 120-124.

Christoforidis, S., McBride, H. M., Burgoyne, R. D., and Zerial, M. (1999). The Rab5 effector EEA1 is a core component of endosome docking. Nature *397*, 621-625.
Chuang, J. Z., and Sung, C. H. (1998). The cytoplasmic tail of rhodopsin acts as a novel apical sorting signal in polarized MDCK cells. J Cell Biol *142*, 1245-1256.
Coco, S., Raposo, G., Martinez, S., Fontaine, J. J., Takamori, S., Zahraoui, A., Jahn, R., Matteoli, M., Louvard, D., and Galli, T. (1999). Subcellular localization of tetanus neurotoxin-insensitive vesicle- associated membrane protein (VAMP)/VAMP7 in neuronal cells: evidence for a novel membrane compartment. J Neurosci *19*, 9803-9812.
Coco, S., Verderio, C., Trotti, D., Rothstein, J. D., Volterra, A., and Matteoli, M. (1997). Non-synaptic localization of the glutamate transporter EAAC1 in cultured hippocampal neurons. Eur J Neurosci *9*, 1902-1910.
Conti, F., DeBiasi, S., Minelli, A., Rothstein, J. D., and Melone, M. (1998). EAAC1, a high-affinity glutamate tranporter, is localized to astrocytes and gabaergic neurons besides pyramidal cells in the rat cerebral cortex. Cereb Cortex *8*, 108-116.
Costes, S. V., Daelemans, D., Cho, E. H., Dobbin, Z., Pavlakis, G., and Lockett, S. (2004). Automatic and quantitative measurement of protein-protein colocalization in live cells. Biophys J *86*, 3993-4003.
Craig, A. M., and Banker, G. (1994). Neuronal polarity. Annu Rev Neurosci *17*, 267-310.
Craig, A. M., Blackstone, C. D., Huganir, R. L., and Banker, G. (1994). Selective clustering of glutamate and gamma-aminobutyric acid receptors opposite terminals releasing the corresponding neurotransmitters. Proc Natl Acad Sci U S A *91*, 12373-12377.
Craig, A. M., Rao, A., and Harms, K. J. (2000). Neuroligation: building synapses around the neurexin-neuroligin link. Nature Neuroscience *3*, 747-749.
Craig, A. M., Wyborski, R. J., and Banker, G. (1995). Preferential addition of newly synthesized membrane protein at axonal growth cones. Nature *375*, 592-594.
Crump, C. M., Xiang, Y., Thomas, L., Gu, F., Austin, C., Tooze, S. A., and Thomas, G. (2001). PACS-1 binding to adaptors is required for acidic cluster motif-mediated protein traffic. Embo J *20*, 2191-2201.
Dabrowski, M., Aerts, S., Van Hummelen, P., Craessaerts, K., De Moor, B., Annaert, W., Moreau, Y., and De Strooper, B. (2003). Gene profiling of hippocampal neuronal culture. J Neurochem *85*, 1279-1288.
Daniels, G. M., and Amara, S. G. (1998). Selective labeling of neurotransmitter transporters at the cell surface. Methods Enzymol *296*, 307-318.
Das, S. S., and Banker, G. (ms. in prep.). the Involvement of the c-terminus of mGluR1a in its dendritic and synatpic localization.
de Hoop, M. J., Huber, L. A., Stenmark, H., Williamson, E., Zerial, M., Parton, R. G., and Dotti, C. G. (1994). The involvement of the small GTP-binding protein Rab5a in neuronal endocytosis. Neuron *13*, 11-22.
de Renzis, S., Sonnichsen, B., and Zerial, M. (2002). Divalent Rab effectors regulate the sub-compartmental organization and sorting of early endosomes. Nat Cell Biol *4*, 124-133.
Dehnes, Y., Chaudhry, F. A., Ullensvang, K., Lehre, K. P., Storm-Mathisen, J., and Danbolt, N. C. (1998). The glutamate transporter EAAT4 in rat cerebellar Purkinje cells:

a glutamate-gated chloride channel concentrated near the synapse in parts of the dendritic membrane facing astroglia. J Neurosci *18*, 3606-3619.
Deora, A. A., Gravotta, D., Kreitzer, G., Hu, J., Bok, D., and Rodriguez-Boulan, E. (2004). The basolateral targeting signal of CD147 (EMMPRIN) consists of a single leucine and is not recognized by retinal pigment epithelium. Mol Biol Cell *15*, 4148-4165.
Dietrich, J., Hou, X., Wegener, A. M., and Geisler, C. (1994). CD3 gamma contains a phosphoserine-dependent di-leucine motif involved in down-regulation of the T cell receptor. Embo J *13*, 2156-2166.
Dotti, C. G., Kartenbeck, J., and Simons, K. (1993). Polarized distribution of the viral glycoproteins of vesicular stomatitis, fowl plague and Semliki Forest viruses in hippocampal neurons in culture: a light and electron microscopy study. Brain Res *610*, 141-147.
Dotti, C. G., and Simons, K. (1990). Polarized Sorting of Viral Glycoproteins to the Axon and Dendrites of Hippocampal Neurons in Culture. Cell *62*, 63-72.
Dotti, C. G., Sullivan, C. A., and Banker, G. A. (1988). The establishment of polarity by hippocampal neurons in culture. J Neurosci *8*, 1454-1468.
Drubin, D. G., and Nelson, W. J. (1996). Origins of Cell Polarity. Cell *84*, 335-344.
Dwyer, N. D., Adler, C. E., Crump, J. G., L'Etoile, N. D., and Bargmann, C. I. (2001). Polarized dendritic transport and the AP-1 mu1 clathrin adaptor UNC-101 localize odorant receptors to olfactory cilia. Neuron *31*, 277-287.
Eiraku, M., Hirata, Y., Takeshima, H., Hirano, T., and Kengaku, M. (2002). Delta/Notch-like Epidermal Growth Factor (EGF)-related Receptor, a Novel EGF-like Repeat-containing Protein Targeted to Dendrites of Developing and Adult Central Nervous System Neurons. J Biol Chem *277*, 25400-25407.
El-Husseini Ael, D., Craven, S. E., Brock, S. C., and Bredt, D. S. (2001). Polarized targeting of peripheral membrane proteins in neurons. J Biol Chem *276*, 44984-44992.
Fache, M. P., Moussif, A., Fernandes, F., Giraud, P., Garrido, J. J., and Dargent, B. (2004). Endocytotic elimination and domain-selective tethering constitute a potential mechanism of protein segregation at the axonal initial segment. J Cell Biol *166*, 571-578.
Fairman, W. A., Vandenberg, R. J., Arriza, J. L., Kavanaugh, M. P., and Amara, S. G. (1995). An excitatory amino-acid transporter with properties of a ligand-gated chloride channel. Nature *375*, 599-603.
Farquhar, M. G. (1985). Progress in Unraveling Pathways of Golgi Traffic. Annual Review of Cell Biology *1*, 447-488.
Farquhar, M. G., and Palade, G. (1998). The Golgi Apparatus: 100 Years of Progress and Controversy. Trends in Cell Biology *8*, 2-10.
Federovitch, C. M., Ron, D., and Hampton, R. Y. (2005). The dynamic ER: experimental approaches and current questions. Curr Opin Cell Biol *17*, 409-414.
Folsch, H., Ohno, H., Bonifacino, J. S., and Mellman, I. (1999). A novel clathrin adaptor complex mediates basolateral targeting in polarized epithelial cells. Cell *99*, 189-198.
Friend, D. S., and Farquar, M. G. (1967). Functions of Coated Vesicles During Protein Absorption in the Rat Vas Deferens. Journal of Cell Biology *35*, 357-376.

Furuta, A., Martin, L. J., Lin, C. L., Dykes-Hoberg, M., and Rothstein, J. D. (1997). Cellular and synaptic localization of the neuronal glutamate transporters excitatory amino acid transporter 3 and 4. Neuroscience *81*, 1031-1042.
Futter, C. E., Connoly, C. N., Cutler, D. F., and Hopkins, C. R. (1995). Newly Synthesized Transferrin Receptors Can Be Detected in the Endosome Before They Appear on the Cell Surface. Journal of Biological Chemistry *270*, 10999-11003.
Futter, C. E., Gibson, A., Allchin, E. H., Maxwell, S., Ruddock, L. J., Odorizzi, G., Domingo, D., Trowbridge, I. S., and Hopkins, C. R. (1998). In polarized MDCK cells basolateral vesicles arise from clathrin-gamma- adaptin-coated domains on endosomal tubules. J Cell Biol *141*, 611-623.
Gan, Y., McGraw, T. E., and Rodriguez-Boulan, E. (2002). The epithelial-specific adaptor AP1B mediates post-endocytic recycling to the basolateral membrane. Nat Cell Biol *4*, 605-609.
Garrido, J. J., Fernandes, F., Giraud, P., Mouret, I., Pasqualini, E., Fache, M. P., Jullien, F., and Dargent, B. (2001). Identification of an axonal determinant in the C-terminus of the sodium channel Na(v)1.2. Embo J *20*, 5950-5961.
Garrido, J. J., Fernandes, F., Moussif, A., Fache, M. P., Giraud, P., and Dargent, B. (2003a). Dynamic compartmentalization of the voltage-gated sodium channels in axons. Biol Cell *95*, 437-445.
Garrido, J. J., Giraud, P., Carlier, E., Fernandes, F., Moussif, A., Fache, M. P., Debanne, D., and Dargent, B. (2003b). A targeting motif involved in sodium channel clustering at the axonal initial segment. Science *300*, 2091-2094.
Ghavami, A., Stark, K. L., Jareb, M., Ramboz, S., Segu, L., and Hen, R. (1999). Differential addressing of 5-HT1A and 5-HT1B receptors in epithelial cells and neurons. J Cell Sci *112*, 967-976.
Gibson, A., Futter, C. E., Maxwell, S., Allchin, E. H., Shipman, M., Kraehenbuhl, J. P., Domingo, D., Odorizzi, G., Trowbridge, I. S., and Hopkins, C. R. (1998). Sorting mechanisms regulating membrane protein traffic in the apical transcytotic pathway of polarized MDCK cells. J Cell Biol *143*, 81-94.
Goldstein, L. S., and Yang, Z. (2000). Microtubule-based transport systems in neurons: the roles of kinesins and dyneins. Annu Rev Neurosci *23*, 39-71.
Gorelick, F. S., and Shugrue, C. (2001). Exiting the endoplasmic reticulum. Mol Cell Endocrinol *177*, 13-18.
Gorvel, J. P., Chavrier, P., Zerial, M., and Gruenberg, J. (1991). rab5 controls early endosome fusion *in vitro*. Cell *64*, 915-925.
Griffiths, G., Pfeiffer, S., Simons, K., and Matlin, K. (1985). Exit of newly synthesized membrane proteins from the trans cisterna of the Golgi complex to the plasma membrane. Journal of Cell Biology *101*, 949-964.
Griffiths, G., and Simons, K. (1986). The trans Golgi Network: Sorting at the Exit Site of the Golgi Complex. Science *234*, 438-443.
Gruenberg, J. (2001). The endocytic pathway: a mosaic of domains. Nat Rev Mol Cell Biol *2*, 721-730.
Gu, C., Jan, Y. N., and Jan, L. Y. (2003). A conserved domain in axonal targeting of Kv1 (Shaker) voltage-gated potassium channels. Science *301*, 646-649.

Gu, F., Crump, C. M., and Thomas, G. (2001). Trans-golgi network sorting. Cellular and molecular life sciences *58*, 1067-1084.
Guillaud, L., Setou, M., and Hirokawa, N. (2003). KIF17 dynamics and regulation of NR2B trafficking in hippocampal neurons. J Neurosci *23*, 131-140.
Gumbiner, B., and Kelly, R. B. (1982). Two Distinct Intracellular Pathways Transport Secretory and Membrane Glycoproteins to the Surface of Pituitary Cells. Cell *28*, 51-59.
Gunawardena, S., and Goldstein, L. S. (2004). Cargo-carrying motor vehicles on the neuronal highway: transport pathways and neurodegenerative disease. J Neurobiol *58*, 258-271.
Haft, C. R., de la Luz Sierra, M., Barr, V. A., Haft, D. H., and Taylor, S. I. (1998). Identification of a family of sorting nexin molecules and characterization of their association with receptors. Mol Cell Biol *18*, 7278-7287.
Hammerton, R. W., Krzeminski, K. A., Mays, R. W., Ryan, T. A., Wollner, D. A., and Nelson, W. J. (1991). Mechanism for Regulating Cell Surface Distribution Na+/K+ ATPase in Polarized Epithelial Cells. Science *254*, 847-850.
Hammond, A. T., and Glick, B. S. (2000). Dynamics of transitional endoplasmic reticulum sites in vertebrate cells. Mol Biol Cell *11*, 3013-3030.
Hannah, M. J., Schmidt, A. A., and Huttner, W. B. (1999). Synaptic vesicle biogenesis. Annu Rev Cell Dev Biol *15*, 733-798.
Hauri, H. P., and Schweizer, A. (1992). The endoplasmic reticulum-Golgi intermediate compartment. Curr Opin Cell Biol *4*, 600-608.
He, C., Hobert, M., Friend, L., and Carlin, C. (2002). The epidermal growth factor receptor juxtamembrane domain has multiple basolateral plasma membrane localization determinants, including a dominant signal with a polyproline core. J Biol Chem *277*, 38284-38293.
He, Y., Hof, P. R., Janssen, W. G., Rothstein, J. D., and Morrison, J. H. (2001). Differential synaptic localization of GluR2 and EAAC1 in the macaque monkey entorhinal cortex: a postembedding immunogold study. Neurosci Lett *311*, 161-164.
Heusser, K., and Schwappach, B. (2005). Trafficking of potassium channels. Curr Opin Neurobiol *15*, 364-369.
Hinners, I., Wendler, F., Fei, H., Thomas, L., Thomas, G., and Tooze, S. A. (2003). AP-1 recruitment to VAMP4 is modulated by phosphorylation-dependent binding of PACS-1. EMBO Rep *4*, 1182-1189.
Hirschberg, K., Miller, C. M., Ellenberg, J., Presley, J. F., Siggia, E. D., Phair, R. D., and Lippincott-Schwartz, J. (1998). Kinetic analysis of secretory protein traffic and characterization of golgi to plasma membrane transport intermediates in living cells. J Cell Biol *143*, 1485-1503.
Hirst, J., Bright, N. A., Rous, B., and Robinson, M. S. (1999). Characterization of a fourth adaptor-related protein complex. Mol Biol Cell *10*, 2787-2802.
Hirst, J., Lui, W. W. Y., Bright, N. A., Totty, N., Seaman, M. N. J., and Robinson, M. S. (2000). A Family of proteins with g-Adaptin and VHS Domains that facilitate Trafficking between the Trans-Golgi Network and the Vacuole/Lysosome. The Journal of Cell Biology *149*, 67-79.

Hirt, R. P., Hughes, G. J., Frutiger, S., Michetti, P., Perregaux, C., Poulain-Godefroy, O., Jeanguenat, N., Neutra, M. R., and Kraehenbuhl, J. P. (1993). Transcytosis of the polymeric Ig receptor requires phosphorylation of serine 664 in the absence but not the presence of dimeric IgA. Cell *74*, 245-255.
Ho, A., Morishita, W., Hammer, R. E., Malenka, R. C., and Sudhof, T. C. (2003). A role for Mints in transmitter release: Mint 1 knockout mice exhibit impaired GABAergic synaptic transmission. Proc Natl Acad Sci U S A *100*, 1409-1414.
Hobert, M. E., Kil, S. J., Medof, M. E., and Carlin, C. R. (1997). The cytoplasmic juxtamembrane domain of the epidermal growth factor receptor contains a novel autonomous basolateral sorting determinant. J Biol Chem *272*, 32901-32909.
Hoekstra, D., Tyteca, D., and van, I. S. C. (2004). The subapical compartment: a traffic center in membrane polarity development. J Cell Sci *117*, 2183-2192.
Hoepfner, S., Severin, F., Cabezas, A., Habermann, B., Runge, A., Gillooly, D., Stenmark, H., and Zerial, M. (2005). Modulation of receptor recycling and degradation by the endosomal kinesin KIF16B. Cell *121*, 437-450.
Hommelgaard, A. M., Roepstorff, K., Vilhardt, F., Torgersen, M. L., Sandvig, K., and van Deurs, B. (2005). Caveolae: stable membrane domains with a potential for internalization. Traffic *6*, 720-724.
Horton, A. C., and Ehlers, M. D. (2003a). Dual modes of endoplasmic reticulum-to-Golgi transport in dendrites revealed by live-cell imaging. J Neurosci *23*, 6188-6199.
Horton, A. C., and Ehlers, M. D. (2003b). Neuronal polarity and trafficking. Neuron *40*, 277-295.
Howarth, M., Takao, K., Hayashi, Y., and Ting, A. Y. (2005). Targeting quantum dots to surface proteins in living cells with biotin ligase. Proc Natl Acad Sci U S A *102*, 7583-7588.
Hunziker, W., and Fumey, C. (1994). A di-leucine motif mediates endocytosis and basolateral sorting of macrophage IgG Fc receptors in MDCK cells. Embo J *13*, 2963-2967.
Hunziker, W., and Kraehenbuhl, J. P. (1998). Epithelial transcytosis of immunoglobulins. J Mammary Gland Biol Neoplasia *3*, 287-302.
Hunziker, W., and Mellman, I. (1989). Expression of macrophage-lymphocyte Fc receptors in Madin-Darby canine kidney cells: polarity and transcytosis differ for isoforms with or without coated pit localization domains. J Cell Biol *109*, 3291-3302.
Jareb, M., and Banker, G. (1998). The polarized sorting of membrane proteins expressed in cultured hippocampal neurons using viral vectors. Neuron *20*, 855-867.
Jones, B. G., Thomas, L., Molloy, S. S., Thulin, C. D., Fry, M. D., Walsh, K. A., and Thomas, G. (1995). Intracellular trafficking of furin is modulated by the phosphorylation state of a casein kinase II site in its cytoplasmic tail. Embo J *14*, 5869-5883.
Kadmon, G., and Altevogt, P. (1997). The cell adhesion molecule L1: species- and cell-type-dependent multiple binding mechanisms. Differentiation *61*, 143-150.
Kaether, C., Skehel, P., and Dotti, C. G. (2000). Axonal Membrane proteins Are Transported in Distinct Carriers: A Two-Color Video Microscopy Study in Hippocampal Neurons. Molecular Biology of the Cell *11*, 1213-1224.

Kametaka, S., Mattera, R., and Bonifacino, J. S. (2005). Epidermal growth factor-dependent phosphorylation of the GGA3 adaptor protein regulates its recruitment to membranes. Mol Cell Biol *25*, 7988-8000.
Kanaani, J., Diacovo, M. J., El-Husseini Ael, D., Bredt, D. S., and Baekkeskov, S. (2004). Palmitoylation controls trafficking of GAD65 from Golgi membranes to axon-specific endosomes and a Rab5a-dependent pathway to presynaptic clusters. J Cell Sci *117*, 2001-2013.
Kanaani, J., el-Husseini Ael, D., Aguilera-Moreno, A., Diacovo, J. M., Bredt, D. S., and Baekkeskov, S. (2002). A combination of three distinct trafficking signals mediates axonal targeting and presynaptic clustering of GAD65. J Cell Biol *158*, 1229-1238.
Kantheti, P., Qiao, X., Diaz, M. E., Peden, A. A., Meyer, G. E., Carskadon, S. L., Kapfhamer, D., Sufalko, D., Robinson, M. S., Noebels, J. L., and Burmeister, M. (1998). Mutation in AP-3 delta in the mocha mouse links endosomal transport to storage deficiency in platelets, melanosomes, and synaptic vesicles. Neuron *21*, 111-122.
Kay, B. K., Williamson, M. P., and Sudol, M. (2000). The importance of being proline: the interaction of proline-rich motifs in signaling proteins with their cognate domains. Faseb J *14*, 231-241.
Keller, P., and Simons, K. (1997). Post-Golgi Biosynthetic Trafficking. Journal of Cell Science *110*, 3001-3009.
Keller, P., and Simons, K. (1998). Cholesterol is Required for Surface Transport of Influenza Virus Hemagglutinin. Journal of Cell Biology *140*, 1357-1367.
Keller, P., Toomre, D., Diaz, E., White, J., and Simons, K. (2001). Multicolour imaging of post-Golgi sorting and trafficking in live cells. Nat Cell Biol *3*, 140-149.
Keller, P. T., D. Diaz, E. White, J. Simons, K. (2001). Multicolor imaging of post-Golgi sorting and trafficking in live cells. Nature Cell Biology *3*, 140-149.
Khanin, R., Segel, L., and Futerman, A. H. (1998). The diffusion of molecules in axonal plasma membranes: the sites of insertion of new membrane molecules and their distribution along the axon surface. J Theor Biol *193*, 371-382.
Kil, S. J., Hobert, M., and Carlin, C. (1999). A leucine-based determinant in the epidermal growth factor receptor juxtamembrane domain is required for the efficient transport of ligand- receptor complexes to lysosomes. J Biol Chem *274*, 3141-3150.
Killisch, I., Dotti, C. G., Laurie, D. J., Luddens, H., and Seeburg, P. H. (1991). Expression patterns of GABAA receptor subtypes in developing hippocampal neurons. Neuron *7*, 927-936.
Killisch, I., Steinlein, P., Romisch, K., Hollinshead, R., Beug, H., and Griffiths, G. (1992). Characterization of early and late endocytic compartments of the transferrin cycle. Transferrin receptor antibody blocks erythroid differentiation by trapping the receptor in the early endosome. J Cell Sci *103 ( Pt 1)*, 211-232.
Kirchhausen, T. (1999). Adaptors for Clathrin-Mediated Traffic. Annual Review of Cell and Developmental Biology *15*, 705-732.
Kobayashi, T., Storrie, B., Simons, K., and Dotti, C. G. (1992). A functional barrier to movement of lipids in polarized neurons. Nature *359*, 647-650.

Koivisto, U. M., Hubbard, A. L., and Mellman, I. (2001). A novel cellular phenotype for familial hypercholesterolemia due to a defect in polarized targeting of LDL receptor. Cell *105*, 575-585.
Kornfeld, R., and Kornfeld, S. (1985). Assembly of asparagine-linked oligosaccharides. Annual Review of Biochemistry *54*, 631-664.
Kreitzer, G., Schmoranzer, J., Low, S. H., Li, X., Gan, Y., Weimbs, T., Simon, S. M., and Rodriguez-Boulan, E. (2003). Three-dimensional analysis of post-Golgi carrier exocytosis in epithelial cells. Nat Cell Biol *5*, 126-136.
Krijnse-Locker, J., Parton, R. G., Fuller, S. D., Griffiths, G., and Dotti, C. G. (1995). The organization of the endoplasmic reticulum and the intermediate compartment in cultured rat hippocampal neurons. Mol Biol Cell *6*, 1315-1332.
Kryl, D., Yacoubian, T., Haapasalo, A., Castren, E., Lo, D., and Barker, P. A. (1999). Subcellular localization of full-length and truncated Trk receptor isoforms in polarized neurons and epithelial cells. J Neurosci *19*, 5823-5833.
Kuismanen, E., and Saraste, J. (1989). Low temperature-induced transport blocks as tools to manipulate membrane traffic. Methods Cell Biol *32*, 257-274.
Kurten, R. C., Cadena, D. L., and Gill, G. N. (1996). Enhanced degradation of EGF receptors by a sorting nexin, SNX1. Science *272*, 1008-1010.
Ladinsky, M. S., Kremer, J. R., Furcinitti, P. S., McIntosh, J. R., and Howell, K. E. (1994). HVEM tomography of the trans-Golgi network: structural insights and identification of a lace-like vesicle coat. J Cell Biol *127*, 29-38.
Ladinsky, M. S., Mastronarde, D. N., McIntosh, J. R., Howell, K. E., and Staehelin, L. A. (1999). Golgi Structure in Three Dimensions: Functional Insights from the Normal Rat Kidney Cell. The Journal of Cell Biology *144*, 1135-1149.
Ladinsky, M. S., Wu, C. C., McIntosh, S., McIntosh, J. R., and Howell, K. E. (2002). Structure of the Golgi and Distribution of Reporter Molecules at 20 degrees C Reveals the Complexity of the Exit Compartments. Mol Biol Cell *13*, 2810-2825.
Le Maout, S., Welling, P. A., Brejon, M., Olsen, O., and Merot, J. (2001). Basolateral membrane expression of a K+ channel, Kir 2.3, is directed by a cytoplasmic COOH-terminal domain. Proc Natl Acad Sci U S A *98*, 10475-10480.
Lee, S. H., Valtschanoff, J. G., Kharazia, V. N., Weinberg, R., and Sheng, M. (2001). Biochemical and morphological characterization of an intracellular membrane compartment containing AMPA receptors. Neuropharmacology *41*, 680-692.
Lehre, K. P., Levy, L. M., Ottersen, O. P., Storm-Mathisen, J., and Danbolt, N. C. (1995). Differential expression of two glial glutamate transporters in the rat brain: quantitative and immunocytochemical observations. J Neurosci *15*, 1835-1853.
Leung, S. M., Ruiz, W. G., and Apodaca, G. (2000). Sorting of membrane and fluid at the apical pole of polarized Madin- Darby canine kidney cells. Mol Biol Cell *11*, 2131-2150.
Levine, T., and Rabouille, C. (2005). Endoplasmic reticulum: one continuous network compartmentalized by extrinsic cues. Curr Opin Cell Biol *17*, 362-368.
Lichtman, J. W., and Fraser, S. E. (2001). The neuronal naturalist: watching neurons in their native habitat. Nat Neurosci *4 Suppl*, 1215-1220.

Lim, S. T., Antonucci, D. E., Scannevin, R. H., and Trimmer, J. S. (2000). A novel targeting signal for proximal clustering of the Kv2.1 K+ channel in hippocampal neurons. Neuron *25*, 385-397.
Lin, C. I., Orlov, I., Ruggiero, A. M., Dykes-Hoberg, M., Lee, A., Jackson, M., and Rothstein, J. D. (2001). Modulation of the neuronal glutamate transporter EAAC1 by the interacting protein GTRAP3-18. Nature *410*, 84-88.
Lin, S. X., Mallet, W. G., Huang, A. Y., and Maxfield, F. R. (2004). Endocytosed cation-independent mannose 6-phosphate receptor traffics via the endocytic recycling compartment en route to the trans-Golgi network and a subpopulation of late endosomes. Mol Biol Cell *15*, 721-733.
Lippincott-Schwartz, J., Roberts, T. H., and Hirschberg, K. (2000). Secretory Protein Trafficking and Organelle Dynamics in Living Cells. Annual Review of Cell And Developmental Biology *16*, 557-589.
Llopis, J., McCaffery, J. M., Miyawaki, A., Farquhar, M. G., and Tsien, R. Y. (1998). Measurement of cytosolic, mitochondrial, and Golgi pH in single living cells with green fluorescent proteins. Proc Natl Acad Sci U S A *95*, 6803-6808.
Lock, J. G., and Stow, J. L. (2005). Rab11 in recycling endosomes regulates the sorting and basolateral transport of E-cadherin. Mol Biol Cell *16*, 1744-1755.
London, M., and Segev, I. (2001). Synaptic scaling *in vitro* and *in vivo*. Nat Neurosci *4*, 853-855.
Low, S. H., Tang, B. L., Wong, S. H., and Hong, W. (1992). Selective inhibition of protein targeting to the apical domain of MDCK cells by brefeldin A. J Cell Biol *118*, 51-62.
Mancias, J. D., and Goldberg, J. (2005). Exiting the endoplasmic reticulum. Traffic *6*, 278-285.
Martin, T. (1997). Stages of Regulated Exocytosis. Trends in Cell Biology *7*, 271-276.
Martinez-Maza, R., Poyatos, I., Lopez-Corcuera, B., E, N. u., Gimenez, C., Zafra, F., and Aragon, C. (2001). The role of N-glycosylation in transport to the plasma membrane and sorting of the neuronal glycine transporter GLYT2. J Biol Chem *276*, 2168-2173.
Martoglio, B., and Dobberstein, B. (1998). Signal sequences: more than just greasy peptides. Trends Cell Biol *8*, 410-415.
Marzolo, M. P., Yuseff, M. I., Retamal, C., Donoso, M., Ezquer, F., Farfan, P., Li, Y., and Bu, G. (2003). Differential distribution of low-density lipoprotein-receptor-related protein (LRP) and megalin in polarized epithelial cells is determined by their cytoplasmic domains. Traffic *4*, 273-288.
Matlin, K. S., and Simons, K. (1983). Reduced temperature Prevents Transfer of a Membrane Glycoprotein to the Cell Surface But Does Not Prevent Terminal Glycosylation. Cell *34*, 233-243.
Matsuoka, K., Schekman, R., Orci, L., and Heuser, J. E. (2001). Surface structure of the COPII-coated vesicle. Proc Natl Acad Sci U S A *98*, 13705-13709.
Matter, K., Hunziker, W., and Mellman, I. (1992). Basolateral Sorting of LDL Receptor in MDCK Cells: the Cytoplasmic Domain Contains Two Tyosine-Dependant Targeting Domains. Cell *71*, 741-753.

Matter, K., Whitney, J. A., Yamamoto, E. M., and Mellman, I. (1993). Common signals control low density lipoprotein receptor sorting in endosomes and the Golgi complex of MDCK cells. Cell *74*, 1053-1064.
Matter, K., Yamamoto, E. M., and Mellman, I. (1994). Structural Requirements and Sequence Motifs for Polarized Sorting and Endocytosis of LDL and Fc Receptors in MDCK cells. Journal of Cell Biology *126*, 991-1004.
Mattera, R., Arighi, C. N., Lodge, R., Zerial, M., and Bonifacino, J. S. (2003). Divalent interaction of the GGAs with the Rabaptin-5-Rabex-5 complex. Embo J *22*, 78-88.
Mays, R. W., Siemers, K. A., Fritz, B. A., Lowe, A. W., Van Meer, G., and Nelson, W. J. (1995). Hierarchy of Mechanisms Involved in Generating Na/ATPase Polarity in MDCK Epithelial Cells. Journal of Cell Biology *130*, 1105-1115.
McBride, H. M., Rybin, V., Murphy, C., Giner, A., Teasdale, R., and Zerial, M. (1999). Oligomeric complexes link Rab5 effectors with NSF and drive membrane fusion via interactions between EEA1 and syntaxin 13. Cell *98*, 377-386.
McCarthy, J. B., Lim, S. T., Elkind, N. B., Trimmer, J. S., Duvoisin, R. M., Rodriguez-Boulan, E., and Caplan, M. J. (2001). The C-terminal tail of the metabotropic glutamate receptor subtype 7 is necessary but not sufficient for cell surface delivery and polarized targeting in neurons and epithelia. J Biol Chem *276*, 9133-9140.
McPherson, P. S. (1999). Regulatory role of SH3 domain-mediated protein-protein interactions in synaptic vesicle endocytosis. Cell Signal *11*, 229-238.
Mellman, I. (1992). The importance of being acid: the role of acidification in intracellular membrane traffic. J Exp Biol *172*, 39-45.
Migliaccio, G., Zurzolo, C., Nitsch, L., Obici, S., Lotti, L. V., Torrisi, M. R., Pascale, M. C., Leone, A., and Bonatti, S. (1990). Human CD8 alpha glycoprotein is expressed at the apical plasma membrane domain in permanently transformed MDCK II clones. Eur J Cell Biol *52*, 291-296.
Miller, E. A., Beilharz, T. H., Malkus, P. N., Lee, M. C., Hamamoto, S., Orci, L., and Schekman, R. (2003). Multiple cargo binding sites on the COPII subunit Sec24p ensure capture of diverse membrane proteins into transport vesicles. Cell *114*, 497-509.
Miranda, K. C., Khromykh, T., Christy, P., Le, T. L., Gottardi, C. J., Yap, A. S., Stow, J. L., and Teasdale, R. D. (2001). A dileucine motif targets E-cadherin to the basolateral cell surface in Madin-Darby canine kidney and LLC-PK1 epithelial cells. J Biol Chem *276*, 22565-22572.
Mironov, A. A., Mironov, A. A., Jr., Beznoussenko, G. V., Trucco, A., Lupetti, P., Smith, J. D., Geerts, W. J., Koster, A. J., Burger, K. N., Martone, M. E., *et al.* (2003). ER-to-Golgi carriers arise through direct en bloc protrusion and multistage maturation of specialized ER exit domains. Dev Cell *5*, 583-594.
Misonou, H., Mohapatra, D. P., Park, E. W., Leung, V., Zhen, D., Misonou, K., Anderson, A. E., and Trimmer, J. S. (2004). Regulation of ion channel localization and phosphorylation by neuronal activity. Nat Neurosci *7*, 711-718.
Misonou, H., Mohapatra, D. P., and Trimmer, J. S. (2005). Kv2.1: a voltage-gated k(+) channel critical to dynamic control of neuronal excitability. Neurotoxicology *26*, 743-752.

Mitsui, S., Saito, M., Hayashi, K., Mori, K., and Yoshihara, Y. (2005). A novel phenylalanine-based targeting signal directs telencephalin to neuronal dendrites. J Neurosci *25*, 1122-1131.
Molloy, S. S., Thomas, L., Kamibayashi, C., Mumby, M. C., and Thomas, G. (1998). Regulation of endosome sorting by a specific PP2A isoform. J Cell Biol *142*, 1399-1411.
Moore, H.-P. H., and Kelly, R. B. (1985). Secretory Protein Targeting in a Pituitary Cell Line: Differential Transport of Foreign Secretory Proteins to Distinct Secretory Pathways. The Journal of Cell Biology *101*, 1773-1781.
Mostov, K. E., Verges, M., and Altschuler, Y. (2000). Membrane traffic in polarized epithelial cells. Curr Opin Cell Biol *12*, 483-490.
Mullin, J. M., and McGinn, M. T. (1987). The phorbol ester, TPA, increases transepithelial epidermal growth factor flux. FEBS Lett *221*, 359-364.
Muniz, M., Morsomme, P., and Riezman, H. (2001). Protein sorting upon exit from the endoplasmic reticulum. Cell *104*, 313-320.
Murk, J. L., Humbel, B. M., Ziese, U., Griffith, J. M., Posthuma, G., Slot, J. W., Koster, A. J., Verkleij, A. J., Geuze, H. J., and Kleijmeer, M. J. (2003). Endosomal compartmentalization in three dimensions: implications for membrane fusion. Proc Natl Acad Sci U S A *100*, 13332-13337.
Musch, A., Cohen, D., Kreitzer, G., and Rodriguez-Boulan, E. (2001). cdc42 regulates the exit of apical and basolateral proteins from the trans-Golgi network. Embo J *20*, 2171-2179.
Musch, A., Xu, H., Shields, D., and Rodriguez-Boulan, E. J. (1996). Transport of Vesicular Stomatitis Virus G Protein to the Cell Surface is Signal Mediated in Polarized and Nonpolarized Cells. Journal of Cell Biology *133*, 543-558.
Muth, T. R., Ahn, J., and Caplan, M. J. (1998). Identification of sorting determinants in the C-terminal cytoplasmic tails of the gamma-aminobutyric acid transporters GAT-2 and GAT-3. J Biol Chem *273*, 25616-25627.
Muth, T. R., and Caplan, M. J. (2003). Transport protein trafficking in polarized cells. Annu Rev Cell Dev Biol *19*, 333-366.
Naisbitt, S., Valtschanoff, J., Allison, D. W., Sala, C., Kim, E., Craig, A. M., Weinberg, R. J., and Sheng, M. (2000). Interaction of the postsynaptic density-95/guanylate kinase domain- associated protein complex with a light chain of myosin-V and dynein. J Neurosci *20*, 4524-4534.
Nakada, C., Ritchie, K., Oba, Y., Nakamura, M., Hotta, Y., Iino, R., Kasai, R. S., Yamaguchi, K., Fujiwara, T., and Kusumi, A. (2003). Accumulation of anchored proteins forms membrane diffusion barriers during neuronal polarization. Nat Cell Biol *5*, 626-632.
Niell, C. M., and Smith, S. J. (2004). Live optical imaging of nervous system development. Annu Rev Physiol *66*, 771-798.
Nishimura, N., and Balch, W. E. (1997). A di-acidic signal required for selective export from the endoplasmic reticulum. Science *277*, 556-558.
Nishimura, N., Plutner, H., Hahn, K., and Balch, W. E. (2002). The delta subunit of AP-3 is required for efficient transport of VSV-G from the trans-Golgi network to the cell surface. Proc Natl Acad Sci U S A *99*, 6755-6760.

Nishimura, T., Kato, K., Yamaguchi, T., Fukata, Y., Ohno, S., and Kaibuchi, K. (2004). Role of the PAR-3-KIF3 complex in the establishment of neuronal polarity. Nat Cell Biol *6*, 328-334.
Nishimura, T., Yamaguchi, T., Kato, K., Yoshizawa, M., Nabeshima, Y., Ohno, S., Hoshino, M., and Kaibuchi, K. (2005). PAR-6-PAR-3 mediates Cdc42-induced Rac activation through the Rac GEFs STEF/Tiam1. Nat Cell Biol *7*, 270-277.
Odorizzi, G., and Trowbridge, I. S. (1997). Structural Requirements for Basolateral Sorting of the Human Transferrin Receptor in the Biosynthetic and Endocytic Pathways of Madin-Darby Canine Kidney Cells. Journal of Cell Biology *137*, 1255-1264.
Ohno, H., Tomemori, T., Nakatsu, F., Okazaki, Y., Aguilar, R. C., Foelsch, H., Mellman, I., Saito, T., Shirasawa, T., and Bonifacino, J. S. (1999). Mu1B, a novel adaptor medium chain expressed in polarized epithelial cells. FEBS Lett *449*, 215-220.
Olkkonen, V. M., and Stenmark, H. (1997). Role of Rab GTPases in membrane traffic. Int Rev Cytol *176*, 1-85.
Orzech, E., Cohen, S., Weiss, A., and Aroeti, B. (2000). Interactions Between the Exocytic and Endocytic Pathways in Polarized madin0Darby Canine Kidney Cells. The Journal of Biological Chemistry *275*, 15207-15219.
Park, M., Penick, E. C., Edwards, J. G., Kauer, J. A., and Ehlers, M. D. (2004). Recycling endosomes supply AMPA receptors for LTP. Science *305*, 1972-1975.
Parton, R. G., Simons, K., and Dotti, C. G. (1992). Axonal and dendritic endocytic pathways in cultured neurons. J Cell Biol *119*, 123-137.
Pearse, B. M., and Robinson, M. S. (1990). Clathrin, adaptors, and sorting. Annu Rev Cell Biol *6*, 151-171.
Perez-Velazquez, J. L., and Angelides, K. J. (1993). Assembly of GABAA receptor subunits determines sorting and localization in polarized cells. Nature *361*, 457-460.
Perret, E., Lakkaraju, A., Deborde, S., Schreiner, R., and Rodriguez-Boulan, E. (2005). Evolving endosomes: how many varieties and why? Curr Opin Cell Biol *17*, 423-434.
Persohn, E., and Schachner, M. (1990). Immunohistological localization of the neural adhesion molecules L1 and N-CAM in the developing hippocampus of the mouse. J Neurocytol *19*, 807-819.
Pfeffer, S. (1999). Transport-vesicle targeting: tethers before SNAREs. Nature Cell Biology *1*, E17-E22.
Pfeffer, S. (2005). A model for Rab GTPase localization. Biochem Soc Trans *33*, 627-630.
Pfeffer, S., and Aivazian, D. (2004). Targeting Rab GTPases to distinct membrane compartments. Nat Rev Mol Cell Biol *5*, 886-896.
Pietrini, G., Matteoli, M., Banker, G., and Caplan, M. J. (1992). Isoforms of the Na,K-ATPase are Present in Both Axons and Dendrites. Proceedings of the National Academy of Sciences USA *89*, 8414-8418.
Pietrini, G., Suh, Y. J., Edelmann, L., Rudnick, G., and Caplan, M. J. (1994). The axonal gamma-aminobutyric acid transporter GAT-1 is sorted to the apical membranes of polarized epithelial cells. J Biol Chem *269*, 4668-4674.

Polishchuk, E. V., Di Pentima, A., Luini, A., and Polishchuk, R. S. (2003). Mechanism of constitutive export from the golgi: bulk flow via the formation, protrusion, and en bloc cleavage of large trans-golgi network tubular domains. Mol Biol Cell *14*, 4470-4485.
Polishchuk, R., Di Pentima, A., and Lippincott-Schwartz, J. (2004). Delivery of raft-associated, GPI-anchored proteins to the apical surface of polarized MDCK cells by a transcytotic pathway. Nat Cell Biol *6*, 297-307.
Polishchuk, R. S., Polishchuk, E. V., Marra, P., Alberti, S., Buccione, R., Luini, A., and Mironov, A. A. (2000). Correlative light-electron microscopy reveals the tubular-saccular ultrastructure of carriers operating between Golgi apparatus and plasma membrane. J Cell Biol *148*, 45-58.
Ponnambalam, S., and Baldwin, S. A. (2003). Constitutive protein secretion from the trans-Golgi network to the plasma membrane. Mol Membr Biol *20*, 129-139.
Powell, S. K., Cunningham, B. A., Edelman, G. M., and Rodriguez-Boulan, E. (1991). Targeting of transmembrane and GPI-anchored forms of N-CAM to opposite domains of a polarized epithelial cell. Nature *353*, 76-77.
Poyatos, I., Ruberti, F., Martinez-Maza, R., Gimenez, C., Dotti, C. G., and Zafra, F. (2000). Polarized distribution of glycine transporter isoforms in epithelial and neuronal cells. Mol Cell Neurosci *15*, 99-111.
Praefcke, G. J., and McMahon, H. T. (2004). The dynamin superfamily: universal membrane tubulation and fission molecules? Nat Rev Mol Cell Biol *5*, 133-147.
Prekeris, R., Foletti, D. L., and Scheller, R. H. (1999). Dynamics of tubulovesicular recycling endosomes in hippocampal neurons. J Neurosci *19*, 10324-10337.
Prekeris, R., Klumperman, J., Chen, Y. A., and Scheller, R. H. (1998). Syntaxin 13 mediates cycling of plasma membrane proteins via tubulovesicular recycling endosomes. J Cell Biol *143*, 957-971.
Presley, J. F., Cole, N. B., Schroer, T. A., Hirschberg, K., Zaal, K. J., and Lippincott-Schwartz, J. (1997a). ER-to-Golgi transport visualized in living cells. Nature *389*, 81-85.
Presley, J. F., Mayor, S., McGraw, T. E., Dunn, K. W., and Maxfield, F. R. (1997b). Bafilomycin A1 treatment retards transferrin receptor recycling more than bulk membrane recycling. J Biol Chem *272*, 13929-13936.
Puertollano, R., van der Wel, N. N., Greene, L. E., Eisenberg, E., Peters, P. J., and Bonifacino, J. S. (2003). Morphology and dynamics of clathrin/GGA1-coated carriers budding from the trans-Golgi network. Mol Biol Cell *14*, 1545-1557.
Puthenveedu, M. A., and Linstedt, A. D. (2005). Subcompartmentalizing the Golgi apparatus. Curr Opin Cell Biol *17*, 369-375.
Rahner, C., Stieger, B., and Landmann, L. (2000). Apical endocytosis in rat hepatocytes In situ involves clathrin, traverses a subapical compartment, and leads to lysosomes. Gastroenterology *119*, 1692-1707.
Rao, A., Kim, E., Sheng, M., and Craig, A. M. (1998). Heterogeneity in the molecular composition of excitatory postsynaptic sites during development of hippocampal neurons in culture. J Neurosci *18*, 1217-1229.
Rapoport, I., Miyazaki, M., Boll, W., Duckworth, B., Cantley, L. C., Shoelson, S., and Kirchhausen, T. (1997). Regulatory interactions in the recognition of endocytic sorting signals by AP-2 complexes. Embo J *16*, 2240-2250.

Rappoport, J. Z., and Simon, S. M. (2003). Real-time analysis of clathrin-mediated endocytosis during cell migration. J Cell Sci *116*, 847-855.
Reich, V., Mostov, K., and Aroeti, B. (1996). The basolateral sorting signal of the polymeric immunoglobulin receptor contains two functional domains. J Cell Sci *109*, 2133-2139.
Reilein, A. R., Rogers, S. L., Tuma, M. C., and Gelfand, V. I. (2001). Regulation of molecular motor proteins. Int Rev Cytol *204*, 179-238.
Rivera, J. F., Ahmad, S., Quick, M. W., Liman, E. R., and Arnold, D. B. (2003). An evolutionarily conserved dileucine motif in Shal K+ channels mediates dendritic targeting. Nat Neurosci *6*, 243-250.
Rivera, J. F., Chu, P. J., and Arnold, D. B. (2005). The T1 domain of Kv1.3 mediates intracellular targeting to axons. Eur J Neurosci *22*, 1853-1862.
Rizzo, M. A., Springer, G. H., Granada, B., and Piston, D. W. (2004). An improved cyan fluorescent protein variant useful for FRET. Nat Biotechnol *22*, 445-449.
Rizzoli, S. O., and Betz, W. J. (2005). Synaptic vesicle pools. Nat Rev Neurosci *6*, 57-69.
Rodriguez-Boulan, E., and Musch, A. (2005). Protein sorting in the Golgi complex: shifting paradigms. Biochim Biophys Acta *1744*, 455-464.
Rodriguez-Boulan, E. J., and Sabatini, D. D. (1978). Assymetric Budding of Viruses in Epithelial Monolayers: a Model fro the Study of Epithelial Polartiy. PNAS USA *75*, 5071-5075.
Rohrer, J., Schweizer, A., Russell, D., and Kornfeld, S. (1996). The targeting of Lamp1 to lysosomes is dependent on the spacing of its cytoplasmic tail tyrosine sorting motif relative to the membrane. J Cell Biol *132*, 565-576.
Rolls, M. M., and Doe, C. Q. (2003). Cell polarity: From embryo to axon. Nature *421*, 905-906.
Rolls, M. M., and Doe, C. Q. (2004). Baz, Par-6 and aPKC are not required for axon or dendrite specification in Drosophila. Nat Neurosci *7*, 1293-1295.
Rosales, C. R., Osborne, K. D., Zuccarino, G. V., Scheiffele, P., and Silverman, M. A. (2005). A cytoplasmic motif targets neuroligin-1 exclusively to dendrites of cultured hippocampal neurons. Eur J Neurosci *22*, 2381-2386.
Roth, M. G. (2004). Phosphoinositides in constitutive membrane traffic. Physiol Rev *84*, 699-730.
Rothman, J. E. (1994). Mechanisms of intracellular protein transport. Nature *372*, 55-63.
Rothman, J. E., and Wieland, F. T. (1996). Protein sorting by transport vesicles. Science *272*, 227-234.
Rothstein, J. D., Martin, L., Levey, A. I., Dykes-Hoberg, M., Jin, L., Wu, D., Nash, N., and Kuncl, R. W. (1994). Localization of neuronal and glial glutamate transporters. Neuron *13*, 713-725.
Ruberti, F., and Dotti, C. G. (2000). Involvement of the proximal C terminus of the AMPA receptor subunit GluR1 in dendritic sorting. J Neurosci *20*, RC78.
Rustom, A., Bajohrs, M., Kaether, C., Keller, P., Toomre, D., Corbeil, D., and Gerdes, H. H. (2002). Selective delivery of secretory cargo in Golgi-derived carriers of nonepithelial cells. Traffic *3*, 279-288.

Salpeter, M., and Farquhar, M. G. (1981). High resolution analysis of the secretory pathway in mammotrophs of the rat anterior pituitary. Journal of Cell Biology *91*, 240-246.
Sampo, B., Kaech, S., Kunz, S., and Banker, G. (2003). Two distinct mechanisms target membrane proteins to the axonal surface. Neuron *37*, 611-624.
Saraste, J., and Kuismanen, E. (1984). Pre- and post-Golgi vacuoles operate in the transport of Semliki Forest virus membrane glycoproteins to the cell surface. Cell *38*, 535-549.
Scannevin, R. H., Murakoshi, H., Rhodes, K. J., and Trimmer, J. S. (1996). Identification of a cytoplasmic domain important in the polarized expression and clustering of the Kv2.1 K+ channel. J Cell Biol *135*, 1619-1632.
Schapiro, F. B., Soe, T. T., Mallet, W. G., and Maxfield, F. R. (2004). Role of cytoplasmic domain serines in intracellular trafficking of furin. Mol Biol Cell *15*, 2884-2894.
Scheiffele, P. M., Roth, M. G., and Simons, K. (1997). Interaction of Influenza Virus HA with Sphingolipid-Cholesterol Membrane Domains Via its Tansmembrane Domain. EMBO Journal *16*, 5501-5508.
Scott, G. K., Gu, F., Crump, C. M., Thomas, L., Wan, L., Xiang, Y., and Thomas, G. (2003). The phosphorylation state of an autoregulatory domain controls PACS-1-directed protein traffic. Embo J *22*, 6234-6244.
Seal, R. P., and Amara, S. G. (1998). A reentrant loop domain in the glutamate carrier EAAT1 participates in substrate binding and translocation. Neuron *21*, 1487-1498.
Setou, M., Nakagawa, T., Seog, D. H., and Hirokawa, N. (2000). Kinesin superfamily motor protein KIF17 and mLin-10 in NMDA receptor- containing vesicle transport. Science *288*, 1796-1802.
Shah, J. V., and Goldstein, L. S. (2000). Does motor protein intelligence contribute to neuronal polarity? Neuron *26*, 281-282.
Shaner, N. C., Campbell, R. E., Steinbach, P. A., Giepmans, B. N., Palmer, A. E., and Tsien, R. Y. (2004). Improved monomeric red, orange and yellow fluorescent proteins derived from Discosoma sp. red fluorescent protein. Nat Biotechnol *22*, 1567-1572.
Shang, W. H., Adachi, Y., Nakamura, A., Copeland, T., Kim, S. P., and Kamata, T. (2004). Regulation of amphiphysin1 by mitogen-activated protein kinase: Its significance in nerve growth factor receptor-mediated endocytosis. J Biol Chem.
Shayakul, C., Kanai, Y., Lee, W. S., Brown, D., Rothstein, J. D., and Hediger, M. A. (1997). Localization of the high-affinity glutamate transporter EAAC1 in rat kidney. Am J Physiol *273*, F1023-1029.
Sheff, D., Pelletier, L., O'Connell, C. B., Warren, G., and Mellman, I. (2002). Transferrin receptor recycling in the absence of perinuclear recycling endosomes. J Cell Biol *156*, 797-804.
Sheikh, H., and Isacke, C. M. (1996). A di-hydrophobic Leu-Val motif regulates the basolateral localization of CD44 in polarized Madin-Darby canine kidney epithelial cells. J Biol Chem *271*, 12185-12190.
Shi, S. H., Jan, L. Y., and Jan, Y. N. (2003). Hippocampal neuronal polarity specified by spatially localized mPar3/mPar6 and PI 3-kinase activity. Cell *112*, 63-75.

Shin, H. W., Hayashi, M., Christoforidis, S., Lacas-Gervais, S., Hoepfner, S., Wenk, M. R., Modregger, J., Uttenweiler-Joseph, S., Wilm, M., Nystuen, A., *et al.* (2005). An enzymatic cascade of Rab5 effectors regulates phosphoinositide turnover in the endocytic pathway. J Cell Biol *170*, 607-618.
Shitara, Y., Kato, Y., and Sugiyama, Y. (1998). Effect of brefeldin A and lysosomotropic reagents on intracellular trafficking of epidermal growth factor and transferrin in Madin-Darby canine kidney epithelial cells. J Control Release *55*, 35-43.
Silverman, M. A., Kaech, S., Jareb, M., Burack, M. A., Vogt, L., Sonderegger, P., and Banker, G. (2001). Sorting and directed transport of membrane proteins during development of hippocampal neurons in culture. Proc Natl Acad Sci U S A *98*, 7051-7057.
Silverman, M. A., Peck, R., Glover, G., He, C., Carlin, C., and Banker, G. (2005). Motifs that mediate dendritic targeting in hippocampal neurons: a comparison with basolateral targeting signals. Mol Cell Neurosci *29*, 173-180.
Simmen, T., Honing, S., Icking, A., Tikkanen, R., and Hunziker, W. (2002). AP-4 binds basolateral signals and participates in basolateral sorting in epithelial MDCK cells. Nat Cell Biol *4*, 154-159.
Simons, K., and Fuller, S. D. (1985). Cell Surface Polarity in Epithelia. Annual Review of Cell Biology *1*, 243-288.
Simonsen, A., Gaullier, J. M., D'Arrigo, A., and Stenmark, H. (1999). The Rab5 effector EEA1 interacts directly with syntaxin-6. J Biol Chem *274*, 28857-28860.
Sönnichsen, B., De Renzis, S., Rietdorf, J., Nielsen, E., and Zerial, a. M. (2000). Distinct Membrane Domains on Endosomes in the Recycling Pathway Visualized by Multicolor Imaging of Rab4, Rab5, and Rab11. Journal of Cell Biology *149*, 901-913.
Soza, A., Norambuena, A., Cancino, J., de la Fuente, E., Henklein, P., and Gonzalez, A. (2004). Sorting competition with membrane-permeable peptides in intact epithelial cells revealed discrimination of transmembrane proteins not only at the trans-Golgi network but also at pre-Golgi stages. J Biol Chem *279*, 17376-17383.
Steiner, P., Sarria, J. C., Glauser, L., Magnin, S., Catsicas, S., and Hirling, H. (2002). Modulation of receptor cycling by neuron-enriched endosomal protein of 21 kD. J Cell Biol *157*, 1197-1209.
Stepanova, T., Slemmer, J., Hoogenraad, C. C., Lansbergen, G., Dortland, B., De Zeeuw, C. I., Grosveld, F., van Cappellen, G., Akhmanova, A., and Galjart, N. (2003). Visualization of microtubule growth in cultured neurons via the use of EB3-GFP (end-binding protein 3-green fluorescent protein). J Neurosci *23*, 2655-2664.
Strous, G., Willemsen, R., vanKerkhof, P., Slot, J., Geuze, H., and Lodish, H. (1983). Vesicular Stomatitis Virus Glycoprotein, Albumin, and Tranferrin Are Transported to the Cell Surface Via the Same Golgi Vesicle. Journal of Cell Biology *97*, 1815-1822.
Swedlow, J. R., Hu, K., Andrews, P. D., Roos, D. S., and Murray, J. M. (2002). Measuring tubulin content in Toxoplasma gondii: a comparison of laser- scanning confocal and wide-field fluorescence microscopy. Proc Natl Acad Sci U S A *99*, 2014-2019.

Tai, A. W., Chuang, J. Z., Bode, C., Wolfrum, U., and Sung, C. H. (1999). Rhodopsin's carboxy-terminal cytoplasmic tail acts as a membrane receptor for cytoplasmic dynein by binding to the dynein light chain Tctex-1. Cell *97*, 877-887.
Tai, A. W., Chuang, J. Z., and Sung, C. H. (2001). Cytoplasmic dynein regulation by subunit heterogeneity and its role in apical transport. J Cell Biol *153*, 1499-1509.
Tang, B. L. (2001). Protein trafficking mechanisms associated with neurite outgrowth and polarized sorting in neurons. Journal of Neurochemistry *79*, 923.930.
Taraska, J. W., Perrais, D., Ohara-Imaizumi, M., Nagamatsu, S., and Almers, W. (2003). Secretory granules are recaptured largely intact after stimulated exocytosis in cultured endocrine cells. Proc Natl Acad Sci U S A *100*, 2070-2075.
Teasdale, R. D., Loci, D., Houghton, F., Karlsson, L., and Gleeson, P. A. (2001). A large family of endosome-localized proteins related to sorting nexin 1. Biochem J *358*, 7-16.
Ter Beest, M. B., Chapin, S. J., Avrahami, D., and Mostov, K. E. (2005). The Role of Syntaxins in the Specificity of Vesicle Targeting in Polarized Epithelial Cells. Mol Biol Cell.
Terada, S., and Hirokawa, N. (2000). Moving on to the cargo problem of microtubule-dependent motors in neurons. Curr Opin Neurobiol *10*, 566-573.
Thomas, D., Brewer, C., and Roth, M. (1993). Vesicular stomatitis virus glycoprotein contains a dominant cytoplasmic basolateral sorting signal critically dependent upon a tyrosine. J Biol Chem *268*, 3313-3320.
Thomas, G. (2002). Furin at the cutting edge: from protein traffic to embryogenesis and disease. Nat Rev Mol Cell Biol *3*, 753-766.
Tsien, R. Y. (1998). The green fluorescent protein. Annu Rev Biochem *67*, 509-544.
Tsukita, S., and Ishikawa, H. (1980). The movement of membranous organelles in axons. Electron microscopic identification of anterogradely and retrogradely transported organelles. J Cell Biol *84*, 513-530.
Tucker, M. S., Khan, I., Fuchs-Young, R., Price, S., Steininger, T. L., Greene, G., Wainer, B. H., and Rosner, M. R. (1993). Localization of immunoreactive epidermal growth factor receptor in neonatal and adult rat hippocampus. Brain Res *631*, 65-71.
van Deurs, B., Petersen, O. W., Olsnes, S., and Sandvig, K. (1989). The ways of endocytosis. Int Rev Cytol *117*, 131-177.
Vieira, O. V., Verkade, P., Manninen, A., and Simons, K. (2005). FAPP2 is involved in the transport of apical cargo in polarized MDCK cells. J Cell Biol *170*, 521-526.
von Essen, M., Menne, C., Nielsen, B. L., Lauritsen, J. P., Dietrich, J., Andersen, P. S., Karjalainen, K., Odum, N., and Geisler, C. (2002). The CD3 gamma leucine-based receptor-sorting motif is required for efficient ligand-mediated TCR down-regulation. J Immunol *168*, 4519-4523.
Waguri, S., Dewitte, F., Le Borgne, R., Rouille, Y., Uchiyama, Y., Dubremetz, J. F., and Hoflack, B. (2003). Visualization of TGN to Endosome Trafficking through Fluorescently Labeled MPR and AP-1 in Living Cells. Mol Biol Cell *14*, 142-155.
Wan, L., Molloy, S. S., Thomas, L., Liu, G., Xiang, Y., Rybak, S. L., and Thomas, G. (1998). PACS-1 defines a novel gene family of cytosolic sorting proteins required for trans-Golgi network localization. Cell *94*, 205-216.

Wandinger-Ness, A., Bennett, M. K., Antony, C., and Simons, K. (1990). Distinct Transport Vesicles Mediate the Delivery of Plasma Membrane Proteins to the Apical and Basolateral Domains of MDCK cells. Journal of Cell Biology *111*, 987-1000.
Warren, R. A., Green, F. A., Stenberg, P. E., and Enns, C. (1998). Distinct Saturable pathways for the endocytosis of different tyrosine motifs. Journal of Biological Chemistry *273*, 17056-17063.
Watson, P., and Stephens, D. J. (2005). ER-to-Golgi transport: form and formation of vesicular and tubular carriers. Biochim Biophys Acta *1744*, 304-315.
West, A. E., Neve, R. L., and Buckley, K. M. (1997). Identification of a somatodendritic targeting signal in the cytoplasmic domain of the transferrin receptor. J Neurosci *17*, 6038-6047.
Wieland, F. T., Gleason, M. L., Serafini, T. A., and Rothman, J. E. (1987). The rate of bulk flow from the endoplasmic reticulum to the cell surface. Cell *50*, 289-300.
Wiest, D. L., Burkhardt, J. K., Hester, S., Hortsch, M., Meyer, D. I., and Argon, Y. (1990). Membrane biogenesis during B cell differentiation: most endoplasmic reticulum proteins are expressed coordinately. J Cell Biol *110*, 1501-1511.
Wilson, J. M., deHoop, M., Zorzi, N., Toh, B.-H., Dotti, C. G., and Parton, R. G. (2000). EEA1, a Tethering Protein of the Early Sorting Endosome, Shows a Polarized Distribution in Hippocampal Neurons, Epithelial Cells, and Fibroblasts. Molecular Biology of the Cell *11*, 2657-2671.
Winckler, B., Forscher, P., and Mellman, I. (1999). A diffusion barrier maintains distribution of membrane proteins in polarized neurons. Nature *397*, 698-701.
Winckler, B., and Mellman, I. (1999). Neuronal polarity: controlling the sorting and diffusion of membrane components. Neuron *23*, 637-640.
Wisco, D., Anderson, E. D., Chang, M. C., Norden, C., Boiko, T., Folsch, H., and Winckler, B. (2003). Uncovering multiple axonal targeting pathways in hippocampal neurons. J Cell Biol *162*, 1317-1328.
Wollner, D. A., Krzeminski, K. A., and Nelson, W. J. (1992). Remodeling the cell surface distribution of membrane proteins during the development of epithelial cell polarity. J Cell Biol *116*, 889-899.
Yang, Z., Roberts, E. A., and Goldstein, L. S. (2001). Functional analysis of mouse C-terminal kinesin motor KifC2. Mol Cell Biol *21*, 2463-2466.
Yap, C. C., Murate, M., Kishigami, S., Muto, Y., Kishida, H., Hashikawa, T., and Yano, R. (2003). Adaptor protein complex-4 (AP-4) is expressed in the central nervous system neurons and interacts with glutamate receptor delta2. Mol Cell Neurosci *24*, 283-295.
Yoshimori, T., Keller, P., Roth, M. G., and Simons, K. (1996). Different Biosynthetic Transport Routes to the Plasma Membrane in BHK and CHO Cells. Journal of Cell Biology *133*, 247-256.
Zerial, M., and McBride, H. (2001). Rab proteins as membrane organizers. Nature Reviews Molecular Cell Biology *2*, 107-117.